Report no. 3

Project Title: Remote sensing, model and in-situ data fusion for snowpack parameters and related hazards in a climate change perspective (SnowBall)

Table of Content

1. GENERALE OBJECTIVE

Overall project objective:

Explore and develop methodology supporting the vision of developing a future service providing national authorities with hind-cast and real-time snow and avalanche information retrieved from earth observation data.

SnowBall is aiming at providing and demonstrating the methods required for a snow service to deliver geospatial products on the seasonal snow cover derived from satellite data, to the scientific community in Romania, policy makers, users of snow information and the public.

To meet its overall objective, SnowBall has identified 6 key project objectives. These key objectives and the related sub-objectives are directly mapped onto the tasks undertaken in each of the work packages.

Project objectives:

- Improve the spatial and temporal resolution of in-situ snowpack parameters measurements (WP2).
- Development of algorithms and implementation of a prototype snow monitoring system combining Sentinel-1/-3 satellite data, weather station data, and hydrological modelling for snowpack parameters estimation (WP3).
- Assess the impact of climate change on the snow-related resources and hazards (WP4).
- Define and test a reliable methodology for the snowmelt infiltration component of the hydrogeological cycle (WP5).
- Develop and implement a data assimilation procedure for adjusting the snowpack related state parameters within the snow models module of the hydrological forecasting models (WP6).
- Develop methods for avalanche detection, modelling, and hazard assessment (WP7).

2. OBJECTIVES of the 2016 reporting period

WP1 Management
Activity 1.1. Project Management

WP2 In-situ snow parameters measurements
Activity 2.2. Snowpack parameters observation and measurements (completition degree 80%);
Activity 2.4. Elaboration of spatial products using the spatial database (completition degree 80%).

WP3 Satellite remote sensing, data fusion and modelling of snow parameters
Activity 3.2. MWS algorithm and product (completition degree 70%);
Activity 3.3. New multilayer snow model module in NOAH (completition degree 88%).

WP4 Climate change impact on snow-related hazards
Activity 4.1. Snow-related climate variability and change and associated impact (completition degree 88%);
Activity 4.2. Variability and change in flash floods with snow melt contribution (completition degree 80%);
Activity 4.3. Variability and change in avalanche statistics (completition degree 88%).

WP5 Aquifer replenishment modelling from snowmelt infiltration
Activity 5.1. Snowmelt infiltration assessment for the unsaturated zone (completition degree 100%);
Activity 5.2. Aquifer modelling (completition degree 100%).
Activity 5.3. Pattern matching and climate scenarios (completition degree 83%)

WP6 Assimilation of snowpack parameters in the National Flood Forecasting and Warning System

Activity 6.3. Implementation of the methodology for data assimilation of snow pack parameters in the main operational hydrological forecasting models (completition degree 100%).

WP7 Avalanche inventory, release and hazard mapping

Activity 7.2. Change-detection algorithm for Sentinel-1 and Sentinel-2 (completition degree 80%);
Activity 7.3. Avalanche simulation (completition degree 80%).

WP8 Promotion and Dissemination

Activity 8.1. Project website (completition degree 88%);
Activity 8.3. Dissemination and training actions (completition degree 85%).

3. SUMMARY

WP1 Management
Activity 1.1. Project Management

Ensuring quality, decision making and project management were performed through taking the following measures: work meetings via Skype, meetings of the work groups, communication via Internet between the partners.
From 16 March 2016 to 6 May 2016 the operational audit mission for SnowBall project took place, performed by the Central Harmonisation Unit for Internal Public Audit within the Ministry of Public Finance.
In view to implement recommendations formulated in the audit Report, in the June – December 2016 interval, periodic meetings took place monthly along with discussions via Skype with an information and consultation purpose among the project partners, as well as with the contracting authority and the Ministry of European Funds. Following the discussions, reports were elaborated concerning the stage of implementing recommendations made at the operational audit performed by the Central Harmonisation Unit for Internal Public Audit on 5 July 2016 and 12 December 2016. Also, the additional Act no. 6 from 31 October 2016 to the financing contract no. 19 SEE/ 2014 was concluded, regulating a series of financial aspects noticed by the operational audit team.
The annual meeting of Project 19 SEE/ 30 June 2014 SnowBall took place in Beitostølen and Oslo in Norway on 8 – 10 November 2016.
The annual meeting of Project 19 SEE/ 30 June 2014 SnowBall took place in Beitostølen and Oslo in Norway on 8 – 10 November 2016. During the meeting, a session of the Project Steering Committee also took place, that analysed the project implementation stage, in accordance with the activity plan and issues were discussed that may affect fulfilment of the project's objectives. The Project Management Plan was also verified and updated and there was a discussion about the latest instructions received from the contracting authority regarding the verification of expenses borne at project level at the accomplishment of the indicators within the Annual 2016 Scientific and Technical Report.
The project management activity was developed by the Romanian National Meteorological Administration, as project promoter, unfolding throughout 2016. The activity encompassed the research, administrative and financial activities, too, also the communication with the National Authority for Scientific Research and Innovation (NASR) of Romania and exploitation of obtained results.

WP2 In-situ snow parameters measurements
Activity 2.2. Snowpack parameters observation and measurements

Snow spectral reflectance data sets
Satellite data derived snowpack parameters require proper calibration/ validation with in-situ data measured during intensive data collection campaigns. As an example, determination of snow wetness from remote sensed images (how much liquid water is contained in the snowpack) implies knowledge of the snow pack optical spectra in the visible and infrared domain. This type of information can only be obtained in-situ from portable spectrometers measuring the reflected light in the visible spectrum and infrared emission of the snow. In January, March and April 2016, during the field campaigns in Sinaia (Vârful cu Dor – Valea Dorului) and Babele (Babele – Pestera), more than 200 snow spectra in the visisble and infrared have been collected using the DSR (StellarNet) portable spectro-radiometer

Measuring methodology of the snow liquid water content (SLW) with the dielectric constant sensor
Instruments for measuring the dielectric properties of snow in the field have been developed worldwide after methods to measure the wetness of snow through its dielectric properties have

been devised. With these methods, the real part of the permittivity of wet snow must be measured and, by weighing, the density of snow. From these the wetness of snow can be calculated.
The **Denoth meter** is a capacitance probe measuring permittivity of snow A separate measurement of density is required to solve for the imaginary part of the permittivity, which is necessary to estimate liquid water content. The accuracy of measurements made by dielectric methods is ±0.5 vol. %. The **Snow Fork** sensor is based on the simultaneous measurement of both the real part and the imaginary part of the dielectric constant of snow. Knowledge of these allows both the density and the wetness to be determined The imaginary part of the dielectric constant is directly related to the wetness and the real part is dependent on the density and wetness. The **Decagon 5TM** sensor is a capacitive sensor as both the Denoth and the Snow Fork, working in the frequency range below 1 GHz. It is closer to the Denoth instrument since both measure only the real part of the dielectric permittivity. The permittivity measured with the 5TM sensor can be converted to snow liquid water content using the Topp and Denoth equations. The 5TM sensor has been selected for snow permittivity measurements in the SnowBall project. The probes will be deployed at the project cal/val sites an weather stations within the project test area.

Activity 2.4. Elaboration of spatial products using the spatial database

Within this activity (achieving gridded climatology), the mean multiannual monthly data (1 October 2005 – 30 December 2016) for the parameters of interest were used for spatial interpolation.
The maps representing the climatological normals were obtained with the Regression-Kriging (RK) method.
Statistical relationships between minimum temperature values and auxiliary variables (PCA predictors) were identified for each month.
Spatial interpolation (at 1000 × 1000 m resolution) of the mean multiannual values corresponding to each month, were computed from data extracted from the climatological database.

WP3 Satellite remote sensing, data fusion and modelling of snow parameters

Activity 3.2. MWS algorithm and product

The main aim of the work in this period has been to further test and validate the algorithms and wet snow maps using a combination of Sentinel-1 SAR and Terra MODIS optical data. The delay of the launch of the Sentinel-3A satellite made the project team to follow the contingency plan and use MODIS data instead of Sentinel-3 SLSTR data this year. More experience with the novel multi-sensor/multi-temporal wet snow (MWS) algorithm and the products gave valuable added experience and further justifications of the algorithms.

Activity 3.3. New multilayer snow model module in NOAH

During this phase, was implemented the first version of the methodology for estimating the snow water equivalent, by data fusion approach, using the distributed model NOAH simulations, ground observations and satellite products.
Within the methodology, the diferrent type of data and information are analyzed and compared, using a series of automatic cross-validation algorithms, and then the snow water equivalent is estimated in grid format, at spatial resolution of 1 km, by multiple succesive steps of interpolations and adjustments, depending on the degree of uncertainty associated with different type of data.
The software implementation was also done using a modular approach, flexible and easy adapted configuration, based on the following stable open source components:
This implementation version will be further developed, tested, and improved in the next working phase, of the project.

WP4 Climate change impact on snow-related hazards
Activity 4.1. Snow-related climate variability and change and associated impact

In the framework of Activity 4.1 an interesting result refers to the number of days with good ski conditions in the winter season that is decreasing in the Romanian Carpathians under climate change.

Activity 4.2. Variability and change in flash floods with snow melt contribution

The research continued for the Activity 4.2 related to variability and change in flash floods with snow melt contribution. The hydrologic modelling have been applied to the sub-basins corresponding to the rivers Argeş (up to the hydrometric station Căteasca) and Dâmboviţa (left tributary of the Argeş River, up to the hydrometric station Lunguleţu), located mainly in mountain areas. The results of the hydrologic model (CONSUL) indicate that multiannual averages of maximum discharges during the interval from November to April show increases compared with present climate (1981-2010) under best (RCP 2.6) and worst (RCP 8.5) climate change scenarios.

Activity 4.3. Variability and change in avalanche statistics

The main activity in 2016 was to analyse variability and change in avalanche statistics (Activity 4.3). In this context, we have firstly identified the climate conditions for avalanches in the Carpathians. Then we computed the composite maps for large scale variables for the days with episodes of avalanches using monthly stratified data. We used the NCEP/NCAR Reanalysis covering the time interval from January 1948 up to present. We selected as large scale variables daily geopotential heights at 500 hPa, daily sea level pressure, daily temperature at 850 hPa and daily zonal wind component at 300 hPa. Composite maps suggest the approach of multifield analog prediction method (Barnett and Preisendorfer, 1979). We selected the month of April, with a large number of avalanches, to build and test the model. The components of the large scale climate vector are the standardized anomalies of geopotential heights at 500 hPa, temperature at 850 hPa, sea level pressure and zonal wind at 300 hPa for the Atlantic European sector. The components of the local scale vector are the snow depth and air temperature averaged over Fagars Masiff for locations above 1800 m. Local data are derived from the high resolution data sets (1 km x 1 km). Daily data available for the study are from 2000 up to 2016. In order to predict the events, we use the Euclidean distance between the past events and the actual conditions, in the hyperspace defined by the first 4 empirical orthogonal function (EOFs) modes. However, the states associated with avalanche events do not significantly cluster themselves, so the skill of the model is not high.

WP5 Aquifer replenishment modelling from snowmelt infiltration

Activity 5.1. Snowmelt infiltration assessment for the unsaturated zone

The assessment of the infiltration of snow melting in the unsaturated zone is describing the processes of aquifers recharge from snow melt. In 2016 the conceptual models of the three study areas were refined and the hydrological characteristics related to aquifers recharge from rainfall were highlighted.

Activity 5.2. Aquifer modelling

The methodology for determining the infiltrations from snow melting and quantification of aquifers recharge has been established.The methodology for determining the infiltration of snow melting presents the procedure of analyzing and interpreting information and data (in-situ, meteorological and satellite data) that lead to the assessment of the aquifers rechargefrom snow melt. This activity highlights the advantages or disadvantage of using models based on the equilibrium energy equation or those based on the temperature index method. Snow melting is a major component of the hydrological cycle and is closely linked to aquifers and surface waters.

Activity 5.3. Pattern matching and climate scenarios

The interpretation of the data from the climate scenarios made in the work package 4. Based on climatic evolution scenarios, snow melt infiltration models were developed in correspondence with the models modeled for real situations.The way climate change influences melting rates during the spring in Bucegi Mountains, Padina area has been evaluated for RCP 2.6 and 8.5 scenarios in terms of

snow thickness, rate of snow melting for the 2015-2050 period and evolution of average snow water equivalent (SWE).

WP6 Assimilation of snowpack parameters in the National Flood Forecasting and Warning System
Activity 6.3. Implementation of the methodology for data assimilation of snow pack parameters in the main operational hydrological forecasting models

The intensification in the last decade of the floods events severity, generated by snowmelt contribution combined with liquid precipitations, even during winter season, highlight the need for more accurate estimation of the snow water equivalent, as support for operational activities.
The final SWE product output from the data fusion methodology, is used for adjusting the snow state parameters within the operational hydrological forecasting models NOAH, NWSRFS and ROFFG, using a direct data assimilation approach.
The NOAH-R distributed hydrological model simulations is also one of the main input data in the data fusion methodology, so the state SWE parameters in the model are updated based on the adjusted gridded SWE output product, from the data fusion methodology, having the same spatial resolution (1Km).
The other two important hydrological forecasting systems (NWSRFS and ROFFG) are using the same conceptual model SNOW-17, for simulating the snowpack evolution, and the adjusted gridded SWE product from the data fusion methodology is used to compute the mean SWE for the sub-basins configured within these operational models implementation.

WP7 Avalanche inventory, release and hazard mapping
Activity 7.2. Change-detection algorithm for Sentinel-1 and Sentinel-2

In this stage of the project the completion and updating of the avalanche inventory and avalanche typology analysis based on VHR satellite and drone images has been finalized. For the activity 7.2, the algorithms for the detection of changes in snow cover generated by avalanches has been modified and validated (deliverable 7.2). The processing chain has been applied in test areas from Norway and Romania using HR SAR and optical image (Sentinel-1 and Sentinel-2 data).

Activity 7.3. Avalanche simulation

For the activity 7.3 related tot the avalanche simulation, potential release areas have been extracted based on morphometric parameters and the avalanche trajectories have been simulated in the central area of Făgăraș Mts., near Transfăgărășan highway. The simulation have been tested for several magnitude scenarious and avalanche size specific for Southern Carpathians and maps of the avalanche extent, snow height and snow pressure have been generated.

WP8 Promotion and Dissemination
Activity 8.1. Project website

The project website (http://snowball.meteoromania.ro) was updated on a continuous base.

Activity 8.3. Dissemination and education activities

The dissemination and education actions have been conducted according to the project dissemination strategy included in the Publicity Plan: awareness of the user community about the opportunities offered by the Snowball project; communication of the results achieved in the project; preparation of the support materials for the products created within the project (eg. documentations, flyers, posters, etc.); ensuring project visibility at national and international level.
The communication channels that have been used in the Snowball project included oral ones (seminars, conferences, workshops, formal and informal meetings, etc.) and written communication channels (brochures, newsletters, articles in scientific journals, articles in generalist publications, postings on social networks, etc.

Representatives of the Snowball consortium has participated with oral presentations and posters at relevant events for the topics addressed in the project. There have also been submitted some articles for publication in relevant national and international journals for the project objectives. At the end of the project will be organized a final conference dedicated to the presentation of the results.
The brochure contains information about the project objectives and results structured in an attractive manner and in non-technical language, understandable by the general public. The second (final) bilingual version was performed.
The second e-newsletter (electronic format) was elaborated and uploaded on the project website and distributed to the end-users of the project SnowBall.

4. SCIENTIFIC AND TECHNICAL DESCRIPTION

4.1. WP1 Management

*4.1.1. **Activity 1.1** Project Management*

The project management activity was developed by the Romanian National Meteorological Administration, as project promoter, unfolding throughout 2016. The activity encompassed the research, administrative and financial activities, too, also the communication with the National Authority for Scientific Research and Innovation (NASR) and exploitation of obtained results.
In the project management activity, an important role was that of PSC, made up of individuals responsible on behalf of partner institutions (P1-Norsk Regnesentral, Norway, P2-Technical University of Civil Engineering, Bucharest, P3-National Institute of Hydrology and Water Management, Bucharest and P4-West University of Timişoara) and led by the project manager.
Ensuring quality, decision making and project management were performed through taking the following measures: work meetings via Skype, meetings of the work groups, communication via Internet between the partners.
From 16 March 2016 to 6 May 2016 the operational audit mission for SnowBall project took place, performed by the Central Harmonisation Unit for Internal Public Audit within the Ministry of Public Finance. The audit mission objectives targeted the following aspects:

- Project implementation stage and audited project budget execution stage;
- Eligibility of declared expenses, disorder prevention, detection, recording and reporting, observance of regulations on acquisitions;
- Justification and recording in accountancy of declared expenses;
- Observance of project information and publicity demands.

The final report of the audit team (no. 370638/02.06.2016) contained a series of findings and recommendations for each specific objective of the audit mission, detailed for each project partner. The final conclusion and opinion of the audit team mentioned that at the level of the Project Partners, NMA ensured the organizing framework necessary to SnowBall project implementation, i.e. to the fulfilment of attributions and responsibilities stipulated for PP in the applicable Set of Regulations but that certain improvements must be made in the following fields: correctness and completion of the Annual Financial Reports; completion of tasks and responsibilities of the persons appointed in the project implementation team; improving activities regarding the CFPP project; manner of dealing with disorders, Publicity and Dissemination; acquisitions and archiving. The audit team assessed that favourable premises exist for finalizing all the activities stipulated within the project.
To elaborate a point of view regarding the findings and recommendations from the audit report, a series of meetings took place in the 6-27 May 2016 interval at the headquarters of MeteoRomania with individuals responsible on behalf of the Romanian partner institutions. The point of view resulted following the discussions contained explanations and justifications on the grounds of administrative and financial documents and was supported on the occasion of the reconciliation meeting on 27 May 2016.
In view to implement recommendations formulated in the audit Report, in the June – December 2016 interval, periodic meetings took place monthly along with discussions via Skype with an information and consultation purpose among the project partners, as well as with the contracting authority and the Ministry of European Funds. Following the discussions, reports were elaborated concerning the stage of implementing recommendations made at the operational audit performed by the Central Harmonisation Unit for Internal Public Audit on 5 July 2016 and 12 December 2016. Also, the additional Act no. 6 from 31 October 2016 to the financing contract no. 19 SEE/ 2014 was concluded, regulating a series of financial aspects noticed by the operational audit team.
On 26 September 2016, on the occasion of the SYNASC - Geoinformatics 2016 Workshop, organized within SnowBall project at the West University of Timişoara, a work meeting took place involving all the project partners. The meeting's agenda comprised (Annex 1):

- Presentation of the project situation in 2016, after the second stage finalized in 2015;

- Presentation of the project's objectives implementation stage;
- Brief description of the results within the Work Packages (WP) and of the associated activities stipulated for 2016;
- Aspects regarding the administrative and technical organization of the project: indicators, scientific/technical and financial reports and delivrables stipulated for 2016;
- Organizing the common field measurement campaigns for the 2016 – 2017 winter;
- Settling the meetings scheduled for 2017, the conferences and scientific papers to be presented.

The annual meeting of Project 19 SEE/ 30 June 2014 SnowBall took place in Beitostølen and Oslo in Norway on 8 – 10 November 2016.

The meeting agenda is presented in Annex 2.

The meeting was joined by researchers from all the institutions involved in the project: National Meteorological Administration - Bucharest, Norwegian Computing Center in Oslo, Technical University in Bucharest, National Institute of Hydrology and Water Management in Bucharest and the West University of Timişoara, the Geography Department. Table 4.1.1 renders the list of participants from the 2016 annual meeting.

During the annual meeting, issues connected to the technical-scientific reporting over 1 January – 31 December 2016 were discussed and there were analysed and clarified a series of aspects connected to the following activities:

- Prototype monitoring system in quasi-real time through combining automatic processing of data from Sentinel 1-3 satellites with in-situ data and with snow layer modelling.
- Satellite image processing algorithms in the optic and radar domain, in view to evaluate and chart the humidity classes of the snow layer.
- Planning and organizing the in-situ field measurement campaigns for the 2016-2017 winter, in view to validate the computation algorithms of the snow layer from satellite data;
- Acquiring knowledge and working techniques necessary to design and implement the sites destined to calibration/validation activities for data from the Earth Observing satellites for applications aiming the evaluation of the snow layer parameters.

Table 4.1.1: List of participants in the SnowBall project annual meeting of 8-10 November 2016.

Name	Institution	E-mail
Gheorghe Stăncălie	Project Manager National Meteorological Administration Bucharest	gheorghe.stancalie@meteoromania.ro
Andrei Diamandi	National Meteorological Administration Bucharest	diamandi@meteoromania.ro
Anişoara Irimescu	National Meteorological Administration Bucharest	anisoara.irimescu@meteoromania.ro
Roxana Bojariu	National Meteorological Administration Bucharest	bojariu@meteoromania.ro
Rune Solberg	Norwegian Computing Center, Oslo – responsible P1	rune.solberg@nr.no
Arnt-Børre Salberg	Norwegian Computing Center, Oslo – P1	arnt-borre.salberg@nr.ro
Øivind Due Trier	Norwegian Computing Center,	trier@nr.no

	Oslo – P1	
Dragoş Găitănaru	Technical University of Bucharest /CCIAS – P2	dragos.gaitanaru@utcb.ro
Ada Pandele	National Institute of Hydrology and Water Management, Bucharest	ada.pandele@hidro.ro
Florina Ardelean	West University of Timișoara, Geography Department – P4	florina.ardelean@e-uvt.ro
Knut R.	Statkraft and Glomma and Laagen Water Management Association) (GLB)	

During the meeting, a session of the Project Steering Committee also took place, that analysed the project implementation stage, in accordance with the activity plan and issues were discussed that may affect fulfilment of the project's objectives. The Project Management Plan was also verified and updated and there was a discussion about the latest instructions received from the contracting authority regarding the verification of expenses borne at project level at the accomplishment of the indicators within the Annual 2016 Scientific and Technical Report.
Peculiar attention was paid to the preparation of the technical-scientific and financial Report over the 1 January – 31 December 2016 interval. On that occasion issues were discussed regarding the implementation stage of the notifications and recommendations received from the National Authority for Scientific research and Innovation (NASR) following the operational audit carried out by the Central Harmonisation Unit for Internal Public Audit within the Ministry of Public Finance.
During the 2016 annual meeting new cooperation opportunities were discussed in the frame of the SEE Programme, to be launched in 2017, with representatives from institutions in Norway (Statkraft and Glomma and Laagen Water Management Association) interested in the development of applications for the use of information regarding the snow layer characteristics for the management of the water volumes in the storage lakes.
Those responsible for activities have been established their teams to achieve the proposed objectives. Also have been nominated the responsible for deliverables for the reported period (Table 4.1.2).

Table 4.1.2: List of Deliverables for 2016.

LIST of DELIVERABLES - 2016					
Del. no.	**Deliverable Name**	**WP no.**	**WP Leader**	**Delivery date**	**Responsable**
1	D1.2. Annual project reports	1	CO	Each year	Gheorghe Stăncălie
2	D2.7 Measuring methodology of SWE dielectric constant sensor – Version 1	2	CO	19	Andrei Diamandi
3	D2.8 Measuring methodology of SWE dielectric constant sensor – Version 2	2	CO	21	Andrei Diamandi
4	D3.4 MWS prototype products for flood and avalanche warnings – Version 2	3	P1	24	Rune Solberg
5	D3.6 Gridded SWE prototype products generated using data fusion methodology – Version 1	3	P3	30	Marius Mătreaţă
6	D4.3 Empirical model linking avalanche frequency and atmospheric conditions	4	CO	24	Roxana Bojariu

7	D5.2 Snowmelt infiltration methodology: The innovative aspect of the new methodology is the integration of measured data from the field test with remote sensing and meteorological data. The methodology will be tailored on the hydrogeological and climatological conditions	5	P2	19	Radu Gogu
8	D6.3 Implementation of the snowpack parameter assimilation into the hydrological forecasting modelling system: NOAH-RNWSRFS (U.S. National Weather Service River Forecast System) and ROFFG	6	P3	30	Marius Mătreaţă
9	D7.2 Validated algorithms for detection of changes in land and snow cover caused by avalanches in HR SAR and optical satellite images	7	P4	30	Mircea Voiculescu
10	D8.4 Project brochure - Version 2	8	CO	30	Denis Mihăilescu
11	D8.6. Visibility products (banners, posters etc.)	8	CO	Each dissemination session	Denis Mihăilescu
12	D8.7. Conference project presentation package	8	CO	Each dissemination session	Vasile Crăciunescu
13	D8.8. Dissemination action report	8	CO	Each year	Oana Nicola
14	D8.9. Project newsletter (e-zine) - digital form	8	CO	Each year	Vasile Crăciunescu

4.2. WP2 In-situ snow parameters measurements

*4.2.1. **Activity 2.2.** Snowpack parameters observation and measurements*

Snow spectral reflectance data sets

Satellite data derived snowpack parameters require proper calibration/ validation with in-situ data measured during intensive data collection campaigns. As an example, determination of snow wetness from remote sensed images (how much liquid water is contained in the snowpack) implies knowledge of the snow pack optical spectra in the visible and infrared domain. This type of information can only be obtained in-situ from portable spectrometers measuring the reflected light in the visible spectrum and infrared emission of the snow (Figure 4.2.1).

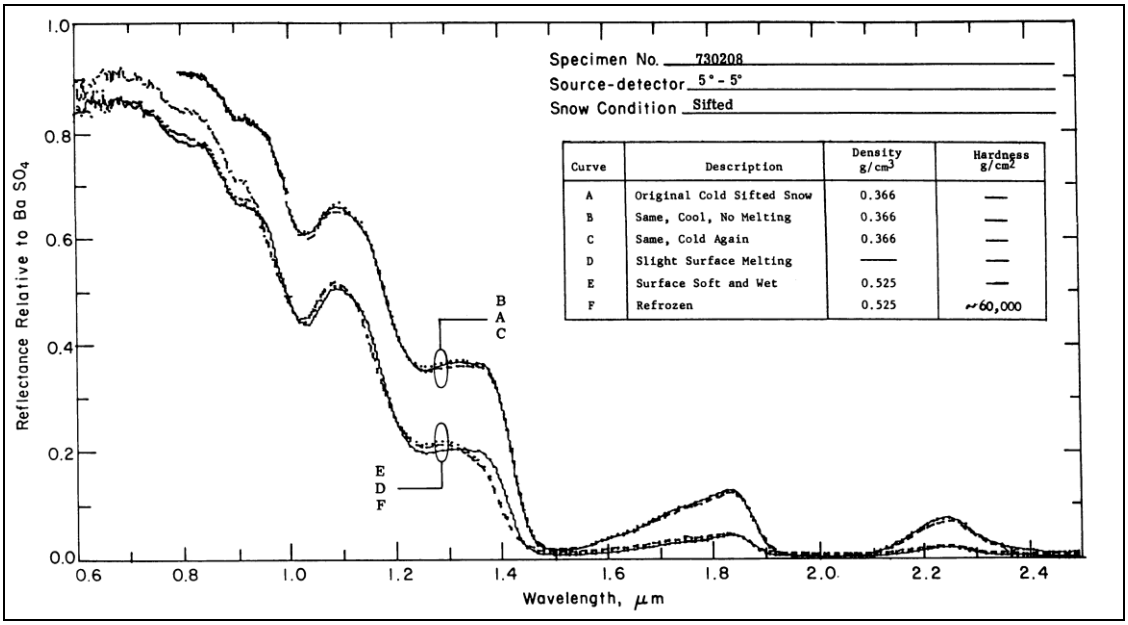

Figure 4.2.1: The effect of snow liquid water spectral reflectance on snow (O'Brien & Munis, 1975).

In January, March and April 2016, during the field campaigns in Sinaia (Vârful cu Dor – Valea Dorului) and Babele (Babele – Pestera), more than 200 snow spectra in the visisble and infrared have been collected using the DSR (StellarNet) portable spectro-radiometer (Figure 4.2.2).

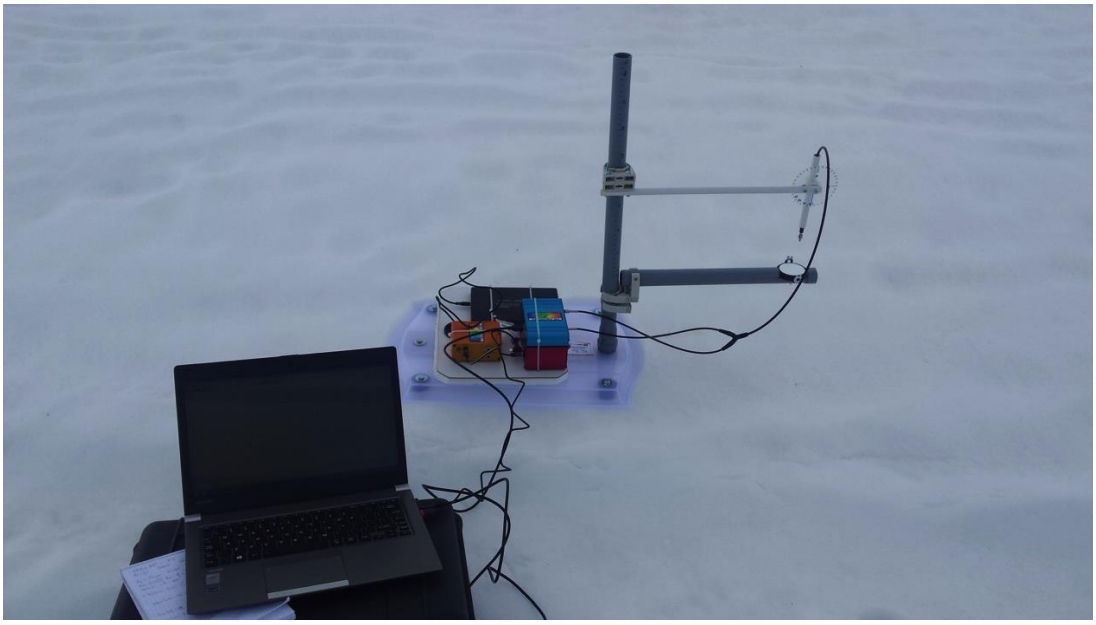

Figure 4.2.2: The DSR spectro-radiometer set up for snow spectra data acquisition, Sinaia 2016.

One can observe on the selection of snow spectra presented in Figures 4.2.3 and 4.2.4 the minima at 1 µm and 1.5 µm as in the plot in Figure 4.2.1, confirming the quality of the data acquisition. The data set obtained so far is covering a wide range of weather and snow conditions (sun angles, spectro-radiometer viewing angles, air temperature, illumination, etc).

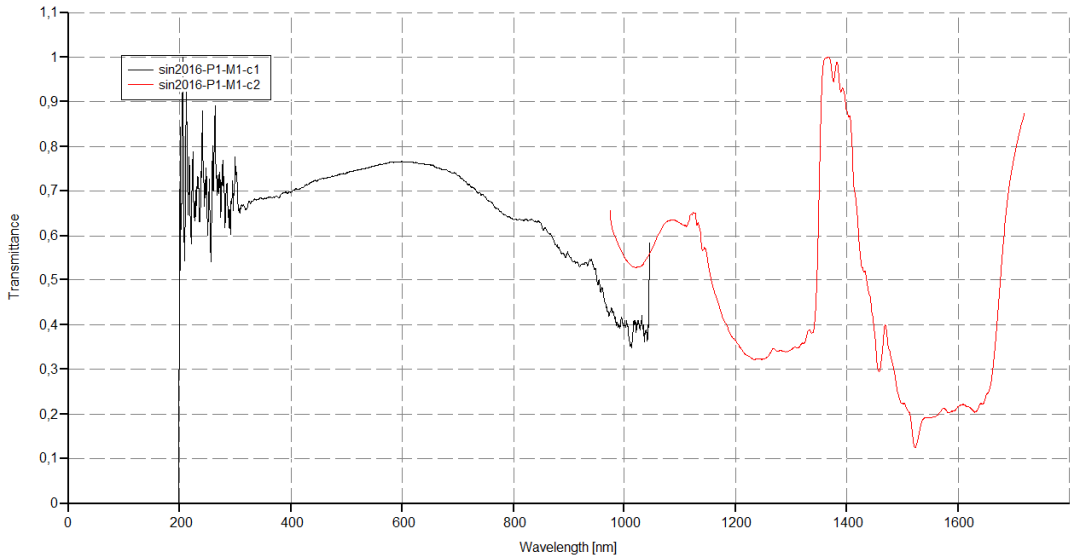

Figure 4.2.3: Transmittance snow spectra, cloudy conditions, Sinaia, 07/04/2016 10:43.

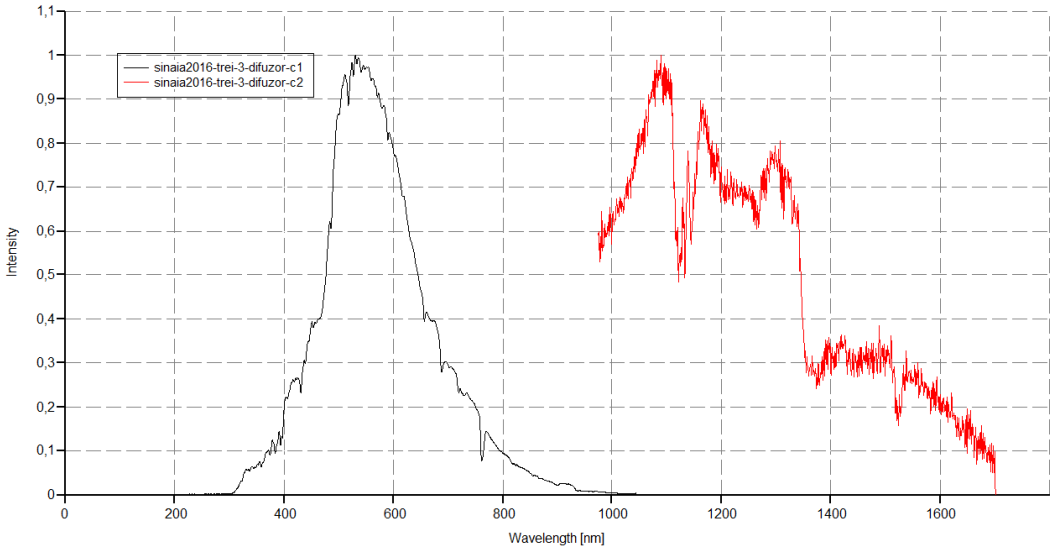

Figure 4.2.4: Irradiance snow spectra, cloudy conditions, Sinaia, 17/03/2016 14:19.

Measuring methodology of the snow liquid water content (SLW) with the dielectric constant sensor

Dry snow is the mixture of ice and air whereas wet snow is the mixture of ice, air, and contents of free liquid water (wetness). The snow wetness or the snow liquid water content (SLW) can be defined as the amount of liquid-phase water in snow and is an important factor in snow avalanche prediction, water ressources management and runoff prediction. The snow wetness is expressed as percent volume (vol%) of the snow.

Liquid water is introduced to snow by rain and/or melt. Melting at the surface depends primarily on the incoming flux of shortwave radiation, which varies with slope aspect and elevation.

There are many methods to measure the liquid water content of snow: centrifugal separation, melting calorimetry, freezing calorimetry, alcohol calorimetry or the dilution method. These methods, summarized by Stein et al., 1981, have all in common the difficulty to perform and, besides,

they are also time-consuming. This makes them impractical for field campaigns as well as for automated operation. Liquid water content can also be estimated by measuring the permittivity of snow. This measurement is diagnostic of liquid water because the permittivity of water (ε=80) is much higher than those of air (ε=1), and ice (ε=5). The dielectric constant of snow measure of the ability of the snow to store electrical energy in the presence of an electrostatic field.

The electromagnetic propagation properties of a material are defined in terms of its magnetic permeability, μ, and its relative complex dielectric constant, ε. For most naturally occuring materials, including snow, $\mu \sim \mu_0$, the magnetic permeability of free space. Hence, the propagation is governed solely by ε, which has the complex form:

$$\varepsilon = \varepsilon' + i\varepsilon'' \tag{1}$$

Since snow is a heterogenous mixture of air, ice and, under certain conditions, liquid water, the dielectric properties of the constituents must be examined first in order to understand the dielectric properties of the mixture. For practical purposes, the characteristics of air are indistinguishable from those of free space. Water and ice, however, exhibit dielectric behaviour which can be described, at least to the first order, by the Debye equation:

$$\varepsilon(\nu) = \varepsilon_\infty = \frac{\Delta\varepsilon}{1 + i2\pi\nu\tau} \tag{2}$$

Separating the real and imaginary parts of the complex dielectric permittivity yields:

$$\varepsilon' = \varepsilon_\infty + \frac{\varepsilon_0 - \varepsilon_\infty}{1 + (2\pi\nu\tau)^2} \tag{3}$$

$$\varepsilon'' = \varepsilon_\infty + \frac{2\pi\nu\tau(\varepsilon_0 - \varepsilon_\infty)}{1 + (2\pi\nu\tau)^2} \tag{4}$$

where $\varepsilon_0 = \lim_{\nu\to 0} \varepsilon$ or the static dielectric constant, dimesionless, $\varepsilon_\infty = \lim_{\nu\to\infty} \varepsilon$ or the optical limit of dielectrical constant, dimesionless, τ = relaxation time of the materisal (s), ν = electromagnetic frequency (Hz). This equation describes the contribution to the polarizability of a polar molecule (H_2O) from the permanent dipole moment of that molecule. An applied electric field tends to align the dipole against the thermal forces which induce disorder or "relaxation" and are a function of the temperature and viscosity of the dielectric material. The relaxation time as derived by Debye for spherical polar molecules in a viscous medium is a good aproximation for water (Styles and Ulaby, 1981):

$$\tau = \frac{4\pi\,\eta\,a^3}{kT} \tag{5}$$

where η is the viscosity, a is the molecular radius, k is Boltzamn's constant and T the temperature. Figure 4.2.5 illustrates the behaviour of ε'_w and ε''_w of water at 0° C as a function of frequency.

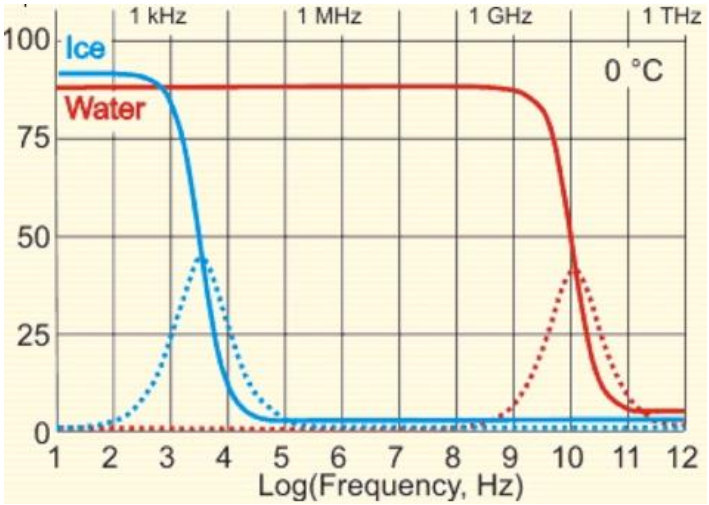

Figure 4.2.5: Complex dielectric constant of water and ice at 0°C from the Debye equation.

For frequencies above 1 MHz, the dominant physical parameter that determines the dielectric constant of dry snow is its density. An alternate and useful expression for density is the volume fraction of ice V_i, which is related to the ice density ρ_i and the snow density ρ_s through $V_i = \rho_s/\rho_i$
Numerous formulae explaining and predicting the dielectric characteristics of wet snow have been presented. These may be mixing formulae that have the permittivities of air, ice, and water as parameters, or they may even be linearized functions of density and wetness. More rigorous mixing theories take into account the microscopic structure of snow and the liquid water distribution. In this case, the resulting formulae usually contain additional parameters (for example, depolarization factors of the ice and water particles).
Instruments for measuring the dielectric properties of snow in the field have been developed after Ambach (1) first suggested a method to measure the wetness of snow through its dielectric properties. With these methods, the real part of the permittivity of wet snow must be measured and, by weighing, the density of snow. From these the wetness of snow can be calculated.
The **Denoth meter** is a capacitance probe measuring permittivity of snow of area 13 × 13.5 cm^2 (Techel and C. Pielmeier, 2011). A separate measurement of density is required to solve for the imaginary part of the permittivity, which is necessary to estimate liquid water content. The accuracy of measurements made by dielectric methods is ±0.5 vol. %. Additional uncertainty can arise if sensors near the surface are affected by solar radiation.
Neglecting the small effects of liquid water geometry, a relatively simple relation between snow permittivity ε, density ρ (g/m^3) and volumetric water content W (vol.%) has been found experimentally (Denoth, 1994):

$$\varepsilon = 1 + 1.92\,\rho + 0.44\,\rho^2 + 0.187\,W + 0.0045\,W^2 \qquad (6)$$

Snow permittivity is measured using flat capacitive sensors to allow both near-surface and volume wetness determinations. The thickness of only 1.5 mm of the platelike sensor offers a nearly non-destructive measurement. For electronic simplicity, a fixed measuring frequency of 20.00 MHz has been selected (Denoth, 1994).
The **Snow Fork** instrument (Figure 4.2.6) has been developed at the Helsinki University of Technology in Finland, by M. Tiuri & A. Sihvola. The snow sensor is based on the simultaneous measurement of both the real part and the imaginary part of the dielectric constant of snow. Knowledge of these allows both the density and the wetness to be determined (4) The imaginary part of the dielectric constant is directly related to the wetness and the real part is dependent on the density and wetness.

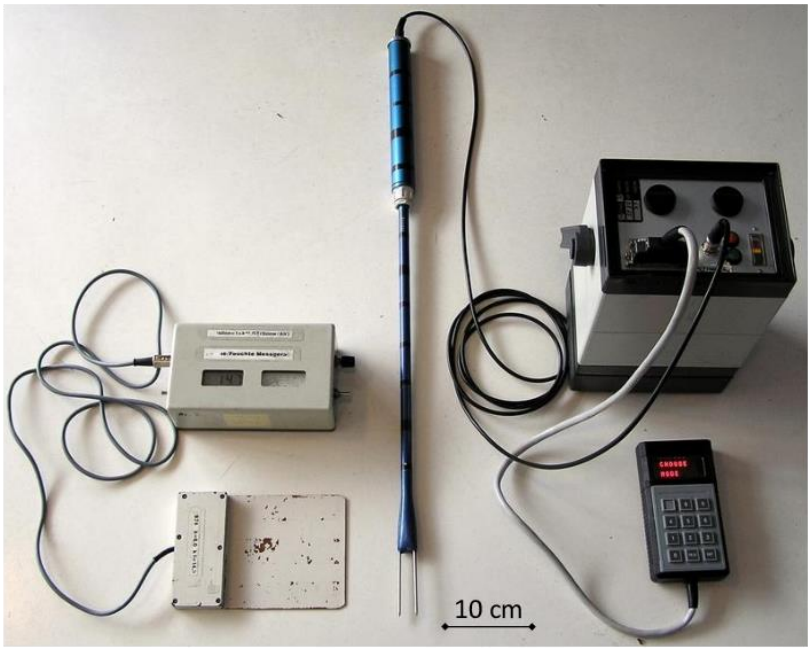

Figure 4.2.6: The Denoth instrument (left) and the Snow Fork (left).

The **Decagon 5TM** sensor was designed to measure soil water volumetric content. It is a capacitive sensor as both the Denoth and the Snow Fork, working in the frequency range below 1 GHz. It is closer to the Denoth instrument since both measure only the real part of the dielectric permittivity.
The sensor uses an electromagnetic field to measure the dielectric permittivity of the surrounding medium. The sensor supplies a 70 MHz oscillating wave to the sensor prongs that charges according to the dielectric of the material. The stored charge is proportional to snow dielectric and snow volumetric water content. The 5TM microprocessor measures the charge and outputs a value of dielectric permittivity from the sensor.
To derive the water volumetric content from the soil dielectric permittivity, the Topp equation is used:

$$WVC = 4.3 * 10^{-6} \varepsilon_a^3 - 5.5 * 10^{-4} \varepsilon_a^2 + 2.92 * 10^{-2} \varepsilon_a - 5.3 * 10^{-2} \quad (7)$$

where ε_a is the real part of the soil dielectric permittivity and WVC the volumetric water content. It is clear that an instrument calibrated for soil moisture cannot measure snow moisture with the same accuracy. However, we deemed that it is worth comparing the snow moisture obtained from the Topp's equation with the values computed using the Denoth formula. We would like to have a look at how well the Topp's snow moisture corresponds to the diurnal variations of the air temperature since measurements of snow temperature can also be used to determine the presence/absence of water.
The Decagon 5TM sensor will be used as both a mobile instrument – with the Decagon ProCheck data logger (Figure 4.2.7) and as a continous measuring device with the snow stations.

Figure 4.2.7: The Decagon 5TM sensor (left) and the Decagon ProcCheck portable data logger (right).

The Decagon 5TM sensor has been selected for capacitive snow wetness mesurements in the SnowBall project. The 5TM probe is much less expensive than the Denoth instrument and can be easily interfaced with microcontroller based data loggers of the type used in the project. The probes will be deployed at the project cal/val sites an weather stations within the project test area.
More details are presented in the deliverables D2.7: „Measuring methodology of SWE dielectric constant sensor – Version 1" and D2.8: „Measuring methodology of SWE dielectric constant sensor – Version 2".

*4.2.2. **Activity 2.4.** Elaboration of spatial products using the spatial database*

Within this activity (achieving gridded climatology), the mean multiannual monthly data (1 October 2005 – 30 December 2016) for the parameters of interest were used for spatial interpolation.
The maps representing the climatological normals were obtained with the Regression-Kriging (RK) method. RK is a multivariate method that can take for computation one or more variables with a spatially continuous distribution (numerical altimetric model, satellite images, etc.).
Due to the existence of the collinearity effect (correlated independent variables), the predictors derived from the numerical altimetric model were filtered by means of principal component analysis

(PCA). Filtering the predictors through PCA is performed through transforming the initial variables into a new set of variables, uncorrelated and of a smaller size.
In this stage, statistical relationships between minimum temperature values and auxiliary variables (PCA predictors) were identified for each month. They were selected for each month by retrograde type stepwise regression. The gridded climatology – mean multiannual monthly maps – was realized for the parameters of interest. Auxiliary data derived from the DEM were also used for spatialization: altitude, mean altitude in a 20-km radius, latitude, distance to the Black Sea and distance to the Adriatic Sea.
The maps representing the climatological normal, obtained with the RK method by summing the surface determined through the least squares method (applied to multiple regression) and the surface obtained through spatially interpolating the regression residuals, using the Kriging method. With this method, the first step consists in statistically validating the deterministic model, in the sense of verifying the intensity of the relationships between predictors and the dependent variable. Here, the multiple regression method can be used. The best regression method is choosed by stepwise regression. For RK, the matrix of the multiple regression grid points represents the large scale variability of the analysed parameter, function of the explanatory variables, interpolated residuals constituting the local peculiarities modelled with the help of the semivariogram (Hengl, Heuvelink, and Rossiter 2007):

$$\hat{Z}(s_0) = \sum_{i=1}^{p} \hat{\beta}_k \cdot q_k(s_0) + \sum_{i=1}^{N} \lambda_i \cdot e(s_i)$$

where $\hat{\beta}_k$ are the coefficients of the regression model, q_k is the value of the predictor in the point localised through the s_0 coordinates for which a new value is estimated and λ_i are the weighting coefficients of the residuals of $e(s_i)$ regression with s_i coordinates. Regression coefficients can be obtained either through the simple method of the least squares or through applying the generalised regression model.
Due to the collinearity effect (correlated independent variables), the predictors derived from the numerical altimetric model were filtered by principal component analysis (PCA) – through transforming the initial variables into a new set of variables, uncorrelated and of a smaller size. The new data set thus obtained contains most part of the original dataset variability (Figure 4.2.8).

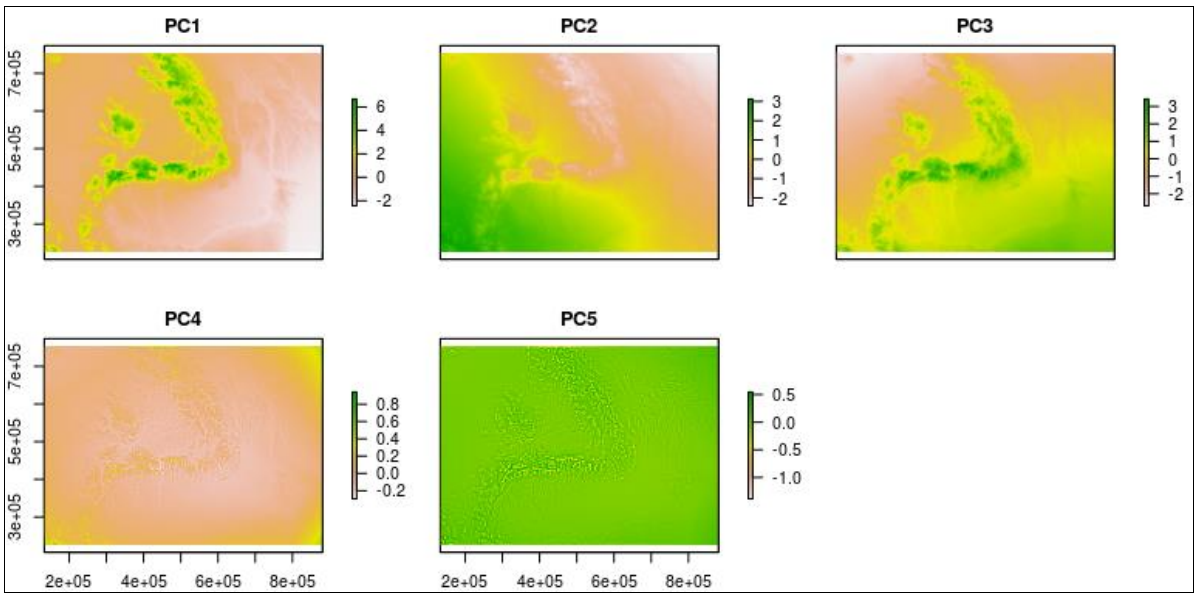

Figure 4.2.8: PCA transformed predictors.

The explained variance of the five principal components is presented in Figure 4.2.9. It is obvious that the first three components explain most of the spatial variability. Hence, only those were taken into account for the spatialization of multiannual values with the RK method.

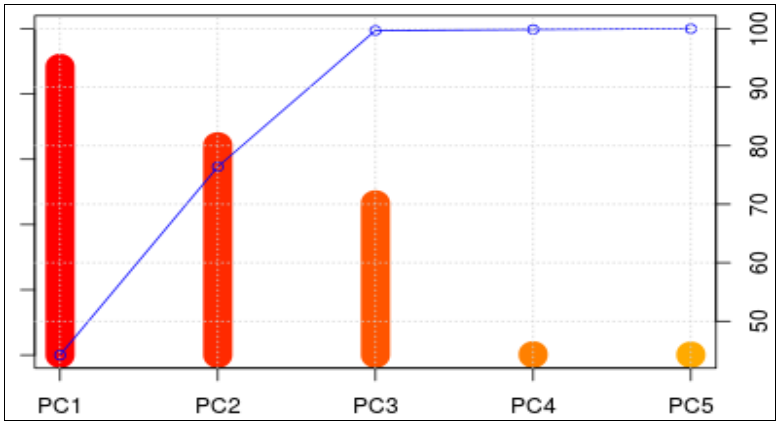

Figure 4.2.9: Variance explained by the principal components (PCA) computed from the set of predictors obtained from the numerical altimetric model.

Minimum air temperature

The statistical relationships between minimum air temperature and auxiliary variables (PCA predictors) were identified for each month, and the statistically significant predictors were selected by retrograde *stepwise regression*. The monthly maps were obtained with RK method at 1000×1000 m spatial resolution representing the multiannual means of the minimum air temperature, 2005-2015 (Figure 4.2.10).

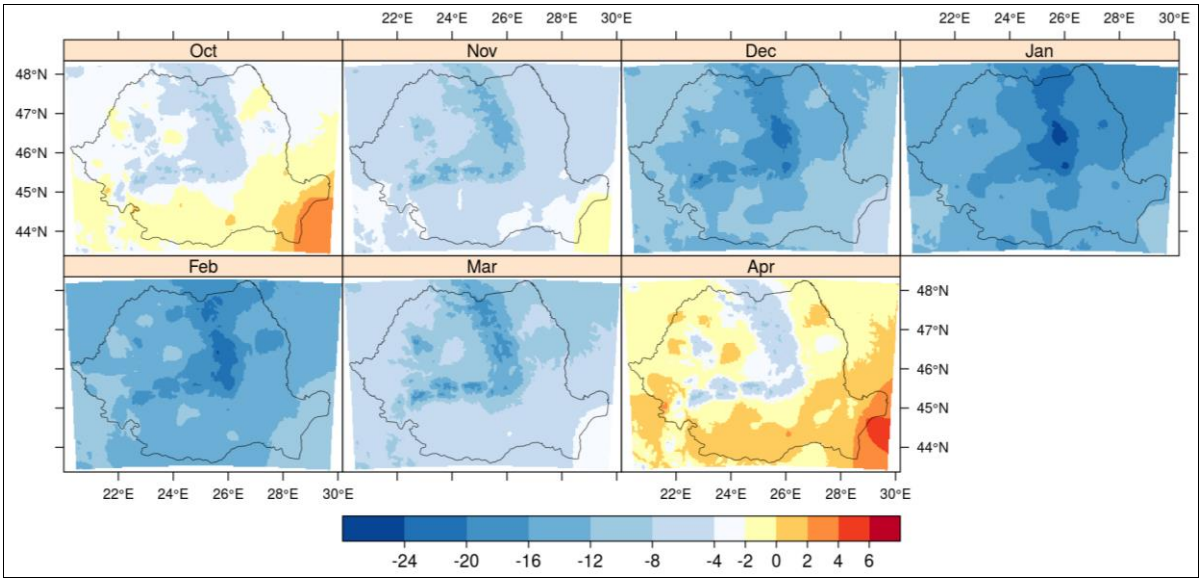

Figure 4.2.10: Mean multiannual minimum air temperatures (°C) 2005-2015.

Mean air temperature

For mean air temperatures, the predictive power of the regressive models is higher during spring and in October, with obtained values of R^2 coefficient higher than 0.9. The influence of predictors in the spatial distribution of the multiannual means is also highlighted by the temperature maps, where the lowest temperature values correspond to the maximum altitudes (Figure 4.2.11).

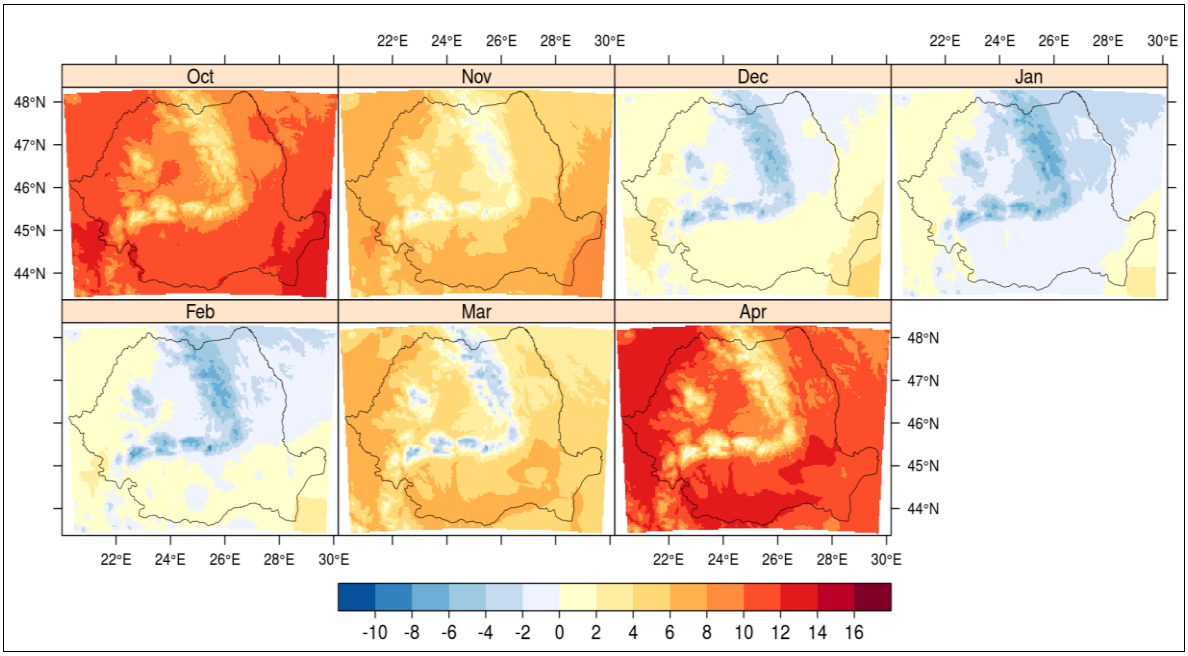

Figure 4.2.11: Mean multiannual air temperatures (°C) 2005-2015.

Maximum air temperature

The maximum air temperature is also strongly conditioned by orography. In most cases regression models explain over 80% of the spatial variability of the mentioned parameter. The largest values of the mean maximum air temperatures exceeded 26 ºC in the south of the Romanian Plain and in the Western Plain in October and April (Figure 4.2.12).

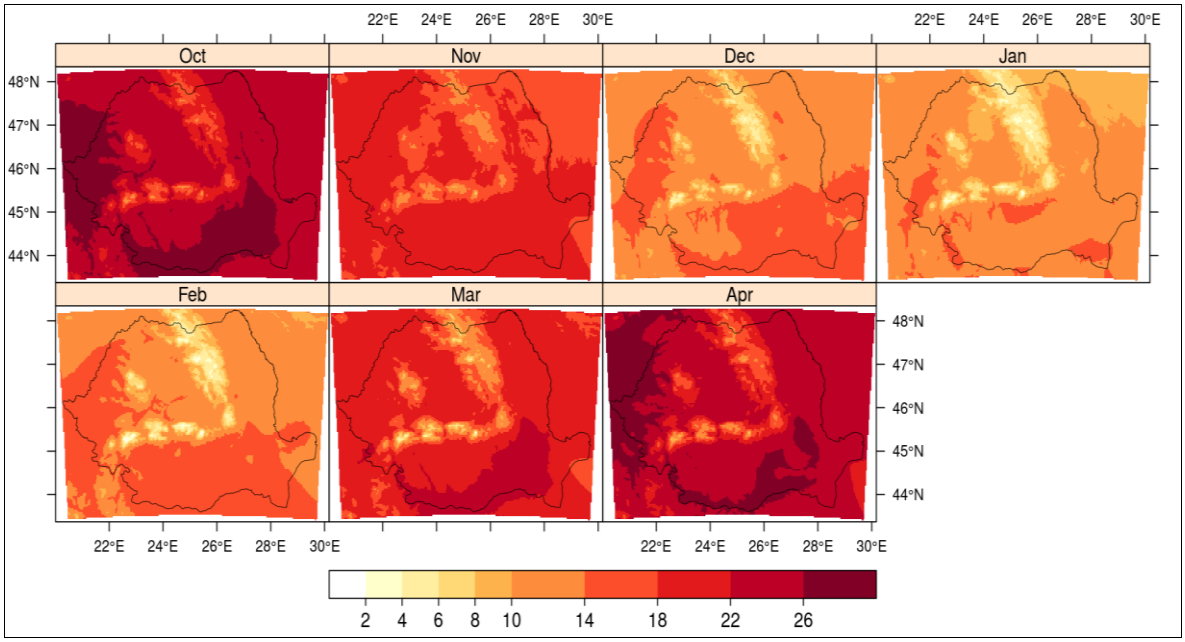

Figure 4.2.12: Mean multiannual maximum air temperatures (°C) 2005-2015.

Precipitation

It is well known that the distribution of the multiannual precipitation is skewed, hence the data series were transformed using the natural logarithm function, resulting into an approximate normalization of the distributions, which made it possible to use geostatistical interpolation methods based on the Gaussian distribution. The inverse of the logarithmic function (exponential function) was used to obtain the maps with real precipitation data.

The spatial and temporal variability of precipitation is much higher than in the case of temperature, which makes the spatialization process of this climatic parameter very difficult, using the predictors derived from the numerical altimetric model. Although the influence of topography on the spatial distribution of mean precipitation is nonlinear, the largest amounts are again recorded in the high mountain areas (Figure 4.2.13).

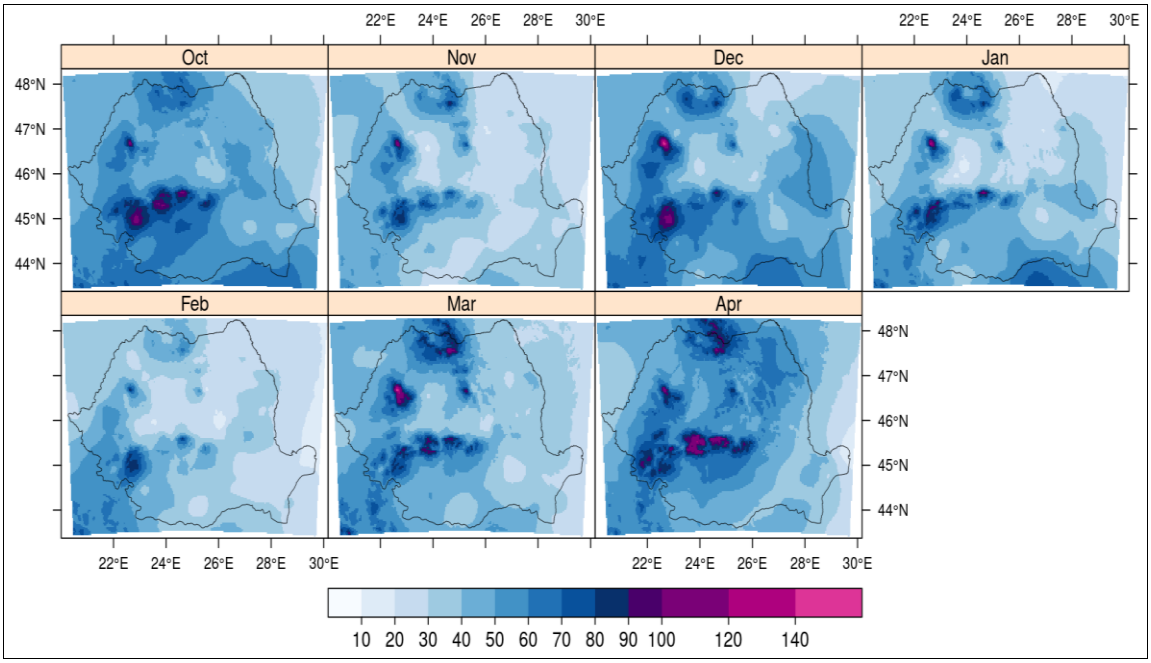

Figure 4.2.13: Mean precipitation amounts (mm) 2005-2015.

Snow depth

The frequency distributions of mean values shows that they show a skewness to the right, therefore the data series were transformed by applying the natural logarithm function in order to obtain a close to normal distribution. It is worth mentioning that in this case the *log1p()* function was used which can also be applied when the data series contain values of zero. To transform data in real values concerning the snowpack depth, *expm1()* function from R language was used (stat.ethz.ch/R-manual/R-devel/library/base/html/Log.html).

The highest values are recorded in the closing months of the cold season (Figure 4.2.14), being generated by persisting negative temperatures at high altitudes, which favours constant accretion of snow.

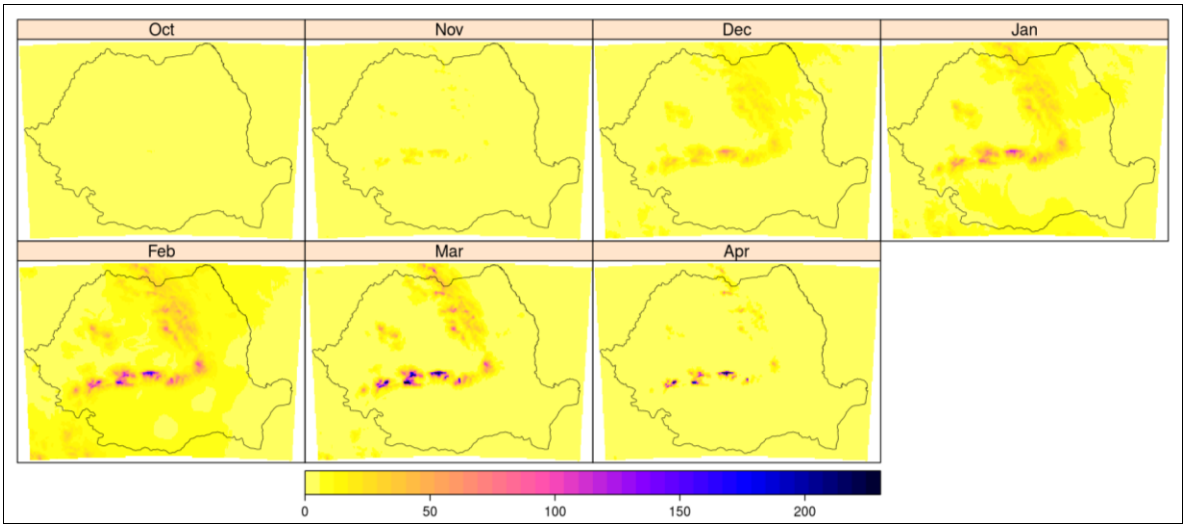

Figure 4.2.14: Mean snowpack depth (cm) 2005-2015.

Snow water equivalent

The distribution of the data series shows strong skewness to the right as well, therefore the data were transformed by applying the same function as in the previous section. The explanatory power of the regression models is great, R^2 values being larger than 0.7 in every case. The spatio-temporal variability of the snowpack water equivalent resembles that of the snow, with the difference that towards the end of the cold season (in March and April) maximum values are very high (in excess of 600 mm), owing to the higher density of the snow, mainly resulted from the accretion of fresh snow at snow temperatures close to 0º C (Figure 4.2.15).

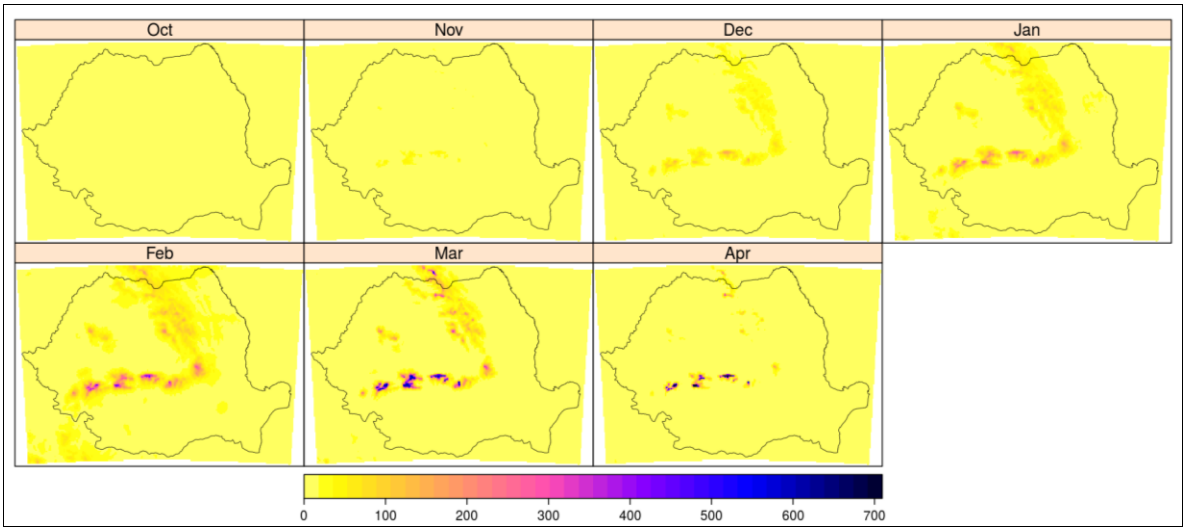

Figure 4.2.15: Snow water equivalent (mm) 2005-2015.

4.3. *WP3 Satellite remote sensing, data fusion and modelling of snow parameters*

4.3.1. Activity 3.2. MWS algorithm and product

Satellite sensors provide the optimal way to monitor the snow conditions as the state of snow might change quickly over vast areas. The Sentinel-1 and Sentinel-3 satellites provide frequent coverage.
The Sentinel-1 C-band SAR can be used to detect wet snow, as the backscatter drops significantly. With C-band SAR however, it is difficult to determine how wet the snow is. It can also be difficult to distinguish bare ground from dry snow cover. Optical sensors, such as Sentinel-3 SLSTR on the other hand, through monitoring of the temperature and snow grain size, can be used to estimate the degree of wetness. However, optical data, are limited by cloud cover. Within the multi-temporal multi-sensor snow wetness algorithm and product, we try to synthetize the best of optical and SAR for improved spatiotemporal coverage.
Due to the delay of the launch of Sentinel-3A satellite, Sea Land Surface Temperature Radiometer (SLSTR) data was not available in the winter 2015/16. The project team followed the contingency plan and used Terra MODIS for further preparation for SLSTR data. One new season of snow wetness observations gave valuable added experience and a larger dataset for final justifications of the algorithms.
The winter 2015/16 was unusually mild with substantially less than average snow cover in Romania. There were only brief events of snow cover at lower altitudes. In the high mountain regions above treeline, the snow layer was rather shallow, and due to wind-transported snow not all the terrain was snow covered. This situation limited the validation work for this season in Romania. For Norway, the situation was quite normal.

Multi-temporal multi-sensor snow wetness algorithm concept

Our approach makes use of a hidden Markov model (HMM) to describe the different states the snow goes through during the melting season, and the possible transitions between these states. The states include dry snow, “moist snow”, “wet snow”, “very wet snow”, “soaked snow cover” and “temporary snow cover”. This model is combined with the available optical and SAR snow wetness products and used to estimate the state of the snow for every 1 km grid cell. The Viterbi algorithm is used to produce the most likely sequence of snow states, given the observations. The result of the method is daily multi-sensor snow wetness products, providing the best estimate for each grid cell for every day.
The HMM approach based on modelling and assimilation was proposed by Solberg et al. (2008) for retrieval of Fractional snow Cover (FSC). A set of snow states is defined, and for each snow state there is a corresponding reflectance and backscatter model. A similar approach was recently developed in the CryoClim project (www.cryoclim.net), where an accuracy of 93% was obtained for snow extent mapping when validating against synoptic weather stations (Rudjord et al., 2015; Solberg et al., 2015).
The basic idea of the approach is to simulate the states the snow surface goes through during the snow season with a state model. The states are not directly observable, but the remote sensing observations give data describing the snow conditions, which are related to the snow states. Solberg et al. 2008 applied a Hidden Markov Model (HMM) to model the states. There are other state modelling frameworks that could be applied as well. However, HMM is building on statistical theory making it possible to establish a sound probabilistic model derived from observational data (Baum and Petrie, 1966). Note that the HMM solution represents not only a multi-sensor model but also a multi-temporal model. The sequence of states over time is required to follow certain optimisation criteria. Note also that the HMM model is applied per pixel, so each pixel’s history through the snow season is modelled.
According to the thematic snow wetness classes applied for the OWS algorithm, four corresponding snow wetness states have been defined in the hidden Markov model (Figure 4.3.1). Additionally, there is a state for patchy snow cover and snow-free ground, *depletion* (< 100% FSC), and *temporary snow* (thin snow layer making full snow cover for a short period, also named ephemeral snow cover). Allowed transitions between states are shown by arrows. As the model shows, the wet snow classes

are “chained” such that the current state might move up to wetter classes or down to drier classes (in terms of liquid water content).

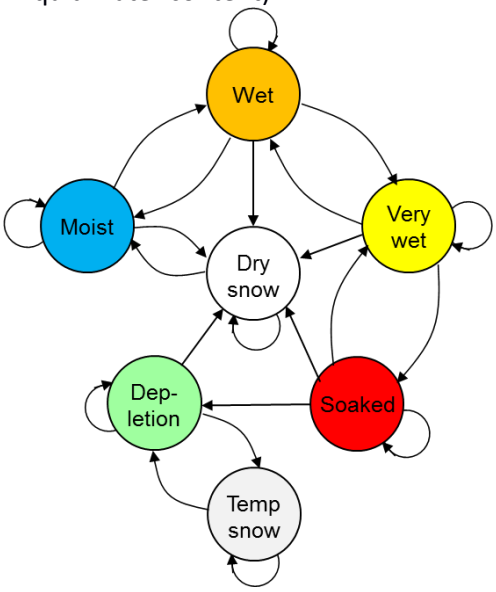

Figure 4.3.1: Hidden Markov model for snow wetness fusing optical and SAR observations.

Hidden Markov Model for snow wetness

In a HMM we observe a system assumed to evolve through a series of different states. Transitions from one state to another happen with certain probabilities. While in a given state the system will produce observables with a certain probability density. We will denote the set of discrete states *Q* of the internal system by:

$$Q = \{S_1, S_2, \dots, S_v\}$$

where *v* is the number of states. Furthermore, the time series of observations, $\bar{X}$, will be denoted by:

$$\bar{X}^T = \{X^1, X^2, \dots, X^T\}$$

where *T* is the number of elements of the sequence. The unknown state of the process at time *t* will be denoted E^t, thus $E^t = S_i$ indicates that the process is in state S_i at time *t*. The states are not directly observable, but are related to observation X^t at times *t*, (*t* = 1, 2,…, *T*) by a probability distribution of measurements:

$$p(X^t | E^t = S_i), i = 1, 2, \dots, v$$

For a given time period, the model is also described by a set of transition probabilities between each pair of states:

$$p\left(E^t = S_i \middle| E^{t-1} = S_j\right), i, j = 1, 2, \dots, v$$

The probabilities of transition between the different states are obviously strongly dependent upon season, thus the process is not stationary and the probabilities of transition are time dependent.
The final parameters of the model are the initial conditions defined by the probability of being in a given state at the initial time:

$$p(E^1 = S_i), i = 1, 2, \dots, v$$

With HMM, the notion of a class from the classification literature becomes the notion of a model in the HMM formalism. Traditionally, ground-cover classification in a temporal sequence of satellite images is the problem of assigning each pixel in the scene to a class based on this pixel’s signal properties (or derived properties). In the HMM case, our aim is to assign each pixel to the model that best explains the observed temporal evolution of the pixel. Solutions to this kind of problem are important in many applications and several algorithms are available. For our problem we have chosen to use the Viterbi algorithm.

The Viterbi algorithm is a dynamic-programming algorithm for finding the most likely sequence of hidden states (the Viterbi path) that result in a sequence of the observables. The Viterbi algorithm was proposed by Viterbi (1967) as a decoding algorithm for convolutional codes over noisy digital communication links. The algorithm requires as input the state probability density functions, the transition probabilities between the different states and the initial probability of each state.
Let $V_{t,k}$ be the probability of the most likely state sequence responsible for the first t observations that has k as its final state, then:

$$V_{1,k} = p(X^1|k)p(E^1 = S_k)$$
$$V_{t,k} = p(X^t|k) \max_i \left(p\left(E^t = S_i \middle| E^{t-1} = S_j\right)V_{t-1,k}\right)$$

The Viterbi path can be retrieved by saving back pointers that remember which state i was used in the second equation.
The algorithm takes as input the optical wet snow (OWS) map, containing wet snow class probabilities, and a SAR wet snow (SWS) map containing probabilities of wet snow.
This year, the training of the HMM was improved from previous versions by making use of a 15-year daily time series (2000-2015) of a 1-km snow surface state product based on a model where data from meteorological stations and numerical weather prediction is combined into a national-wide product provided through the seNorge web portal (Saloranta 2012). This is used to determine a "snow wetness probability" for each grid cell for every day of the year. This simplified parameter is used to find an estimate of transition probabilities and initial probabilities for the HMM states.

Validation Results

The algorithm validation results are presented for the test sites in Norway and Romania. The validation is here limited to comparison with air temperature for the 2015/2016 winter season, but will be extended with results from Sentinel-3 when these become available for the 2016-2017 winter season.

Norway

In the following, validation against weather stations for a time series of multi-sensor wet snow (MWS) products for southern Norway is shown for the winter season 2016. Nine weather stations operated by the Norwegian Meteorological Institute (MET Norway) have been used in this study. The stations' locations and names are indicated in Figure 4.3.2.

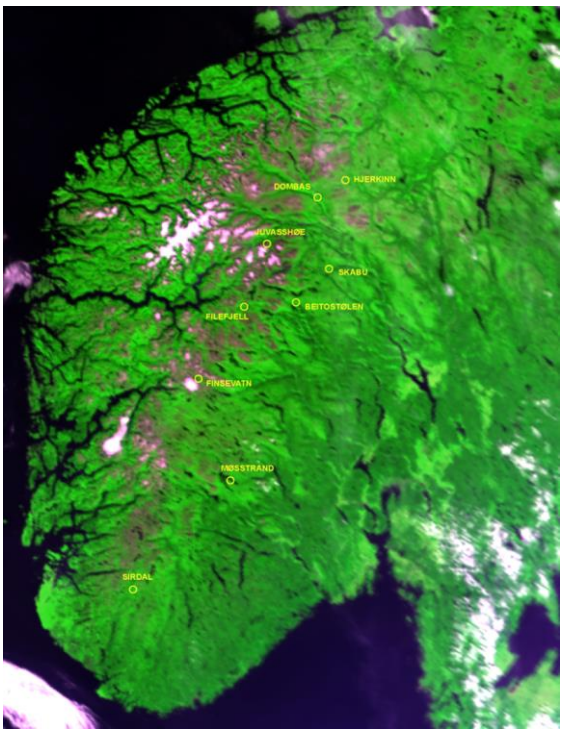

Figure 4.3.2: The locations of the weather stations (circles) applied. The background image is acquired by MODIS.

Table 4.3.1 provides the weather stations' daily mean temperatures for the days of satellite data acquisitions.

Table 4.3.1: Mean daily temperatures (in degrees Celsius) for the MET Norway weather stations applied in this study.

Date	Beitostølen	Dombås	Filefjell	Finse	Hjerkinn	Juvasshøe	Møsstrand	Sirdal	Skåbu
25 February	-4.7	-2.7	-4.5	-7.2	-4.8	-10.7	-6.8	-10.8	-4.7
15 March	4.1	1.9	2.6	2.8	2.8	4.9	1.7	2.3	4.5
6 May	4.7	7.8	4.1	2.2	4.9	-0.8	4.2	8.6	5.4
11 May	6.1	8.8	5.2	3.4	6.7	3.2	5.8	11.1	6.7
20 May	4.1	7.1	3.9	2.0	4.0	-1.5	3.9	7.0	4.4
24 May	5.8	6.6	6.2	3.9	3.4	-1.3	6.9	11.0	5.5

Winter 2015/16 progressed about normally with respect to temperatures, but with less snow precipitation in the southeast. The south west, dominated by the prevailing wind systems and precipitation from west, resulted in significant amounts of snow. There were a few mild events through the winter, with one strong event 14–17 March. April was rather cold in general, and the spring entered in the beginning of May with rapid snowmelt after the first week of May.
The MWS map for 25 February (Figure 4.3.3, left) shows typical winter snow conditions with no wet snow at all in the entire southern Norway. It can be seen that there is not full snow cover above the treeline in the northern part of the mountains, reflecting conditions of less than usual snow cover in parts of southern Norway. All the weather stations show temperatures substantially below freezing point this day (-2.7 – -10.8°C), confirming that dry snow should be expected everywhere.

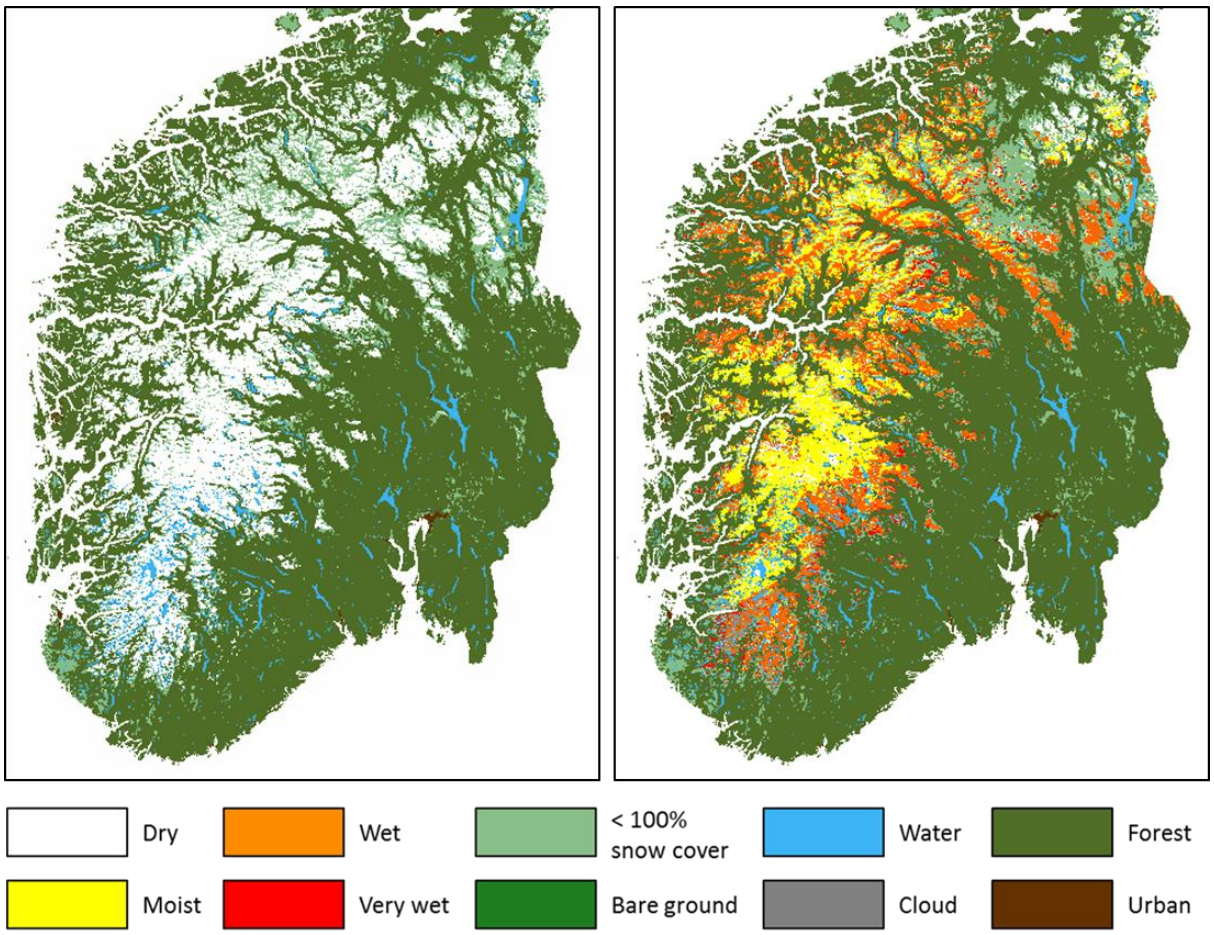

Figure 4.3.3: MWS maps for southern Norway based on Terra MODIS and Sentinel-1 for 25 February and 15 March 2016.

The MWS map for 15 March (Figure 4.3.3, right) shows an event of mild air covering the entire southern Norway. According to the map, the snow is wettest in the south-eastern part of the mountains and the lowland mountains along the west coast. In the south, at Hardangervidda, wet snow stretches high up covering all the southern part of the mountain plateau. The rest of the high mountains show moist snow. All the weather stations show temperatures above zero. The situation is not adiabatic, with some high-mountain regions having relatively high temperatures. Beitostølen and Skåbu show higher temperatures than stations higher up in the same region of Norway, confirming wet snow at lower mountain altitudes and moist snow at the higher.

The MWS map for 6 May (Figure 4.3.4, left) shows an early stage of the rather intensive spring melt building up. Only very high mountain areas, including the large glaciers, are shown as dry snow in the map. The melting intensity relates well to altitude in general, but is more intensive in the southern part of Hardangervidda where significant areas have very wet snow. The weather stations show a quite adiabatic situation. The only station with temperatures below zero is Juvasshøe (1844 m.a.s.l.). The snow map agrees that the highest mountains in this area have dry snow. Sirdal is showing the highest temperature (8.6°C), which agrees very well with the intensive melting (very wet snow) in the southern part of Hardangervidda. The mountain station Finse shows a moderate positive temperature (2.2°C), agreeing well with moist snow on the map.

The MWS map for 11 May (Figure 4.3.4, right) shows a situation with very intensive melting in the mountains from low to high altitudes. Only a few mountain regions in the north show moist snow. The situation seems to be adiabatic in general with the lowest mountain regions showing very wet snow, while the highest are wet. All stations are showing rather high temperatures (3.2 – 11.1°C). The highest stations (Juvasshø, Finse, Filefjell and Hjerkinn) are showing lowest temperatures (3.2 – 6.7°C), while the lowest stations (Dombås and Sirdal) are showing the highest temperatures (6.6 – 11.1°C).

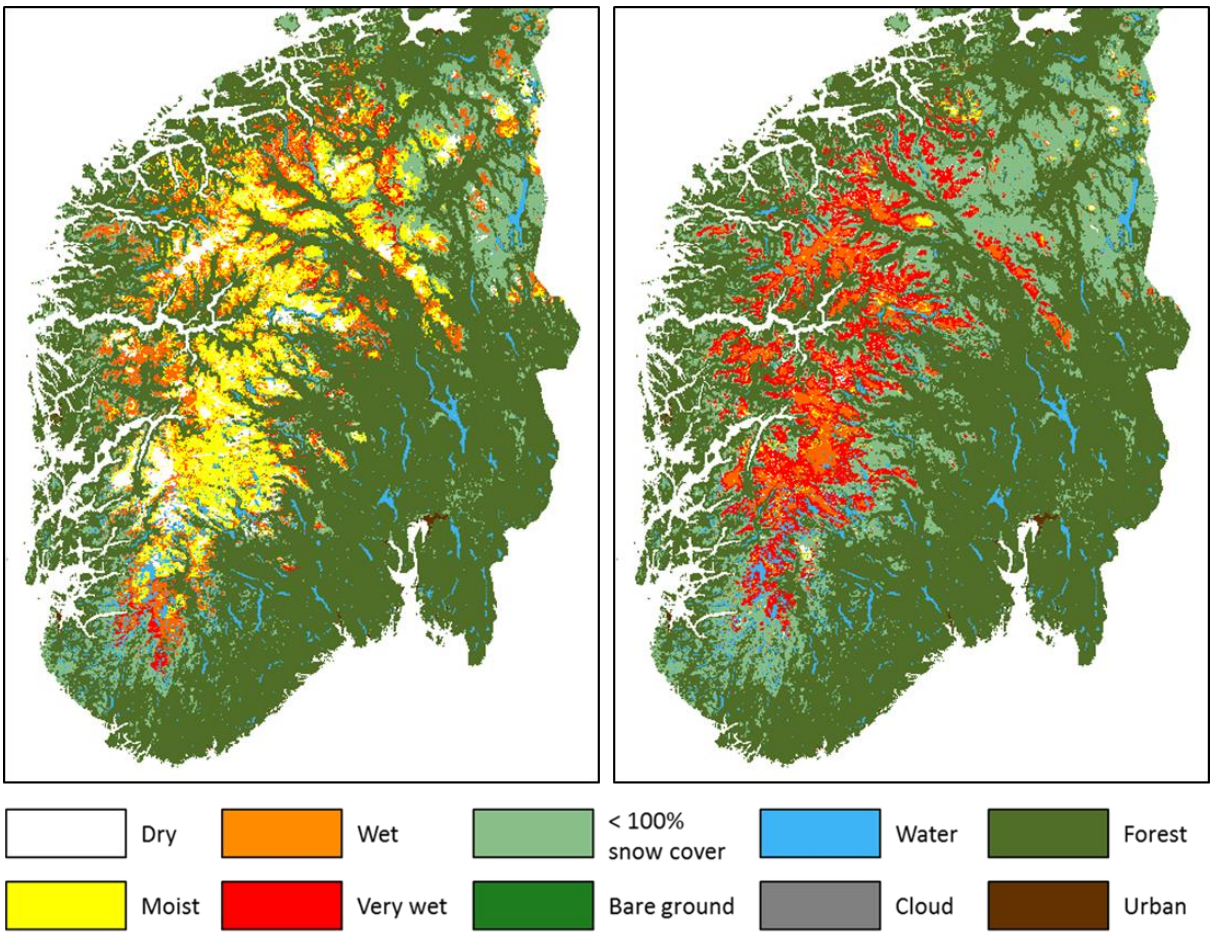

Figure 4.3.4: MWS maps for southern Norway based on Terra MODIS and Sentinel-1 for 6 May and 11 May 2016.

The MWS map for 20 May (Figure 4.3.5, left) shows a spring-melt situation which is less intensive than in the previous map. Hardangervidda is still fairly intensive with wet snow rather high up, while mountain regions of similar altitude show moist snow north of Hardangervidda. The glaciers as well as areas of altitude above around 1700–1800 m.a.s.l. are showing dry snow. All the weather stations are showing temperatures above freezing point except for Juvasshøe (-1.5°C). This agrees well with dry snow in the highest regions. The lowest regions show rather high temperatures (7.0 – 7.1°C), agreeing well with wet snow on the maps in these regions. Other high mountain stations (Finse, Filefjell and Hjerkinn) show positive, but moderate temperatures (2.0 – 3.9°C), agreeing well with moist snow and nearby transitions to wet snow in these regions.
The MWS map for 24 May (Figure 4.3.5, right) shows a situation with very intensive melting, even higher up in the southern part of the mountains with extensive areas of very wet snow. There is clearly a reduced area of full snow cover than in the map of 11 May. The northern part is somewhat less intensive with larger areas of wet snow. There is moist snow only a few places, all in the north, and shown most prominently on Jostedalsbreen (the largest glacier in mainland Norway). All weather station temperatures are above zero except for Juvasshøe (-1.3°C). The Juvasshø area is on the map shown as wet, with a few exceptions of moist and dry (the dry is one grid cell corresponding to the mountain peak Galdhøpiggen). The terrain relief is steep in this region, so a 1 km grid cell would easily be a mixture of at least two snow wetness categories if they follow the elevation zones, which might explain that most of the area is shown as wet. The highest stations – except for Juvasshøe – (Finse, Filefjell and Hjerkinn) are showing lowest positive temperatures (3.9 – 6.2°C), while the lowest stations (Dombås and Sirdal) are showing the highest temperatures (6.6 – 11.0°C). The south-north gradient is also pronounced in the temperature data with lower temperatures in the north, very well agreeing with the snow map.

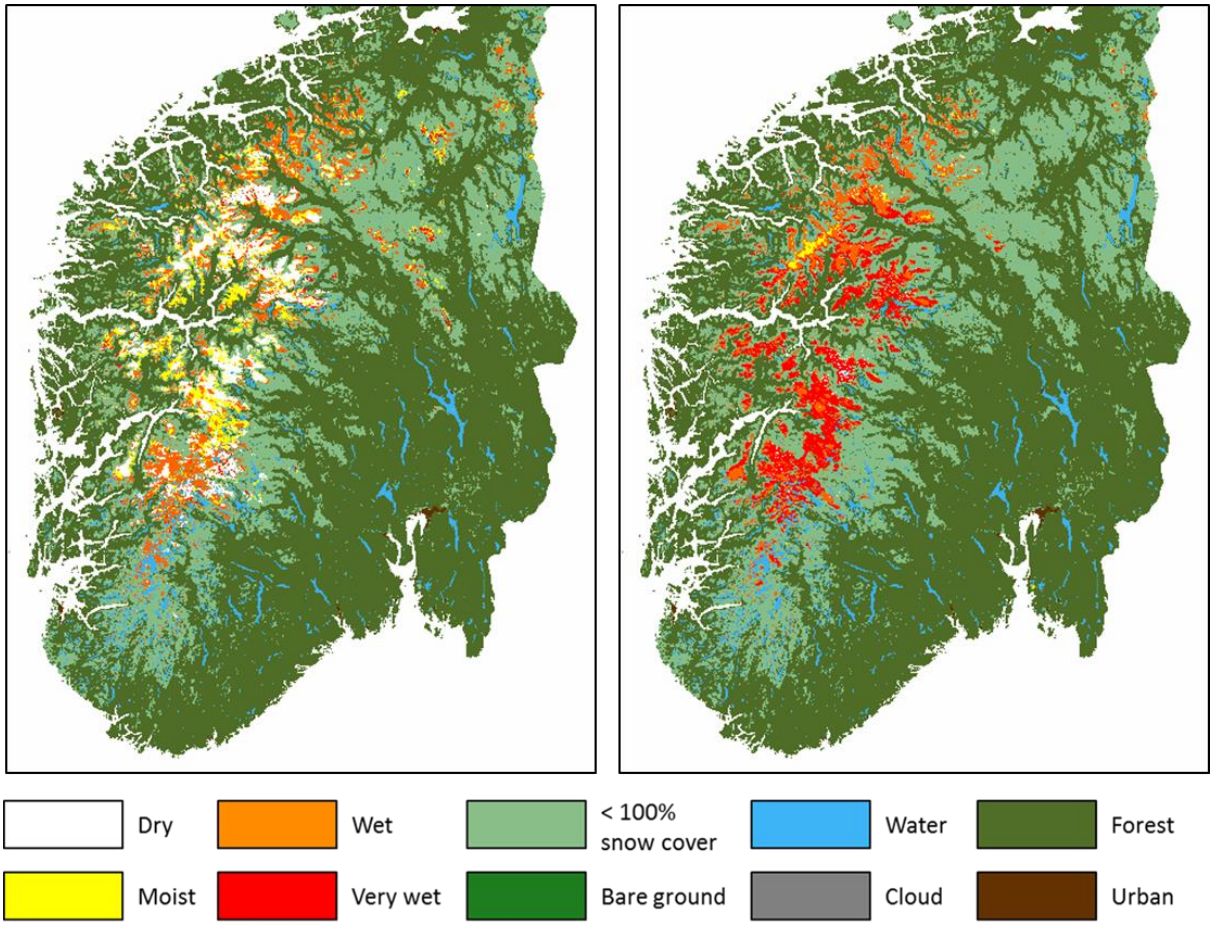

Figure 4.3.5: MWS maps for southern Norway based on Terra MODIS and Sentinel-1 for 20 May and 24 May 2016.

Romania

The validation analysis of multi-sensor wet snow (MWS) products for Romania for the winter season 2015 – 2016 is presented below. The measurements of air temperature, snow cover and snow depth recorded at national weather stations have been used in this study. The stations' locations and names are indicated in Figure 4.3.6.

Figure 4.3.6: Romanian weather stations network.

Below are presented examples for Romania, based on MWS products obtained from Sentinel-3 SLSTR and Sentinel-1 data.

First example is from early winter season (Figure 4.3.7). The warm winter is highlighted by the reduced snowfall and reduces snow layer. Only at the high altitude (over 2000 m.a.s.l.) is a very low snow layer (less than 15 cm). The only exceptions are registered at Balea Lac (snow depth = 68 cm) and Vf. Omu (snow depth = 100 cm); the explanations are related to the orographic conditions of the two weather stations: Balea Lac is in a glacier caldera and on the North slope of Fagaras Mountains, and Vf. Omu is at very high altitude at 2500 m.a.s.l. The air temperature profiles, for the mention weather stations, are positive most of the day. It means that the very vet snow seen on the MWS map is correct classified.

The second example is from end of January, second melting period (Figure 4.3.8). The warm air advection in the Southern Romania determines the snow melting, seen on the MWS map as moist, wet and very wet snow. The most intense areas with snow melting are recored next to the Carpathian Curvature (known as area with most intense foehn wind in Romania), at the Black Sea coastal area under the sea breeze influence and in the South-West region along the Danube River low lands.

The moist and wet snow recorded in the central part of the country is determined by the foehn wind on the Northern slope of Fagaras Mountains (low lands). The cold air advection in the North-West determines the dry snow in that area.

The MWS classification is very well correlated with the temperature profiles of the day.

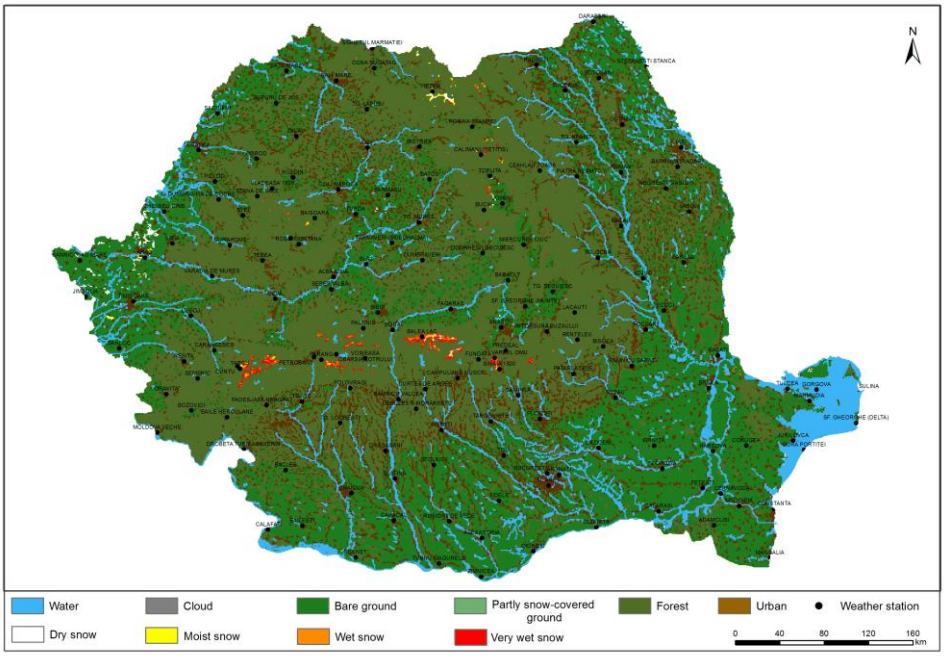

Figure 4.3.7: MWS map for Romania based on Terra MODIS and Sentinel-1 for 24 December 2015.

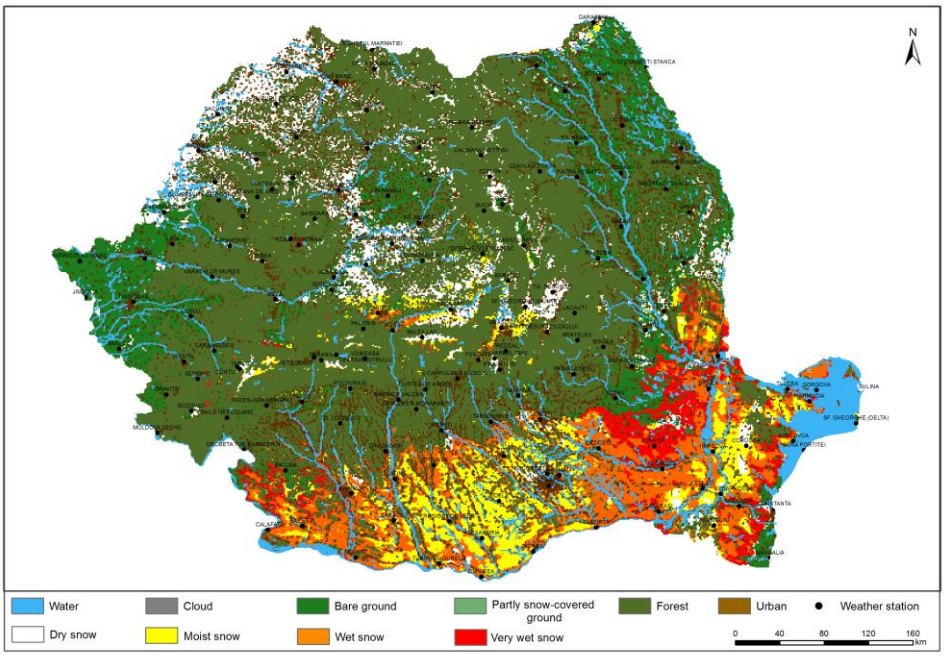

Figure 4.3.8: MWS map for Romania based on Terra MODIS and Sentinel-1 for 28 January 2016.

The last example is from 27th of April 2016 (Figgure 4.3.9). The snow layer is present only at the highest altutides (above 2000 m.a.s.l.): Balea Lac = 87 cm, Vf. Omu = 147 cm, Tarcu =45, Cuntu = 3 cm, Parang = 5 cm, Iezer = 3 cm. The positive air temperature during the day time determines the snow melting, as seen on the MWS map. The anomalies are in the Western regions of the country where the dry snow is present on the MWS map, while the weather stations recorded no snow cover. This situation can be determined by the noise of SAR data in agricultural areas. This problem is well-known problem in the snow SAR community, but not fully understood. Ploughed fields give high backscatter signals when the ground is wet, which can be the case when a wet soil exists under a layer of dry snow. In some situations agriculture fields, during summer, can give erroneous, false

snow cover. So, the problem is more complex and probably related to the use of reference data in the algorithms that might result from a mixture of soil tillage in the reference data giving significant variation in the backscatter properties of some agricultural fields.

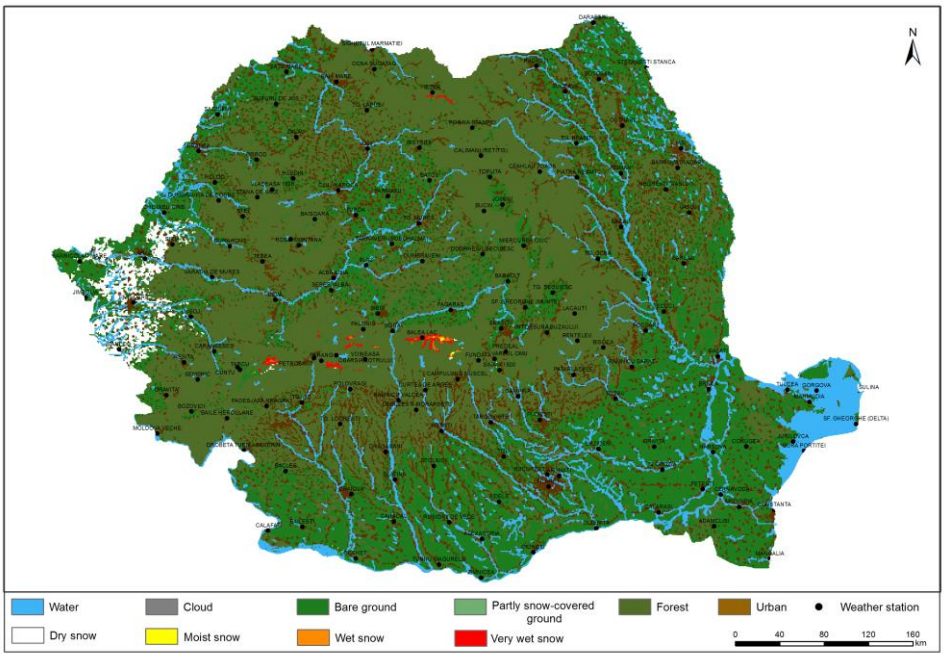

Figure 4.3.9: MWS map for Romania based on Terra MODIS and Sentinel-1 for 27 April 2016.

More details are presented in the deliverable D3.4: „MWS prototype products for flood and avalanche warnings – Version 2".

*4.3.2. **Activity 3.3.** New multilayer snow model module in NOAH*

During this phase, was implemented the first version of the methodology for estimating the snow water equivalent, by data fusion approach, using the distributed model NOAH simulations, ground observations and satellite products (was elaborated the **deliverable D3.6**.).
The main parameters of the snow layer (snow layer depth, water equivalent) have a particularly high spatial and temporal variability, which generate a very high degree of uncertainty in estimating these parameters at river basin level using only observations from the national monitoring networks, especially in the mountain region.
The observations on snow covered area can be obtained in general from direct measurements at ground level or by remote sensing / satellite products.
The proposed data fusion procedure, for estimating the water equivalent in the snow layer, uses the main following type of input data:

- snow water equivalent simulations performed with a distributed hydrological model;
- observations of the snow layer from the national monitoring networks;
- satellite products for the snow cover extent.

Given the relatively high degree of uncertainty associated with different categories of input data within the methodology, both at the level of the measured values at stations as well as at the values simulated with the distributed hydrological model, and the satellite snow extent products, for the implementation of the main processing steps, we used methods based on fuzzy logic systems, and the overall processing stage use a cellular automata approach with variable neighbourhood and possibility to work in cellular spaces with different spatial resolutions.
Within the data fusion process, the different type of data and information are analysed and compared, using a series of automatic cross-validation algorithms, and then the snow water equivalent is estimated in grid format, at spatial resolution of 1 km, by multiple successive steps of

interpolations and adjustments, depending on the degree of uncertainty associated with different type of data.

The implementation of the methodology was done based on the following general design principles:

- Adaptive – use all the data available in real-time, from different sources, adapting the processing workflow in function of data availability;
- Automated procedure, non-interactive, operational ready, daily run.
- Modular and multistep approach, with a flexible workflow.
- Specific adequate processing approach, taking into account the relative high uncertainty associated with all the type of input data (approach based on a combination of Cellular Automata and Fuzzy Logic System)

The data fusion method use the following input data, with national coverage:

- Model simulation, grid format (1 km spatial resolution), from the new multilayer snow distributed model.
- Station observations: snow depth, snow water equivalent, snow density (with different frequency: daily, every 5 days), 24 hours precipitation, mean, minimum and maximum daily air temperature.
- Satellite product with snow cover extent.

The software implementation was also done using a modular approach, flexible and easy adapted configuration, based on the following stable open source components:

- Use Java and R custom program mainly for data interfaces with existing systems.
- Use R and TerraME (http://www.terrame.org/doku.php) custom scripts for main processing and data analysing steps.
- Use OddJob (http://rgordon.co.uk/oddjob/index.html) scheduler for processing workflow control.

The data fusion computation follows the main processing steps:

- Automatic quality check of all the input data.
    - Point observation and grid cell values (model simulation or satellite products).
    - As output of this step, all the available data are categorized on 3 classes, based on their estimated quality (very good, good, acceptable), and all the observation not passing the tests are set to missing.
    - The snow satellite products, 24 hours precipitation and air temperature data are used as input data for quality check of station data and model simulation.
    - The quality check algorithm analyse/check not only the last values but also the variation from the previous estimation (previous day).
    - For each cell a history/time series data is stored in a local database, to be used in a second phase, to further improve the quality checks algorithms.
- First general data fusion processing step – objective: establish/determine the most probable value for each cells
    - Analyse the cells with at least one data source in the category “very good”, and compute for each cell the most probable value.
    - Interpolate the values using the values from the first class of cells.
    - Validate and adjust the interpolation results using the cells with at least one data source in the category “good”, and the other data source values in the same category, “acceptable” category or missing.
    - Validate and adjust the interpolation results using the cells with at least one data source in the category “acceptable”, and the other data source values in the same category or missing.
- Second general data fusion processing step – objective: final determination of the cells without snow (SWE = 0), using satellite snow cover extent product and station data, as a final adjustment of the interpolated field.

Details can be found in deliverable D3.6. “Gridded SWE prototype products generated using data fusion methodology – Version 1”.

4.4. WP4 *Climate change impact on snow-related hazards*

4.4.1. Activity 4.1. Snow-related climate variability and change and associated impact

In the framework of Activity 4.1 the impact of reductions in snow cover depth on ski conditions in the Romanian Carpathians have been analyzed. The number of days with good ski conditions in a season is decreasing in the Carpathians under climate change (Figure 4.4.1).

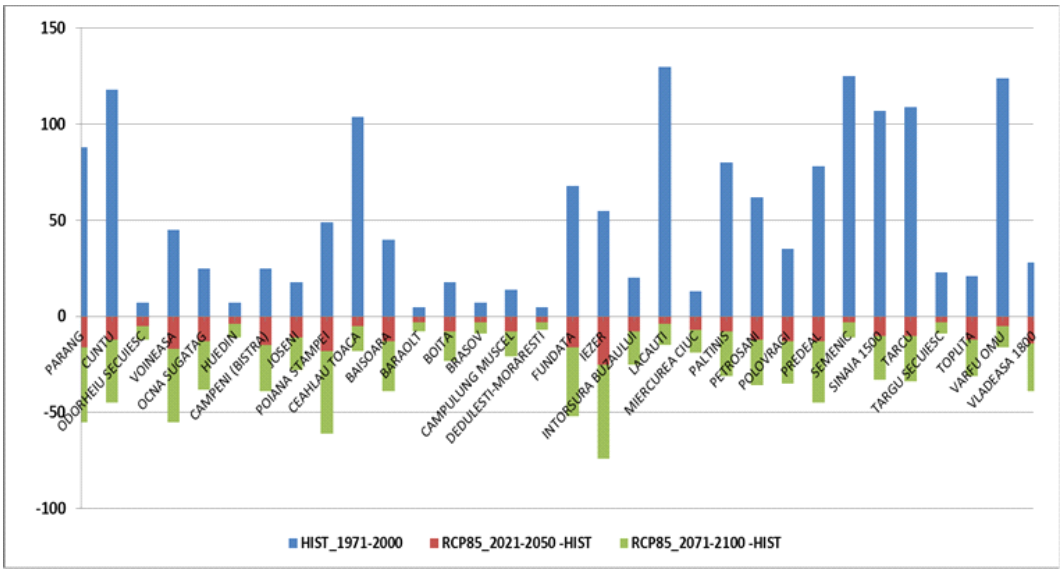

Figure 4.4.1: Mean number of days in a ski season with ski conditions (i.e. snow depth larger than 30 cm) at 32 Romanian mountain stations, in the interval 1971-2001 (blue) and changes under RCP 8.5 scenario for periods 2022-2050 (red) and 2072-2100 (green) based on bias-corrected outputs of 5 RCM models.

4.4.2. Activity 4.2. Variability and change in flash floods with snow melt contribution

The reserch regarding the variability and change in flash floods with snow melt contribution, considered the application of the hydrologic modelling to the sub-basins corresponding to the rivers Argeş (up to the hydrometric station Cătеasca) and Dâmboviţa (left tributary of the Argeş River, up to the hydrometric station Lunguleţu), located mainly in mountain areas; this activity succeded to add more local details about the maximum discharge and flood statistics there. The results of the hydrologic model (CONSUL) indicate that multiannual averages of maximum discharges during the interval from November to April show increases compared with present climate (1981-2010) under best (RCP 2.6) and worst (RCP 8.5) climate change scenarios. For sub-basins with larger areas, the increases are systematically larger under the worst scenario compared to those under the best one showing how the climate change signal overcome the noise beyond specific spatial scales of river basins.

4.4.3. Activity 4.3. Variability and change in avalanche statistics

In order to analyze the variability and change in avalanche statistics we have firstly identified the climate conditions for avalanches in the Carpathians. First avalanche recorded in the Romanian Carpathians occurred in April 1704 in the Ceahlău massif and stroked Sihăstria monastery killing twenty monks (Bălan, 2001). Historically, a number of 845 avalanche cases have been recorded by now, in all massifs of Romanian Carpathians. Figure 4.4.2 reveals that most of the avalanches happened during March (27 %), April (20.3 %) and February (17.1 %), and very few in June (0.7 %) and September (0.1 %).

The statistics of avalanche cases in Romanian Carpathians was based on data provide by the National Meteorological Administration program for snow and avalanches, by the Mountain Rescue Teams, from various articles, works, media and even literature (Bilanţul nivologic al sezonului de iarnă, 2004-

2016; http://www.dinumititeanu.blogopedia; Gaspar and Munteanu, 1968; Milian N. et al., 2010; Milian and Stăncescu, 2012; Moţoiu, 2008). Synoptic conditions for each avalanche day were analyzed using surface pressure, geopotential at the 500 hPa level, temperature and wind at the 850 hPa level from the NCEP/NCAR Reanalysis (www.wetter3.de/archive). This kind of approaches has been used by several Avalanche Services worldwide (Fitzharris, 1987; Hansen and Underwood, 2012; Höller, 2009).

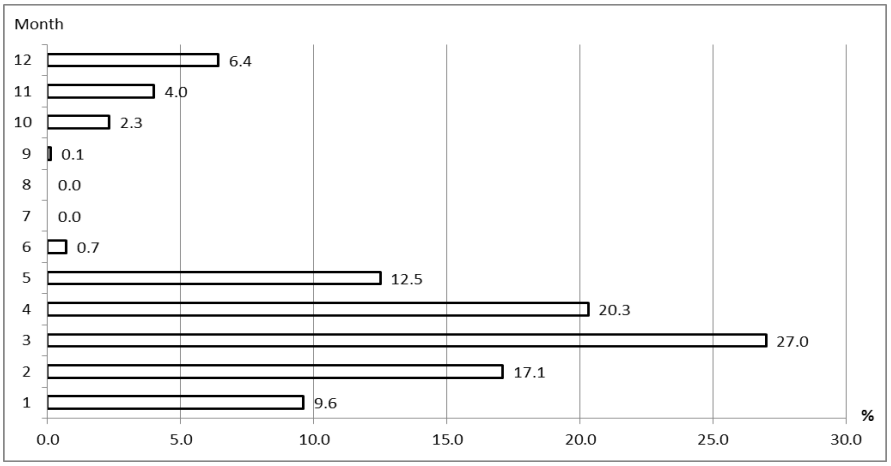

Figure 4.4.2: Avalanche cases by month.

From the standpoint of pressure systems that influenced Romania during the days with avalanches, one could identify 35.9% of cases with associated ridges from Azores or East-European High. As for surface pressure criterion, 39.4% of avalanches occurred on high pressure conditions (above 1020 mb), from which 6.9% under pressure greater than 1030 mb. For 25.2% cases, surface pressure values were between 1015 to 1020 mb, 17.1% cases were between 1010 and 1015 mb and 18.3% cases were lower than 1010 mb (Figure 4.4.3).

From the standpoint of the 850 hPa level isotherm, most frequent avalanches cases had associated values for of 1 to 5 degrees (23.6%) and 5 to 10 degrees (22.9%). 46.5% of cases were related to warming weather episodes (850 hPa isotherm between +2°C and +10°C) and 45.1% for temperatures between -10°C to +1°C, when most snowfalls are taking place (Figure 4.4.3). As for the geopotential pattern, 43.0% of the avalanche cases happened under troughs, 25.5% under ridges, 17.2% under other configurations. A percent of 10.6% from the avalanches cases were under westerly flows and 3.5% of them in the presence of *in nuce* or well-developed cut-off structures (Figure 4.4.3).

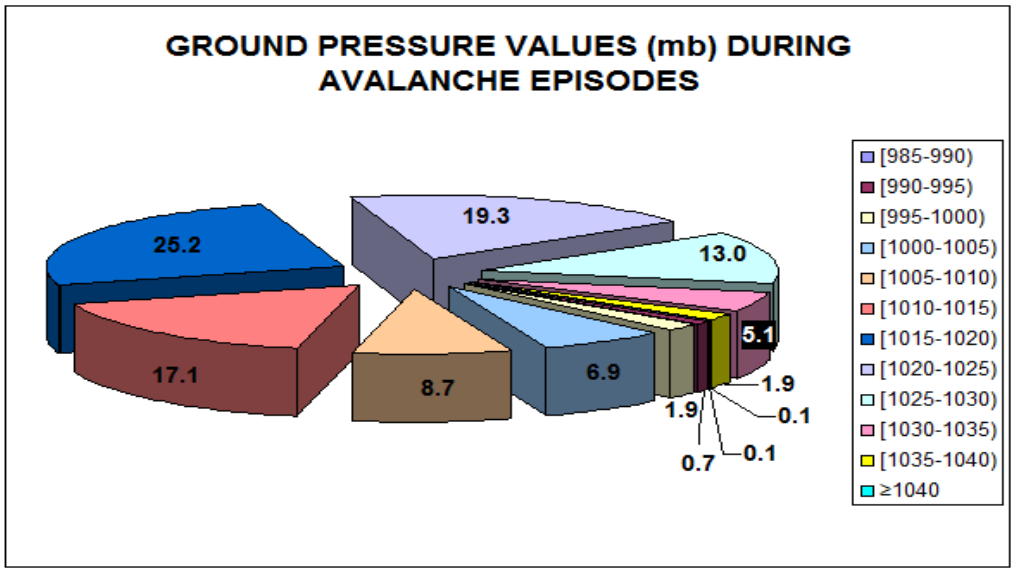

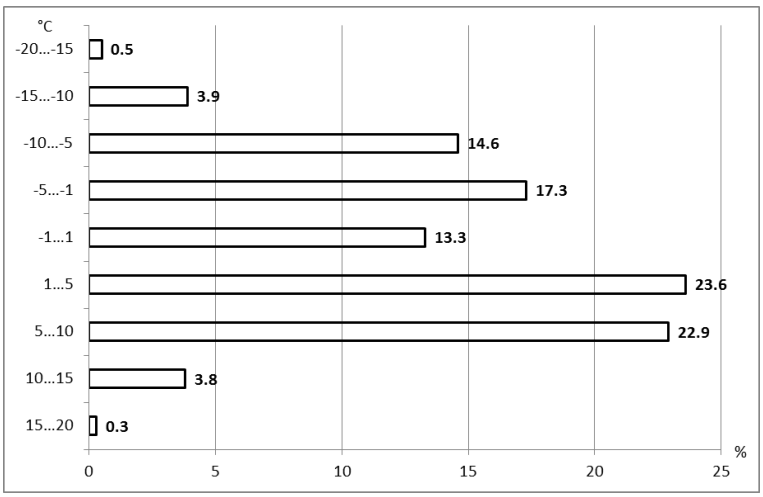

Figure 4.4.3: Avalanche cases by sea-level pressure values (top) and 850 hPa level temperatures (down).

The wind direction at the 500 hPa level was from the North in 7% of the avalanche cases. In 2% of them, the wind blew from the North-East and 2% of situations were characterized by easterly winds. In 4% of avalanche cases the wind direction was from the South-East and 6% of avalanche-related winds were southerlies. In 34% of avalanche cases the wind blew from the South-West. The winds were westerlies in 23% of cases and in 20% of them the wind direction was from the North-West. It can be easily seen that most of avalanches happened while high altitude flow was mainly from the West (South-West to North-West directions cover 67% of avalanche cases), all other direction being relatively poor represented. South-West flows are often associated with warming episodes and strong winds (Paşol et al., 2017) – (Figure 4.4.4).

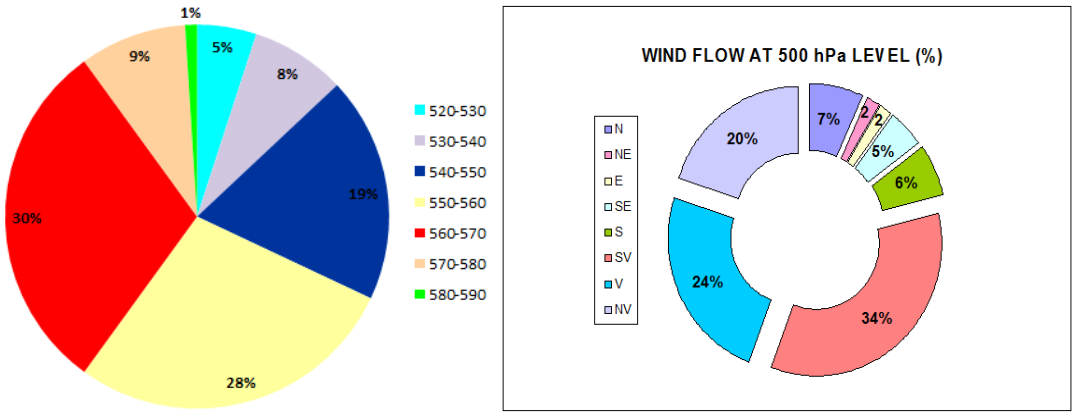

Figure 4.4.4: Avalanche cases by 500 hPa geopotential (left) and flow(right).

One could consider that avalanches occur under very different synoptic conditions, in all the Romanian Carpathians and during the whole cold season. However, they are significantly more frequent during the interval February-April, under westerly flows associated with warming episodes if the preexisting snow cover is consistent.

In order to build a statistical model, we computed the composite maps for large scale variables for the days with episodes of avalanches using monthly stratified data. We used the NCEP/NCAR Reanalysis covering the time interval from January 1948 up to present. We selected as large scale variables daily geopotential heights at 500 hPa (e.g. figure 4.4.5 and 4.4.6), daily sea level pressure, daily temperature at 850 hPa and daily zonal wind component at 300 hPa.

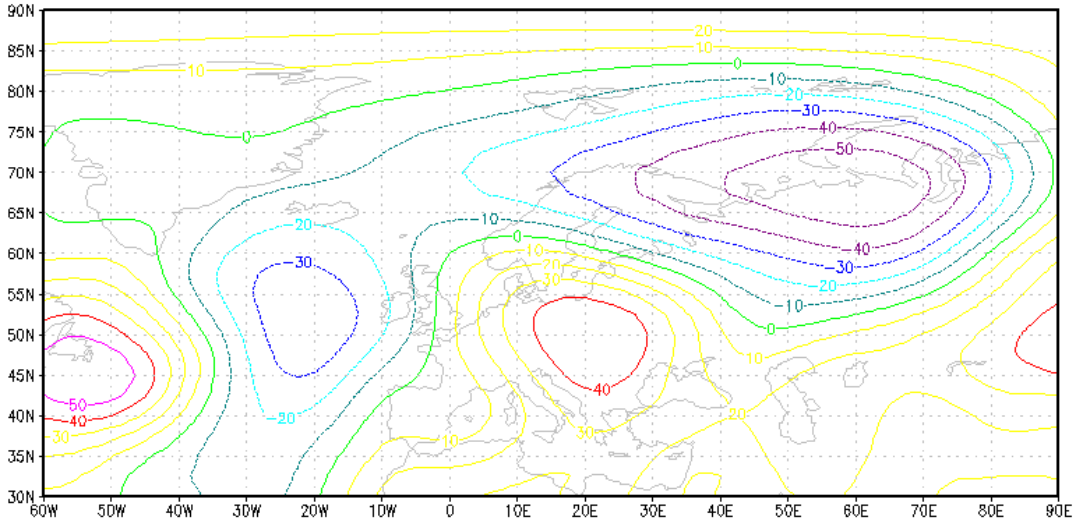

Figure 4.4.5: Composite map of geopotential heights at 500 hPa (in gpm) for days with avalanches in April in Fagaras Mountains. Geopotential data are from the NCEP/NCAR Reanalysis.

Composite maps suggest the approach of multifield analog prediction method (Barnett and Preisendorfer, 1978). We selected the month of April, with a large number of avalanches, to build and test the model. The components of the large scale climate vector are the standardized anomalies of geopotential heights at 500 hPa, temperature at 850 hPa, sea level pressure and zonal wind at 300 hPa for the Atlantic European sector (e.g. Figure 4.4.5 and 4.4.6).

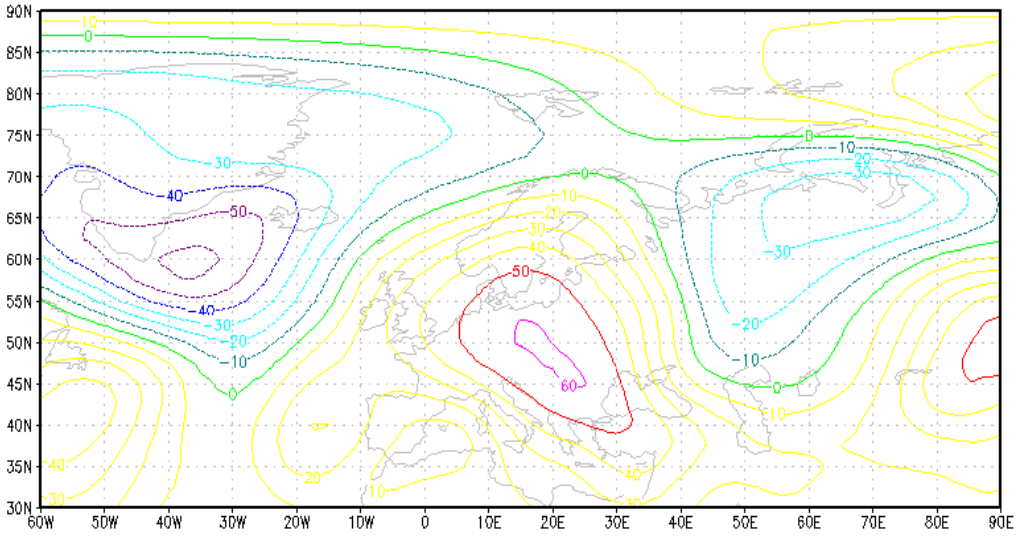

Figure 4.4.6: Composite map of geopotential heights at 500 hPa (in gpm) for days with avalanches in April in Bucegi Mountains. Geopotential data are from the NCEP/NCAR Reanalysis.

The standardized anomalies are computed by averaging the values over significant areas from the composite maps associated to the specific month (in our case, March and April). The components of the local scale vector are the snow depth and air temperature averaged over Fagars Masiff for locations above 1800 m. Local data are derived from the high resolution data sets (1 km x 1 km). Daily data available for the study are from 2000 up to 2016. In order to predict the events, we use the Euclidean distance between the past events and the actual conditions, in the hyperspace defined by the first 4 empirical orthogonal function (EOFs) modes. However, the states associated with avalanche events do not significantly cluster themselves, so the skill of the model is not high.
More details are presented in the deliverable D4.3: „Empirical model linking avalanche frequency and atmospheric conditions".

4.5. WP5 *Aquifer replenishment modelling from snowmelt infiltration*

4.5.1. Activity 5.1. Snowmelt infiltration assessment for the unsaturated zone

The assessment of rainfall recharge was done for three study areas: **(1) Bolboci study area - Omu Peak (upper basin of Ialomita Valley):**From a geomorphologic point of view the study area belongs to Bucegi Mountains and to Leaota Mountains. The accumulation and flow of groundwater is also favored by the existence of a well-developed fracture system. The area of Bucegi Mountains is characterized by a good regime of precipitation, both liquid and solid which favors the aquifers recharge. **(2) Prahovova-Teleajen alluvial cone study area.**We find developed a complex structure, consisting of two overlapping and independent aquifer complexes:(a) the confined complex (the lower one), included in Cândesti strata; (b) the unconfined complex (the upper one) included in the alluvial deposits. Afeter analyzing and interpreting the state network borehole data it resulted that the aquifer system that develops between the Prahova River and the Teleajen River presents a complex structure both from a lithological point of view and from a hydrodynamic point of view.**(3) Colentina area, Bucharest city.** This area was study because it has three essential characteristics: there is a sedimentary aquifer in this area, the area is an urban area and it is hydrogeologicallycharacterized. In Colentina area there is an experimental hydrogeological monitoring site consisting of five hydrogeological wells up to 25 m and a geophysical survey well up to a depth of 60 m. The studied formations from this area are Colentina and Mosiştea aquifer formations.

4.5.2. Activity 5.2. Aquifer modelling

The Aquifer Shaping activity together with the ***Assessment of the infiltration of snow melting in the unsaturated area*** were the basis for accomplishing the main delivery task of work package 5. Delivery task D5.2. Aquifers act as natural reservoirs which can be used as drinking or/and irrigation water supply. The estimation of snow melt is also extremely important for flood forecasting, for hydrological modeling of river basin processes (surface runoff, overexploitation, sediment transport, nutrient transport, depth of frozen soil), for general design projects (highways, footbridges, sewer systems, etc.) and for projects regarding safety and recreational activties (avalanche warnings, ski and road conditions),(Voight, S., 2003).

The physical processes occurring in the snow layer and snow melt are extremely complex, involving mass and energy balances, as well as heat and mass transport.When daytime temperatures are high enough, the snow melting process starts. At first, the soil absorbs water and allows a slow infiltration. Smaller nocturnal temperatures interrupt the snow melting processand the recharge from the snow layer, but the flow in the unsaturated zone continues throughout the night.

Two approaches are used to quantify the melting phenomenon of snow (USDA, 2004):

- Empiric - using temperature index models with a limited number of parameters. The most common method in this approach is the "day - to - day" method, where air temperature is used to index all energy flows.
- Physics-based process, which requires a more detailed description of the mass equilibrum or energy balance.

Temperature-index methods are commonly used, under the assumption that process-based models require too much input.To test this, we used a process-based physical model to simulate snow melting using air temperature, relative air humidity, wind speed and nebulosity as input data.To estimate the snow melt infiltration, you can use Hydrus 1D program, which is based on the finite element method.Hydrus does not work with the thickness of the snow layer but with the equivalent of snow water (SWE).In order to assess the accumulation of the snow layer it is necessary to introduce as input data the air temperature, considering the upper limit condition the atmosferic data. The Hydrus program used to estimate the snow layer's evolution uses the flow modulus that solves the Richards equation for water flow in saturated and unsaturated zones and the heat transfer module by solving the convection-dispersion equation.

If the direct problem is a simulation model in which the hydraulic loads are calculated, the inverse problem is to determine the soil parameters for which the modeling error between the calculated and the observed values is minimal. MVG Mualem-van Genuchten model (1980), which implements Van Genuchten's functions using the Mualem model pore size distribution (Mualem, Y., 1976), was used for the case study.
Due to the nonlinearity of the flow equation in the unsaturated zone, the estimation of the parameters is quite difficult.
For determining the parameters, the inverse problem combines the numerical solution of the flow equation with optimization techniques.The Hydrus program (Šimůnek, J., M. Šejna, and van Genuchten, M. Th., 1998) uses the Gauss-Levenberg-Marquardt method to solve the inverse problem.
Also, the Hydrus program uses the Rosetta sub-program that estimates the parameters of the Mualem-van Genuchtenpe model based on pedotransfer functions using artificial neural networks, calibrating the parameters for each horizon.
The modeling of the snow melting recharge is based on three stages:

1. Local snow melting modelfor wet snow and / or forest conditions using METZ.
2. Local snow infiltration for wet snowand / or forest conditions using Hydrus.

Extrapolating the results obtained for the studied area using satellite data.

More details are presented in the deliverable D5.2: „Snowmelt infiltration methodology: The innovative aspect of the new methodology is the integration of measured data from the field test with remote sensing and meteorological data. The methodology will be tailored on the hydrogeological and climatological conditions".

4.5.3. Activity 5.3. Pattern matching and climate scenarios

Under activity 5.3. the effects of climate change on water resources, especially the snow melt infiltration, have been analyzed. According to the 4th Global Intergovernmental Panel on Climate Change (IPCC-AR4) Global Climate Change Assessment Report (IPCC-AR4, 2007), the increase in atmospheric temperature has been increasing in the last few centuries, and since the pre-industrial period, Earth's atmosphere has warmed by about 0.76 C and a continuation of this phenomenon is predicted to be exceeded even by 1.8 °C - 4°C until the end of this century. Due to industrial development and massive deforestation, GHG concentration in the atmosphere has increased causing global warming with damaging effects on life. Increasing GHG concentrations in the atmosphere, especially carbon dioxide, has been the main cause of global warming. (Meinshausen, M. et al., 2011)
Observed effects of global warming:

- increased average temperature with significant regional variations: air temperature increase was more pronounced at high latitudes in the Nordic Hemisphere, being faster for regions covered by land than water covered;
- reducing the volume of ice caps and, implicitly, increasing ocean levels;
- modification of the hydrological cycle;
- increasing aridity;
- changes in seasons;
- increased frequency and intensity of extreme climatic phenomena;
- reducing biodiversity;
- decreasing the productivity of all grains at low latitudes;
- increased mortality due to heat waves, floods and droughts.

As regards snow and ice coverage, this has diminished globally due to rising temperatures. Thus at high latitudes and altitudes there is the defrosting of permafrost areas. In many regions, changing precipitation patterns or melting snow and ice alter hydrological systems, affecting water resources in terms of quantity and quality (IPCC-AR5,2014).

As far as Europe is concerned, the average temperature has risen by almost 1° C in the last century, faster than the global average. Rain and snow have grown considerably in northern Europe, while droughts have become more frequent in the southern continent (Busuioc, A. et al., 2012).
For Romania, on the basis of daily snow thickness, cumulated precipitation and average temperatures from 105 meteorological stations in 1961-2010, several significant trends were identified: increasing the number of days with positive temperature, a slight decrease in rainfall, a decrease in snow thickness, a decreasing in snow cover days (Birsan, MV, Dumitrescu, A. 2014). The amount of melted snow increases linearly with the temperature, so diminishing snow-covered surfaces will reduce water availability for irrigation and agriculture. Due to the early melting effect of snow in the low-altitude areas, the contribution of the water from the melting of the snow layer to the soil supply is reduced. In contrast to higher altitudes, there is an increase in snow melt flow rates during spring thaw.

4.6. WP6 Assimilation of snowpack parameters in the National Flood Forecasting and Warning System

*4.6.1. **Activity 6.3.** Implementation of the methodology for data assimilation of snow pack parameters in the main operational hydrological forecasting models*

One of the main application of the improved detailed estimations of the snow water equivalent, is to update this important state parameter in the operational hydrological forecasting models.
During this phase, was implemented the methodology for the snowpack parameter assimilation into the operational hydrological forecasting modelling system: NOAH-R, NWSRFS and ROFFG" (it was elaborated the **deliverable D6.3**.).
The Romanian National Hydrological Forecasting and Modelling System is composed by specialized hydrological modelling modules, adequate for the real-time simulation and forecasting of hydrological processes at different spatial and temporal scales:

- The first main component of this hydrological modelling system is represented by a complete implementation of the National Weather Service River Forecasting System – USA (NWSRFS).
- The second component is the distributed modelling component, which is mainly based on the NOAH-R model.
- The system also includes a Flash-Flood Guidance component, which is an adaptation of the HRC Flash Flood Guidance System used in various regions of the world for operational flash floods warning support.

Taking into account that the gridded SWE product generated using the data fusion approach represent the best estimate of this parameter, using detailed model simulation, satellite products and ground observation, the direct insertion method is used as data assimilation approach. This approach makes the explicit assumption that the models simulations have no supplemental useful information, other than the information used to derive the data fusion product.
The NOAH-R distributed hydrological model simulations is also one of the main input data in the data fusion methodology, so the state SWE parameters in the model are updated based on the adjusted gridded SWE output product, from the data fusion methodology have the same spatial resolution (1Km).
The other two important hydrological forecasting systems (NWSRFS and ROFFG) are using the same conceptual model SNOW-17, for simulating the snowpack evolution.
SNOW-17 is a conceptual model, most important physical processes occurring in the snowpack are explicitly included in the model, but only in a simplified form. This model of accumulation and snowmelt was first described by Anderson in 1973, as one of the modelling component of the River Forecasting System of the US Weather Service.
SNOW-17 model is part of the index-type snow models, using air temperature as sole index to determine and characterize the energy exchange processes that occur at the snow-air interface. In addition to data on air temperature, the only supplementary input data necessary for running the model is the precipitation.
The adjusted gridded SWE product, output from the data fusion methodology, is used to compute the mean SWE for the sub-basins configured within the NWSRFS and respectively ROFFG operational models implementation. Taking into account the uncertainty related to the real time data, the mean sub-basin SWE from the model will be adjusted only if the difference is > 10 %. Using the same gridded SWE product for each basin it is computed also the basin areal snow cover extent (based on the distribution of cells with 0 SWE). Also, the areal snow cover extent will be adjusted only if the difference is > 10 %.
An important aspect to be considered is the fact that in general when the value of the snowpack water equivalent simulated by the SNOW-17 model is modified, the snowpack cover percentage at the level of the river basin need also to be modified accordingly, excepting the situation in which it is maintained at 100%.

It is possible that the snowpack cover percentage at the level of the river basin need to be modified even if the snow water equivalent is close to reality.

This takes into account that there may be variations in the snow depletion curve from one year to another, respectively the fact that the model can use a depletion curve resulting from the calibration process that differs significantly from the particular situation at a given time.

The specific data assimilation processing steps have been implemented using the same main open-source software components, as for the data fusion method: OddJob – process execution control, Java and R languages for custom processing and data transfer.

Starting with the next winter season the data assimilation will be applied in operational mode, using the output from the data fusion methodology.

Detais can be found in deliverable D6.3. “Implementation of the snowpack parameter assimilation into the hydrological forecasting modelling system: NOAH-R, NWSRFS (U.S. National Weather Service River Forecast System) and ROFFG”.

4.7. WP7 Avalanche inventory, release and hazard mapping

4.7.1. Activity 7.2. *Change-detection algorithm for Sentinel-1 and Sentinel-2*

Completion of the avalanche inventory and avalanche typology analysis based on-data derived from satellite and drone based images

În this stage of the project, avalanche mapping has beend extended and the spatial database has been updated using new data from Geo-Eye-1 images that covered the central part of Făgăraș Mts. and based on drone images aquired in April 12, 2016 (Figure 4.7.1).

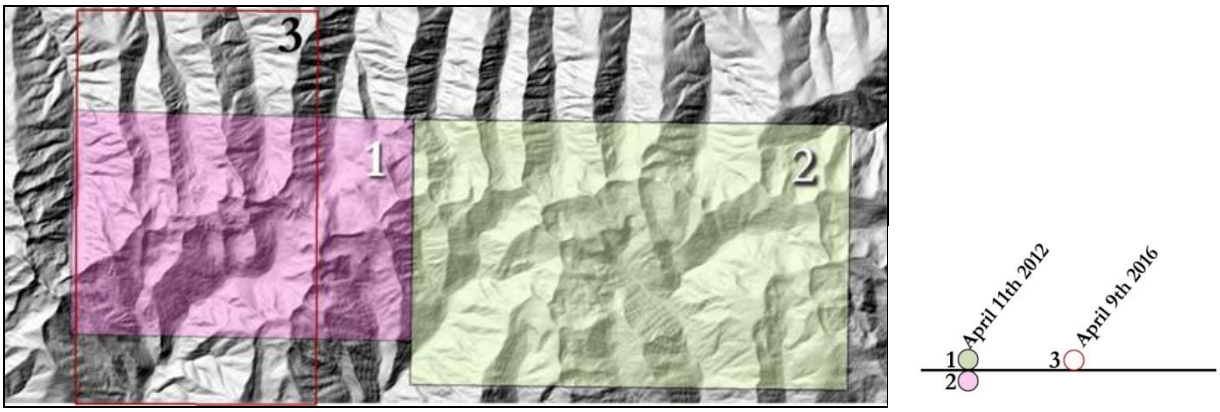

Figure 4.7.1: Coverage of GeoEye-1 scenes (1-2), and aerial image from drone (3) and their aquisition dates.

Avalanche mapping for the central-eastern sector of Făgăraș Mts. based on GeoEye-1

The avalanche identified in the previous stages of the project have been digitized using different band combination or band transformation technique. In the same time several areas with texture similar to avalanche deposits have been identified (Figure 4.7.2). These areas are spatial patterns of snow created by wind or areas with a pattern that might be a result of melting processes, caused by a rain/snow event or by increasing air temperature (Frauenfelder et al., 2015).

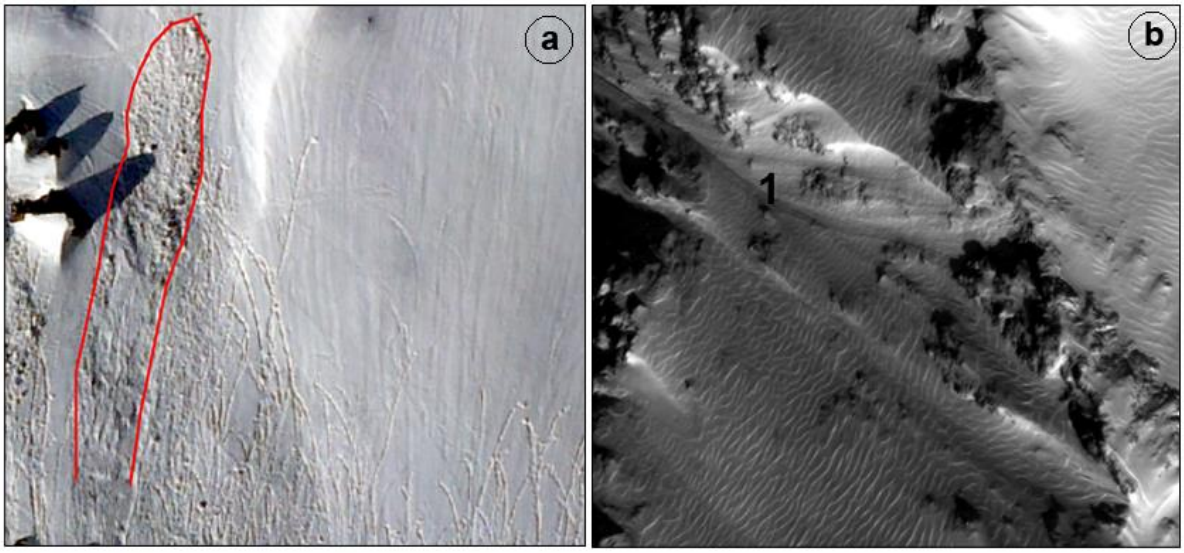

Figure 4.7.2: a) Coarse texture generated by snow patterns and the delineation of an avalanche on a steep slope (red) b) Snow patterns generated by wind that makes almost impossible the delineation of avalanches (1). (pancromatic band of GeoEye-1, at resolution of 0,5 m).

Older avalanches, triggered with 5-6 days before image acquisition have been observed with difficulty. The snow texture in older deposits has no significant contrast with the snow cover due to snow melting, the snowfalls and wind influence (Figure 4.7.3). Only avalanches significantly large as

size have been mapped, when the snow volume has generated a thick deposit that was still visible even in the case of recent snowfalls (Figure 4.7.3).

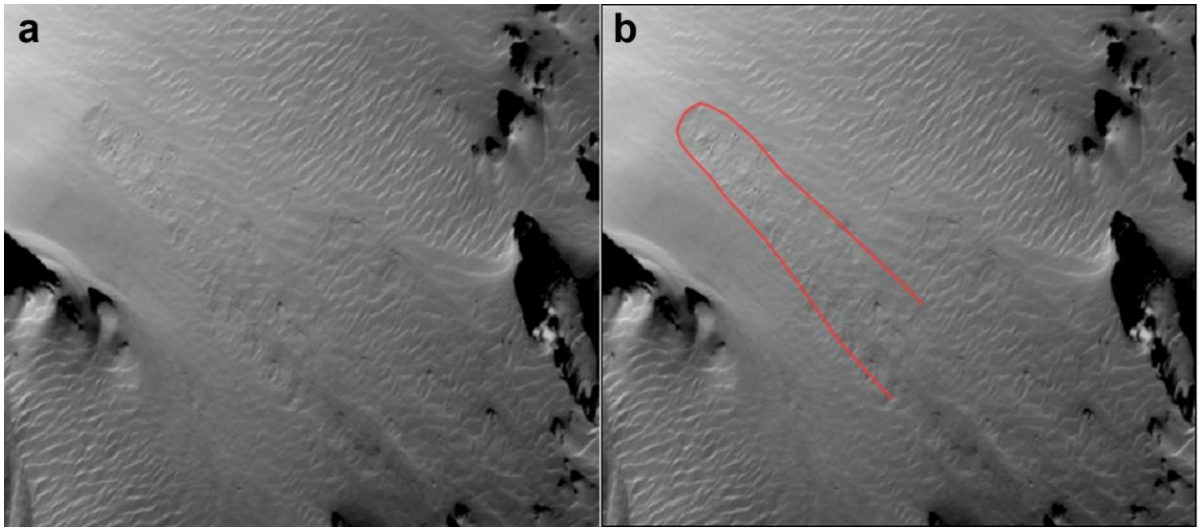

Figure 4.7.3: Old avalanche deposit with low contrast in texture as seen in the pancromatic band (a) and the delineation of avalanche (in red) (b).

In the case of winter images (covered by snow), the spectral bands are highly correlated as compared to summer images. High positive correlations exist between NIR and visible bands (Table 4.7.1). For improvement, we used principal component analysis (PCA), and the first PC is highly correlated with the spectral bands, but the last two PC were not correlated. The avalanches were identified better in PC3 as dark tones elongated shapes.

Table 4.7.1: Correlation coefficients for the multispectral bands, panchromatic and PCA for GeoEye-1 image.

	Green	**Blue**	**Red**	**NIR**	**Pan**	**PCA1**	**PCA2**
Green							
Blue	0.963						
Red	0.989	0.932					
NIR	0.976	0.919	0.984				
Pan	0.962	0.899	0.976	0.958			
PCA1	0.996	0.955	0.995	0.986	0.978		
PCA2	0.056	0.287	-0.054	-0.061	-0.151	0.124	
PCA3	0.014	-0.053	0.027	0.137	-0.135	0.052	0.079

The topography of the test areas being rough with steep slopes and high relief energy, the sun angle varies as a function of slope and aspect, generating the topographic effect, with differences in reflectance values (Mather, 2004). Band ratioing is used as improvement method. We used NDI (normalized difference index) which partially removes the topographic effect and can separate the types of snow. Dozier (1989) showed that NIR radiation is sensitive to the size of snow grains, in the spectral interval 0.9 to 1.3 nm (Figure 4.7.4).

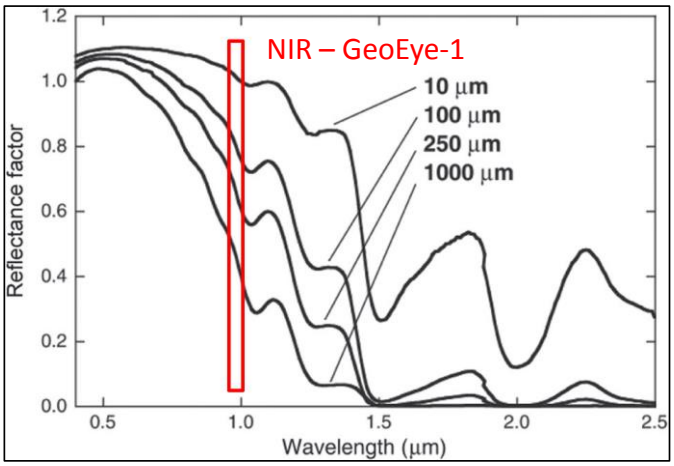

Figure 4.7.4: Spectral signature a s a function of snow grain size and the interval of NIR band (in red) in the GeoEye-1 senzor (modified after Dozier, 1989).

Bühler et al. (2015) disscuss the potential of NIR radiation to distinguish and mapping of different type of snow as a function of snow grain size. For this purpose, a normalized index (NDI, normalizwed difference index) derived from NIR and RED band has been used, as follows:

$$NDI = (RED-NIR)/(RED+NIR)$$

Using the results of NDI for the central areas of Făgăraș Mts. we could separate the avalanche deposits with higher accuracy than in the pancromatic band (0.5 m resolution), although the resolution of NDI was 2 m, coarser than the pancromatic band. The avalanches can be observed even in the shaded areas, as a result of reducind the topographic effect by band ratioing. Theoretically the values are between -1 and 1, and there is an invers relation between the values of NDI and the size of snow grains. Avalanches have values between 0.01 and 0.05, and this is a fisrt approach when NDI values are used to detect snow avalanche deposits (Figure 4.7.5).

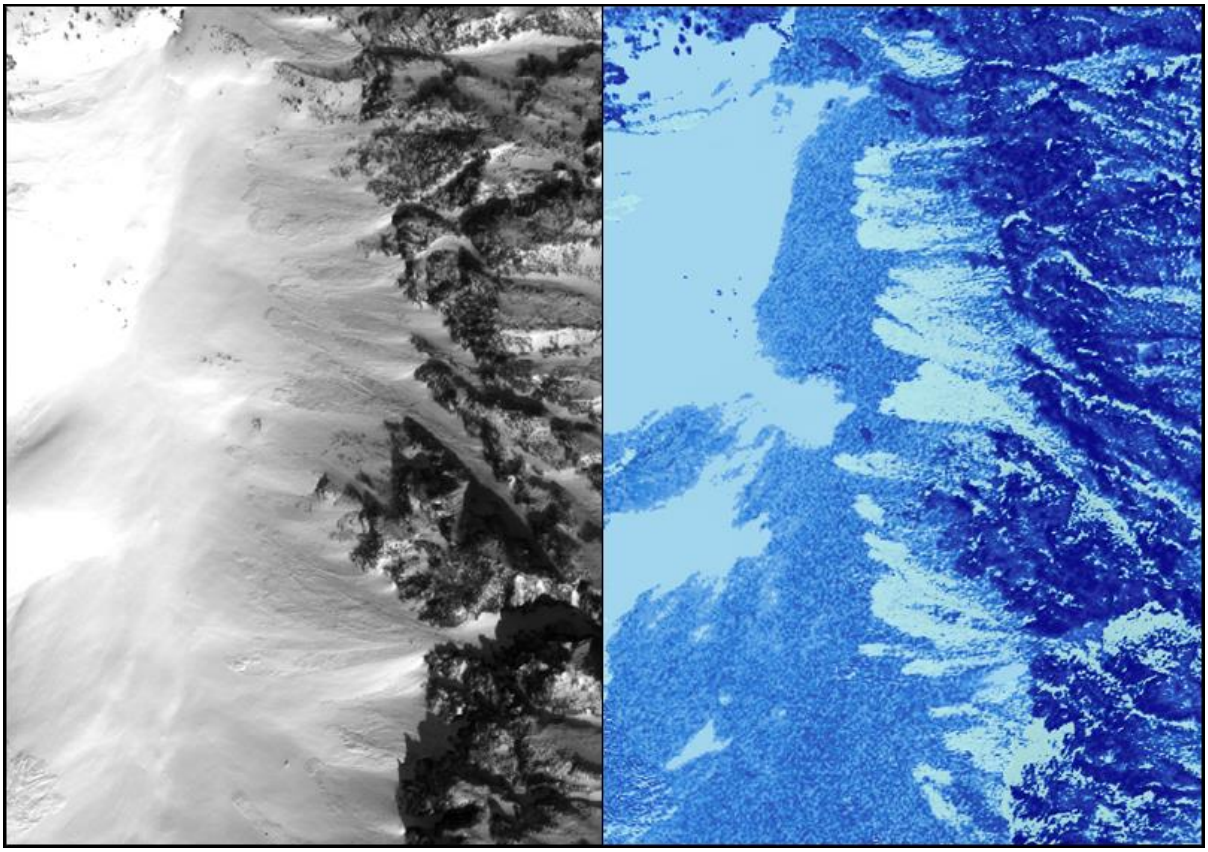

Figure 4.7.5: Avalanches as seen in panchromatic band at 0.5 m (left) and in NDI at 2 m resolution (right).

For most of the areas, the digitizing has been made based on panchromatic band and for overexposed and shaded areas we used composite images (several combinations, including PCA and NDI). The best results have been achieved using fals color composite (Figure 4.7.6) based on PCA and panchromatic (as Red), NDI (as Green), and PCA3 (as Blue). Using the NDI included in the composite images has significantly improved the detection, even in the overexposed and shaded areas (Figure 4.7.6).
For digitizing we used ArcGIS 10.1 software and as complementary data we integrated beside the images, also the slope and hillshade models derived from the DEM to update the existing avalanche database.

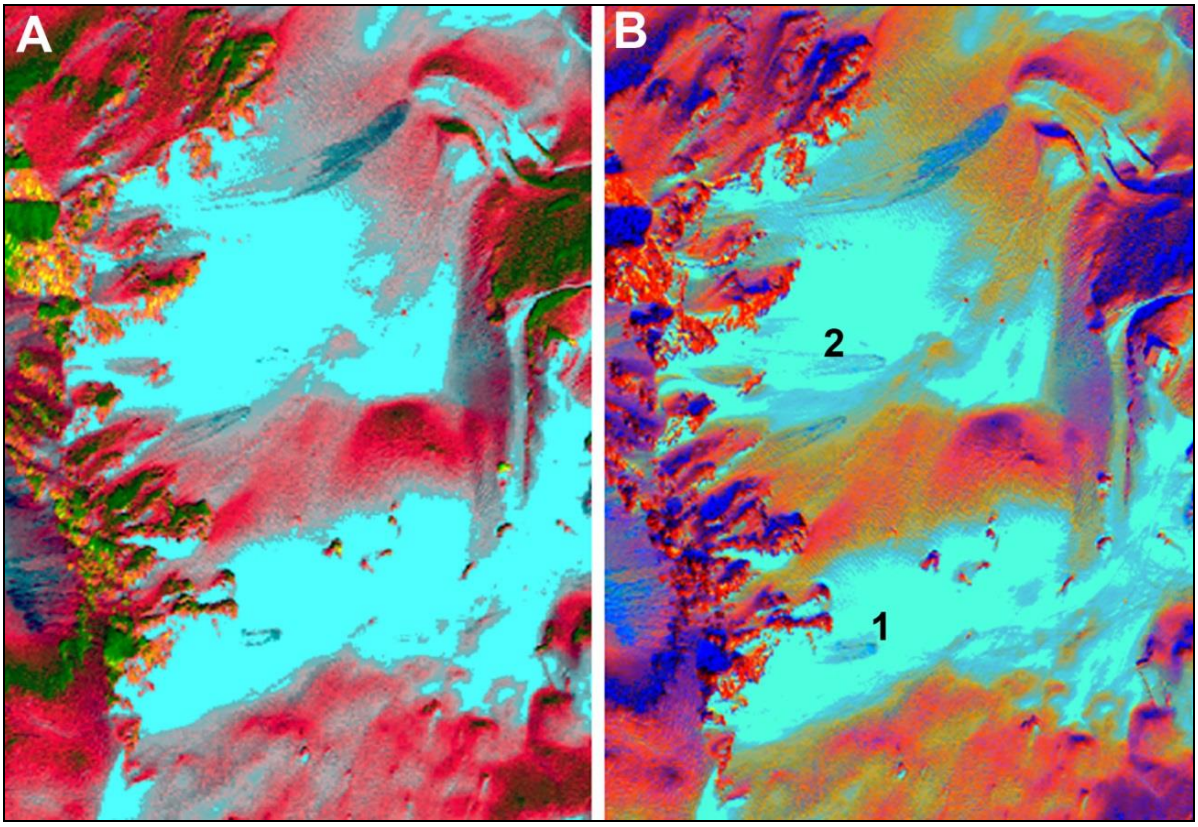

Figure 4.7.6: Fals color composite images in Făgăraș Mts: A. combination of PCA, B. composite image as combination of panchromatic, NDI and PCA3; on the right side image two avalanches (marked as 1 and 2) are visible, whisch was not the case in the left image.

Avalanche mapping based on drone derived products

The aerial images from April 12, 2016, were acquired in good weather conditions, clear sky, using a drone, type DYI (Do It Yourself), with a NIKON D810 DSRL, 36,2 megapixels digital camera. 1296 images were generated from 1390 m fly altitude and a horizontal resolution of 17.8 cm/pixel. The mosaic image covers an area of 40.8 sk km and is overlapping the GeoEye-1 image in the central part of Făgăraș Mts. (Figure 4.7.7).
For the the corections and generation of the DSM, Agisoft Photoscan Pro software has been used with 11 control points (GCP) measured with a double frequency GPS. The mean error was 0.140027 m (XY) and 0.121772 m (Z) respectively.
The resulted DSM (surface reflectance model) is different from the DEM, revealing the height of the objects in the terrain, in this case the snow cover, vegetation and buildings in the central Făgăraș Mts. (Figure 4.7.8). The orthophotoplan and the DSM have been resampled at 0.5 m resolution, same as GeoEye-1 satellite images.

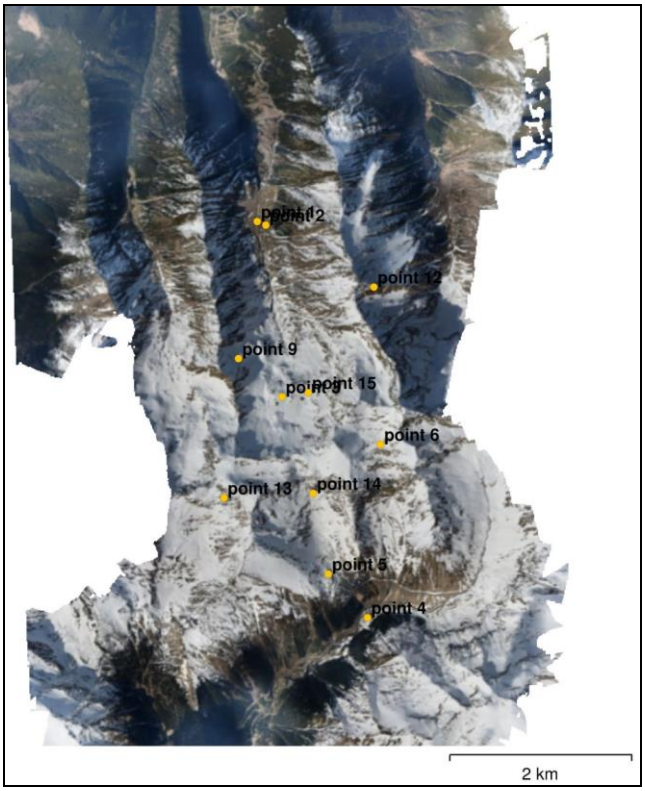

Figure 4.7.7: Orthopho generated from aerial images and the control points using for georeferencing.

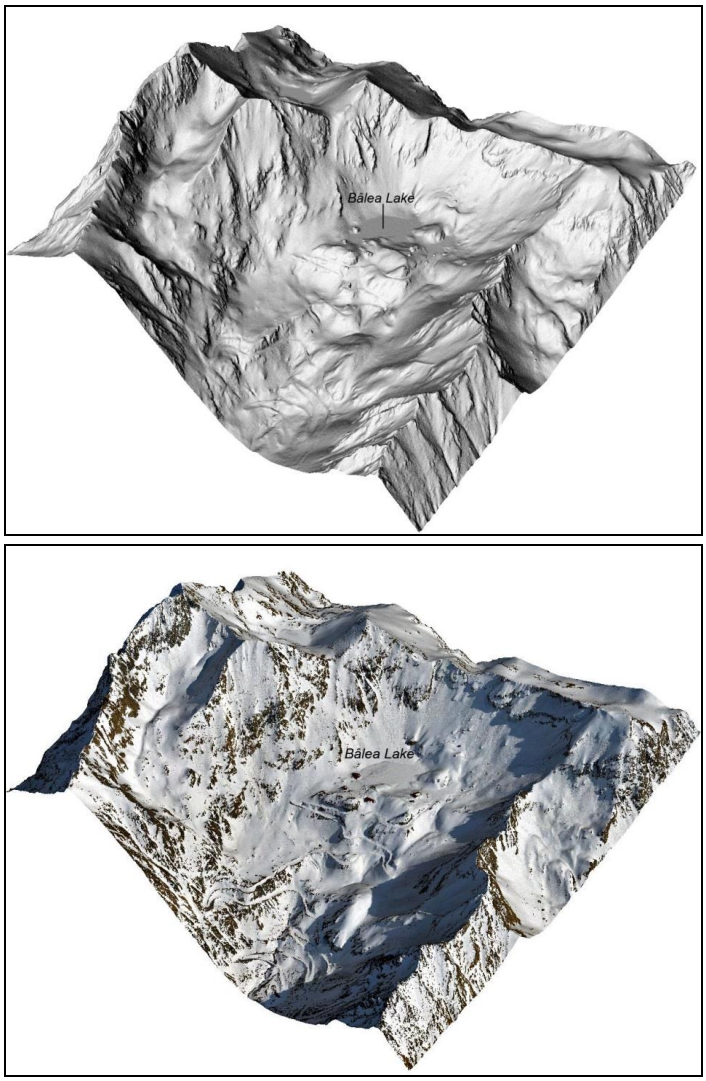

Figure 4.7.8: DSM at 0.5 m resoltion (top) and orthophoto (bottom) overlaid on DSM for Bâlea glacial area, northern slope of Transfăgărășan highway.

The spectral resolution of the drone based image was limited compared with GeoEye-1 scene because the sensor covered only visible domain. For manual detection of avalanches we used only the natural colours image. Because the UAV image acquisition time was between 14 and 15.30, the image exposure was better than that of the satellite image, which was photographed at 9.21 a. m., when the sun altitude was lower. Thus, there were only few areas over dexposed or highly shaded and the manual detection of avalanches was easier.
Based on the UAV images, 429 avalanches were mapped, and 55 were older, being partially covered by fresh snow (Figure 4.7.9 and Figure 4.7.10).

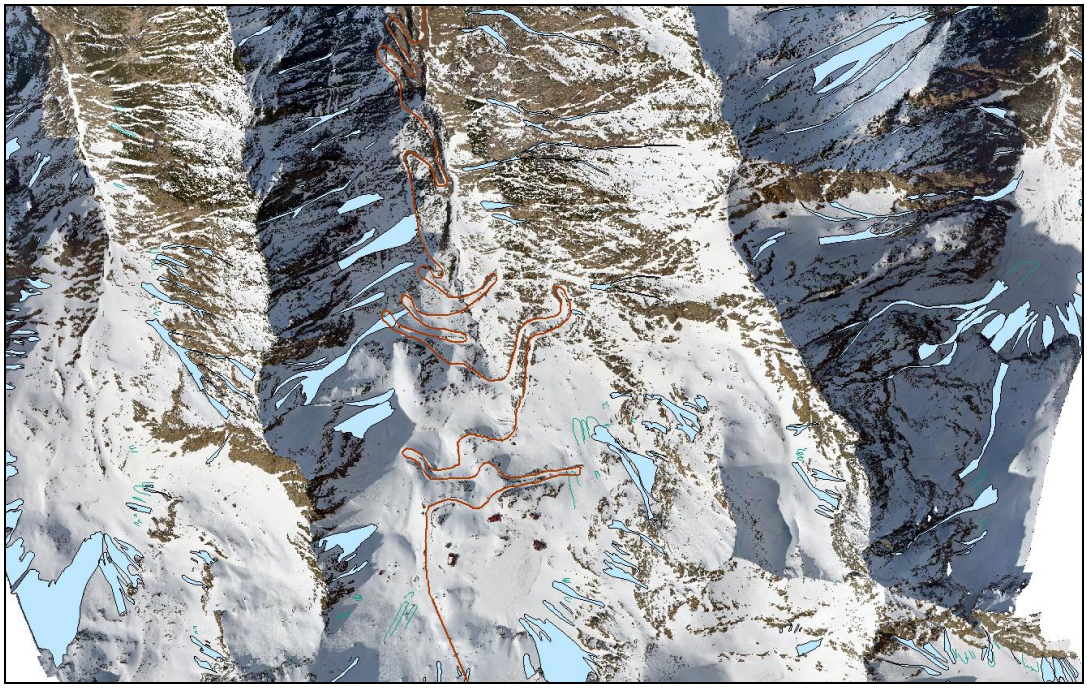

Figure 4.7.9: Avalanches mapped based on UAV image in the Transfăgărășan highway, (April 12, 2016).

Figure 4.7.10: Avalanches triggered at 5-6 days interval, mapped based on UAV image, the old avalanches were mapped only when the deposits had a good contrast.

In total, 1069 avalanche were mapped based on GeoEye-1 and 429 based on UAV image. We estimate that a higher number of avalanches was probably in reality in 2012 satellite image, but there were many overexposed area and thus several avalanches were not detected.
The significant small number of avalanches detected on southern slopes (only 20%) is explained by the differences in morphometry as compared to the northern areas, and by differencies in solar radiation. This last factor correlated with sun azimut (119 degrees) and sun elevation (36.2 degrees) from the moment when the image was acquired, were the cause of the overexposed areas located on the southern, south – estern and eastern slopes. Aproximately 17% of the satellite scene was overexposed.
Even though the optical satellite images and UAV products depend on cloud cover percetage, the use of drones might be a better alternative, the user could choose the time of the aquisition when the exposure conditions are optimal and no areas will be overexposed or shaded. However the use od UAV is limited by the extent of the study area and by the sensor resolution.
In the same time we succesfully applied the NDI in combination with PCA and other bands that improved the avalanche mapping.

Change-detection based mapping of avalanches in Sentinel-1 images

Due to the cloud penetrating property of microwave, SAR is able to acquire "cloud-free" images in all weather conditions, and being an active remote sensing device, it is also capable of night-time operations.
The proposed method for detecting avalanches in Sentinel-1 images relies on the hypothesis that compacted rough snow of an avalanche has very high backscatter values (σ^0) compared to homogeneous snow cover and bare ground, even if the snow is wet (Wiesmann et al., 2001). This principle was utilized also by Malnes et al., 2013.
Further an extensive collection of images used as training data, covering Norway and Romanian mountain areas, was created and the algorithm was modified for best performance in those conditions.

The processing chain develop for the automated detection of changes in avalanche deposits consists of the following modules (Figure 4.7.11):

- Module for downloading Sentinel-1 data. SAR images for a given region and dates are downloaded from the Copernicus Open Access Hub
- Module for calibration and geocoding of SAR images
- Module for mosaicking of SAR images corresponding to the region of interest.
- Module for generation of reference image and corresponding variance image. A reference image for «ascending» and one for «descending» orbit directions are constructed.
- Module for change detection. This supports several techniques for change detection based on the difference between the event image and reference image, with and without correction for pixel-based variance
- Module for avalanche mapping. Based on output from the change detection, a water mask and slope mask, potential avalanches are identified and written to a shape file.

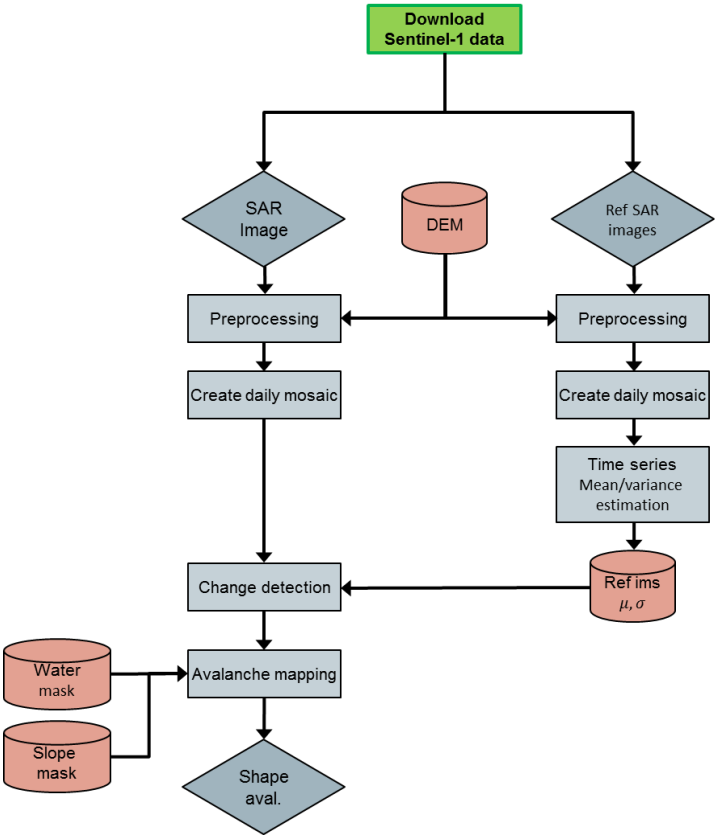

Figure 4.7.11: Sentinel-1 avalanche detection processing chain.

Avalanche detection in Troms, Norway, 2016

In the end of 2015 and beginning of 2016 several avalanches were reported in the Troms Region in Norway. Sentinel-1 data from 1 November to April 30 were analyzed with the SnowBall Sentinel-1 avalanche detection processing chain (Figures 4.7.12, 4.7.13, 4.7.14). Avalanches were detected in each image in the time series, and for a given event image, a unique color were given corresponding to the age of the avalanche. The avalanche age was estimated from the image where a given avalanche was first observed. From the analysis we observe that the avalanches are visible for many days after the avalanche event was triggered.

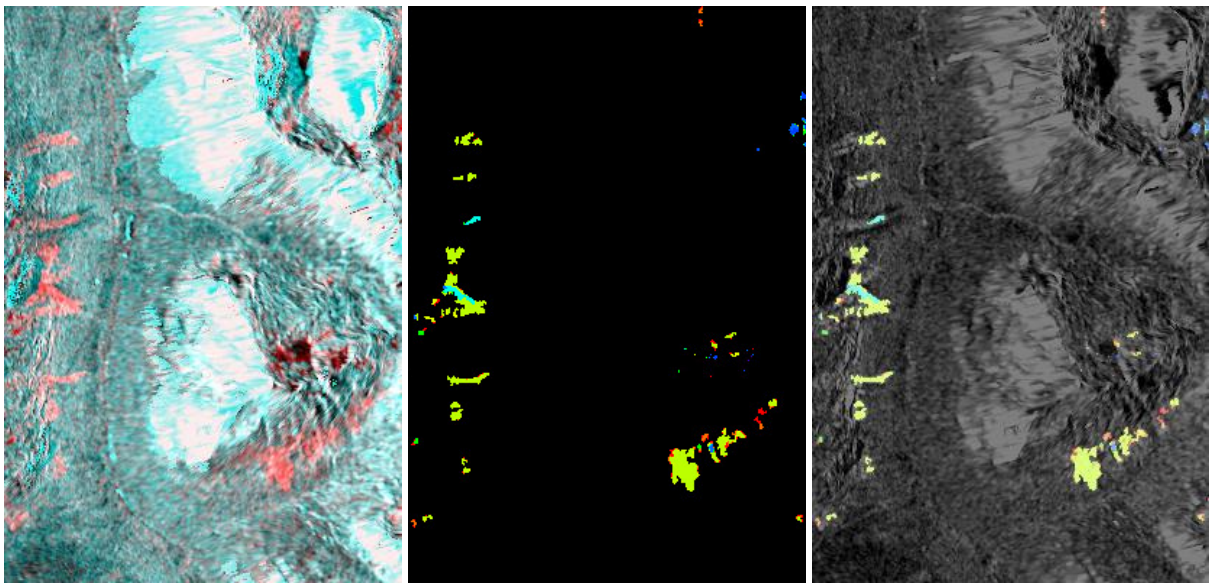

Fiure 4.7.12: Left: False color image with event image from 30 January 2016 (red channel) and reference image (blue and green channel). Middle: Avalanche detections: green - 25 days old, blue - 49 days old, and red - 13 days old. Right: SAR image with detections overlaid.

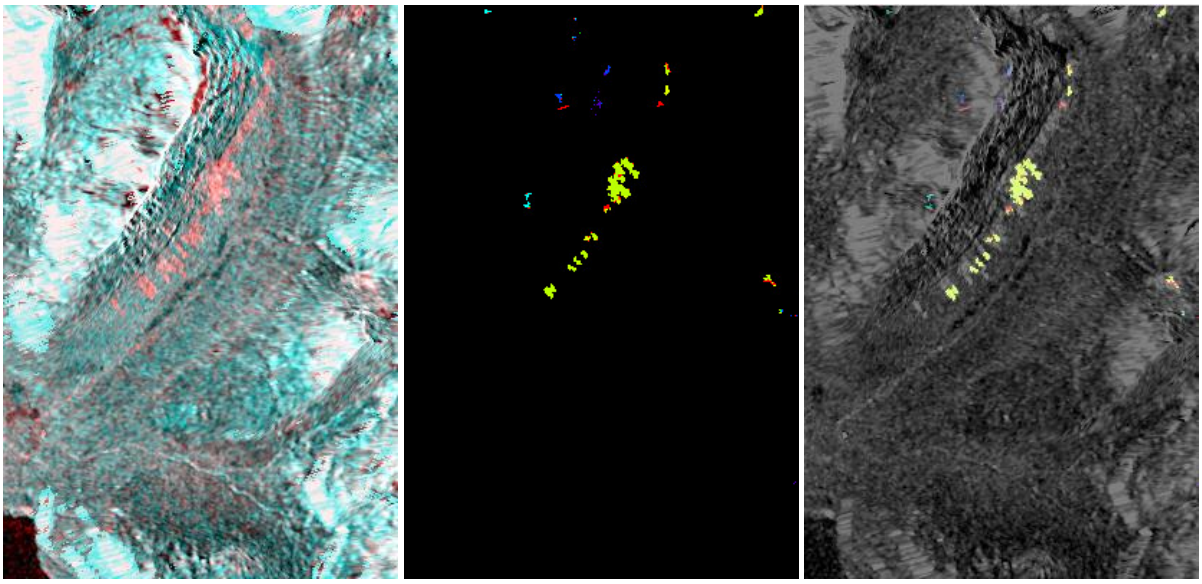

Figure 4.7.13: False color image with event image from 30 January 2016 (red channel) and reference image (blue and green channel). Middle: Avalanche detections: green - 25 days old, blue - 49 days old, dark blue – 71 days old, and red - 13 days old. Right: SAR image with detections overlaid.

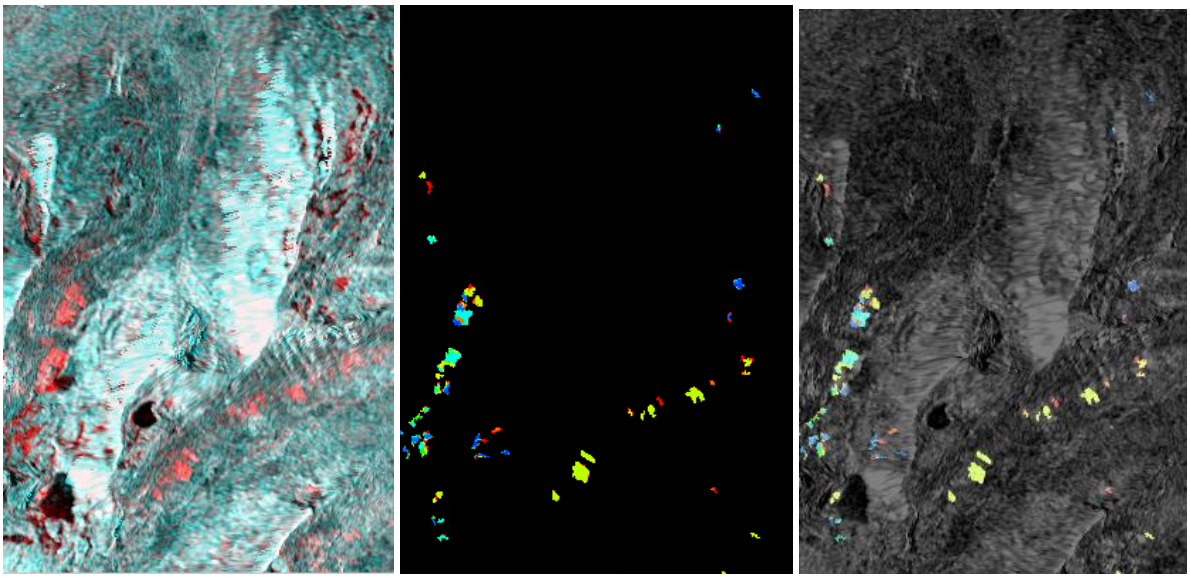

Figure 4.7.14: False color image with event image from 30 January 2016 (red channel) and reference image (blue and green channel). Middle: Avalanche detections: green - 25 days old, blue - 49 days old, dark blue – 71 days old, and red - 13 days old. Right: SAR image with detections overlaid.

Avalanches on the Svalbard island

Due to bad weather conditions a number of avalanches were reported on the Svalbard island, Norway, around November 11, 2016. However, due to its location only a few images are available in the IW mode, and for only with single polarity (HH).

The following Sentinel-1 images were used to detect potential avalanches at Svalbard in the period 31 October 2016 to 11 November 2016:

- S1A_IW_GRDH_1SSH_20161112T154500_20161112T154525_013911_016641_24BA.SAFE
- S1A_IW_GRDH_1SSH_20161031T154500_20161031T154525_013736_0160B5_F4EA.SAFE

Both images are acquired with HH polarization. The 11 November image is the event image, and the 31 October image is the reference images.

A false color image was created from the Sentinel-1 images where the red channel is the event image and the blue and green channel is the reference image. About 700 potential avalanches were

detected (Figure 4.7.15). The processing chain manages to delineate the avalanche area with high precision for many of the avalanches, however, some objects are not detected as avalanche since the maximum slope is not steep enough (Figure 4.7.16).

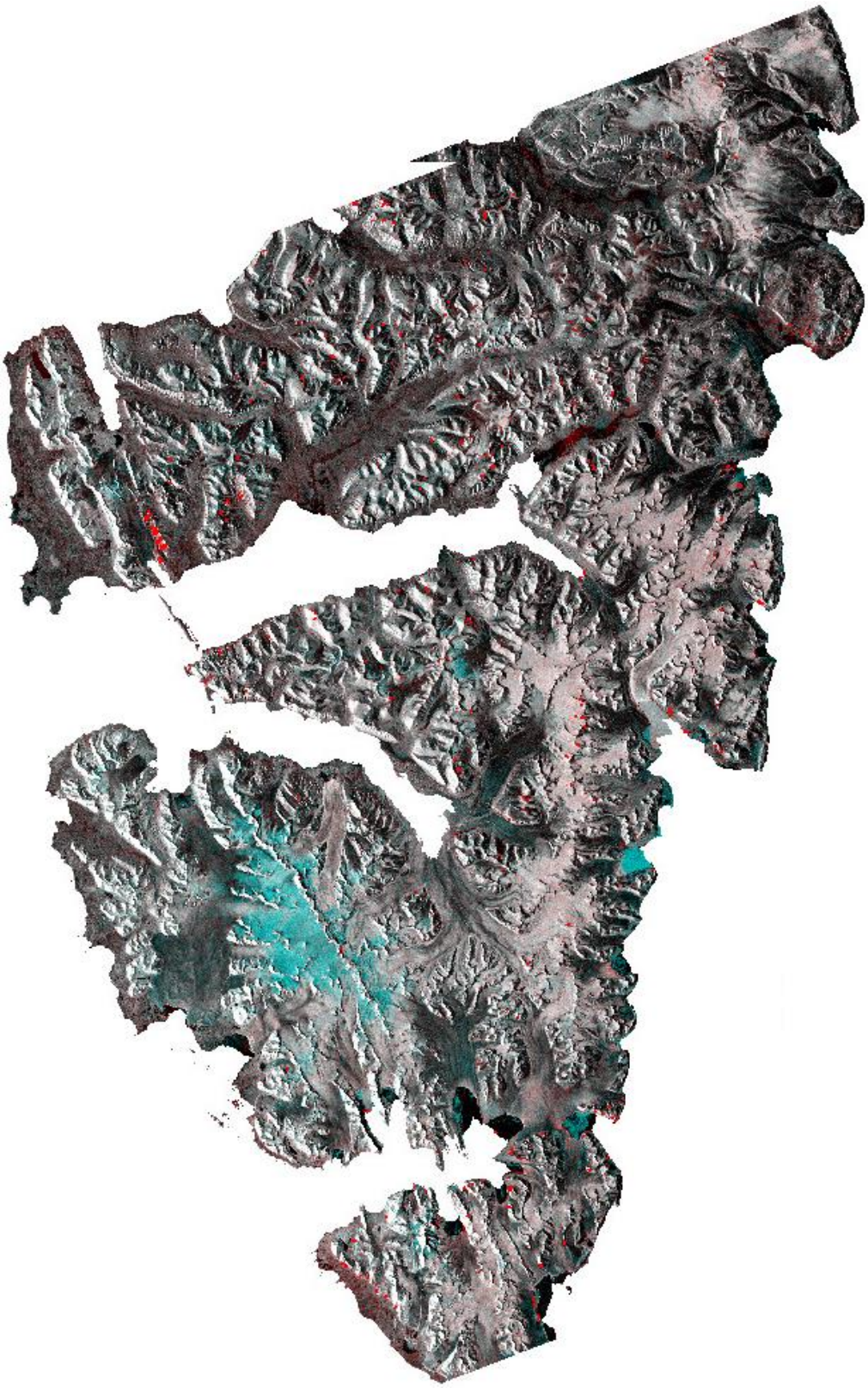

Figure 4.7.15: Sentinel-1 images over Svalbard. The RGB channels are 11 November 2016 (R), and 31 October 2016 (G, B). Red objects indicate potential avalanches.

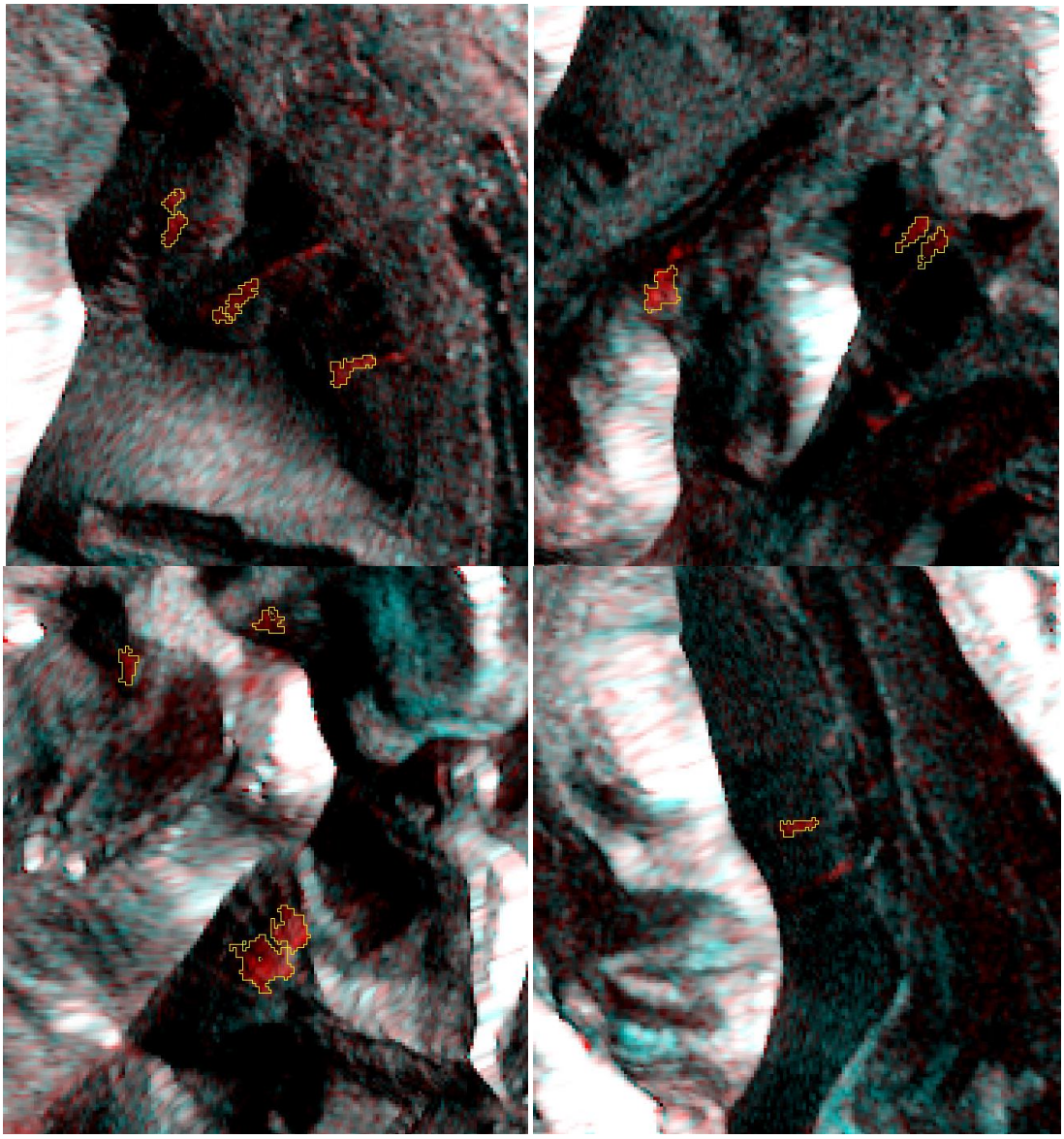

Figure 4.7.16: Zoom on some avalanche detections. Detected avalanches are indicated with yellow polygon.

Avalanches in the central part of Făgăraș Mts.

The processing chain was applied to detect avalanches in the Făgăraș Mts. The event image was acquired on 11th of April 2016, whereas the reference image was from October 26, 2016 (the same repeat cycle as the event image in order to reduce terrain effects in the difference image). A false color image was created from the event and reference images.
Very high resolution optical images were acquired by an unmanned aerial vehicle, and inspected manually for avalanches. The detected avalanches are overlaid as yellow polygons (Figure 4.7.17).
None of the avalanches detected in the drone image are visible in the Sentinel-1 image. There may be many reasons for this, including that:

- the avalanches are too small
- the avalanches are caused by point release
- there are severe terrain effects
- the snow conditions are not suitable for detecting avalanches.

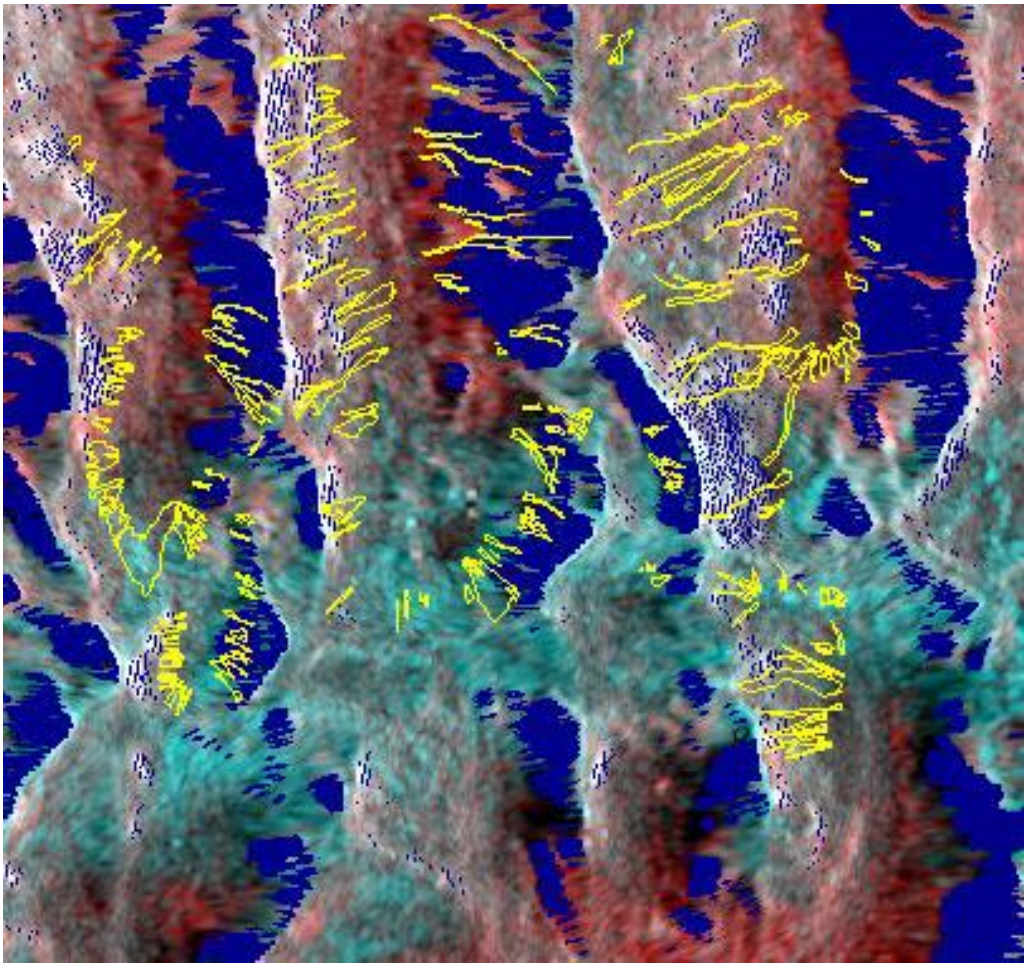

Figure 4.7.17: Sentinel-1 images over Fagaras. The RGB channels are 11 April 2016 (R), and 26 October 2016 (G, B). Yellow polygons show avalanches detected in a VHR optical drone image. The dark blue areas indicate SAR layover and shadow areas.

The benefit with SAR based detection scheme is that there are no cloud issues. Hence, we receive SAR images for all weather conditions. When the avalanches look like bright “blobs”, the algorithm detects them in most cases. Large avalanches are reliably detected; however, the algorithm struggles to detect avalanches if the blob contrast is weak. The algorithm also detects some non-identified objects that appears as bright blobs and has favorable DEM conditions.
A challenge with SAR is the side-look geometry, which may result in severe layover and shadow areas, in particular for steep mountain regions like the Făgăraș. In the layover and shadow areas avalanche detection is not feasible.
Currently, the processing chain is only applicable for semi-automatic operation due to the high number of false detections.

Change analysis and avalanche mapping in Sentinel-2 images

The MSI (MultiSpectral Instrument) of the Sentinel-2 satellite, aquires images în 13 spetcral bands în visible, NIR and SWIR domains, the spațial resolution being different, as follows: 4 bands în 10 m spatial resolution (490 nm (B2), 560 nm (B3), 665 nm (B4), 842 nm (B8)), 6 bands at 20 m (705 nm (B5), 740 nm (B6), 783 nm (B7), 865 nm (B8a), 1 610 nm (B11), 2 190 nm (B12)) and 3 bands at 60m (443 nm (B1), 945 nm (B9) și 1 375 nm (B10)).
Considering that the size of avalanches (length and width) has been calculated from VHR images from 2012 and 2016, we can assume that the avalanches from Southern Carpathians, as suggested by Greene et al., (2010) are in general small and medium size. From the database, 39,73 % from all

mapped avalanches were small (length less then 100 m), 60,10% were medium size avalanches (100 - 1000m) and only 0,17% were considered large size (>1000 m length). Thus, the only bands that theoretically migh be usefull in detecting these categories are visible and NIR, with the most detailed resolution of 10 m.
Starting with the launching of Sentinel-2 (June 2015) up to present (April 2017), for the study area a number of 120 images from the intervals when the snow layer is present (November to May) have been identified. Yet, only two images were useful, all the other being with a high percentage of cloud cover. The images used for Făgăraș Mts. were aquired in 4th of April 2016 and 26th of January 2017.
Both scenes have been analyzed in separate bands and in composite images, as natural color 234 and in combinations visible-NIR, 348 (Figures 4.7.18, 4.7.19).

Figure 4.7.18: Sentinel-2 scene over Făgăraș; Mts., 4th of April 2016. Composite image (G, R, and NIR).

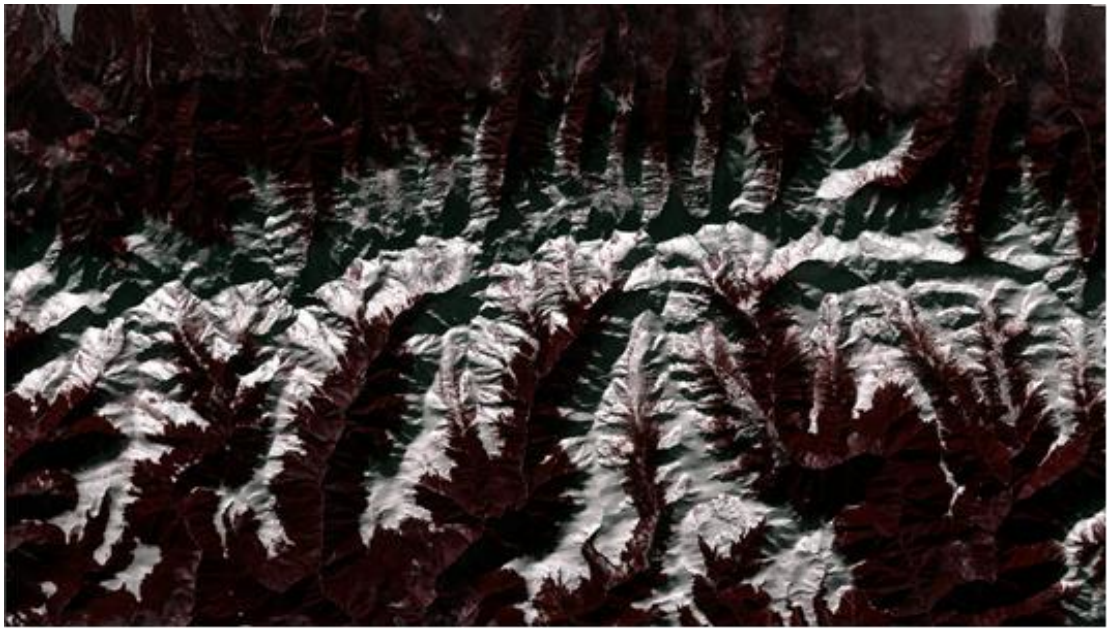

Figure 4.7.19: Sentinel-2 scene over Făgăraș; Mts., 26th of January 2016. Composite image (G, R, and NIR).

Although for the date when the image was aquired, several avalanches were reported in the Transfăgărășan area, none of these events were visible in Sentinel-2. The avalanches mapped from VHR images aquired with UAV – drone only a few days after the Sentinel-2 (in April 12, 2016) have

been used as additional data, but the resolution in Sentinel-2 is too coarse for the detection of these avalanches.
Moreover, the image from January, has several areas in shadow, where no details can be distinguished. Although the images were aquired approximately at the same time (9:35 and 9:23), the exteded shadow that can be seen in January was caused by a low altitudine of the Sun at azimuth of 65.21°, as compared to the image from April (azimuth 41.35°) (Figure 4.7.20).

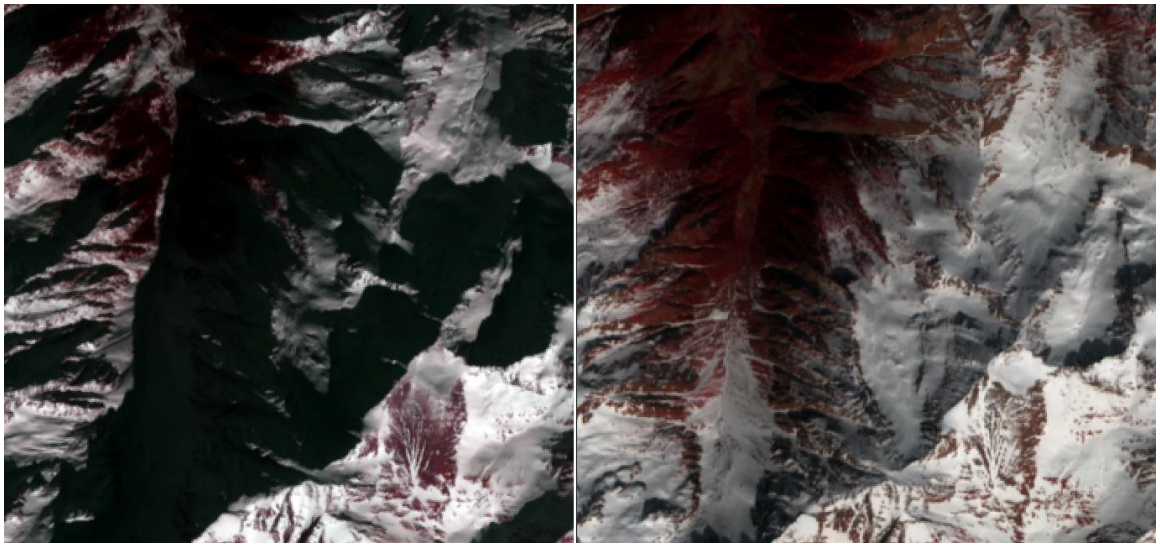

Figure 4.7.20: Areas affected by shadow in image from January (left), as compared to the same areas in April (right).

The NDI (normalized difference index) generated from red and NIR bands has been succesfully used in manual and automated detection of avalanches in VHR optical images. In the case of Sentinel-2, using the NDI index, we couldn't separate the avalanche deposits. Only a few avalanches mapped in VHR images were overllaped on areas with NDI values of 0.01 and 0.05, that suggest the presence of avalanches (Figure 4.7.21). The NDI was inefficient in this case, that might be explained through the values of NIR band, which is in the interval of 727 - 957 nm, and the maximum potential of radiation in NIR to distinguish the type of snow cover as a function of snow grain size is between 0.9 and 1.3 nm (Dozier, 1989).

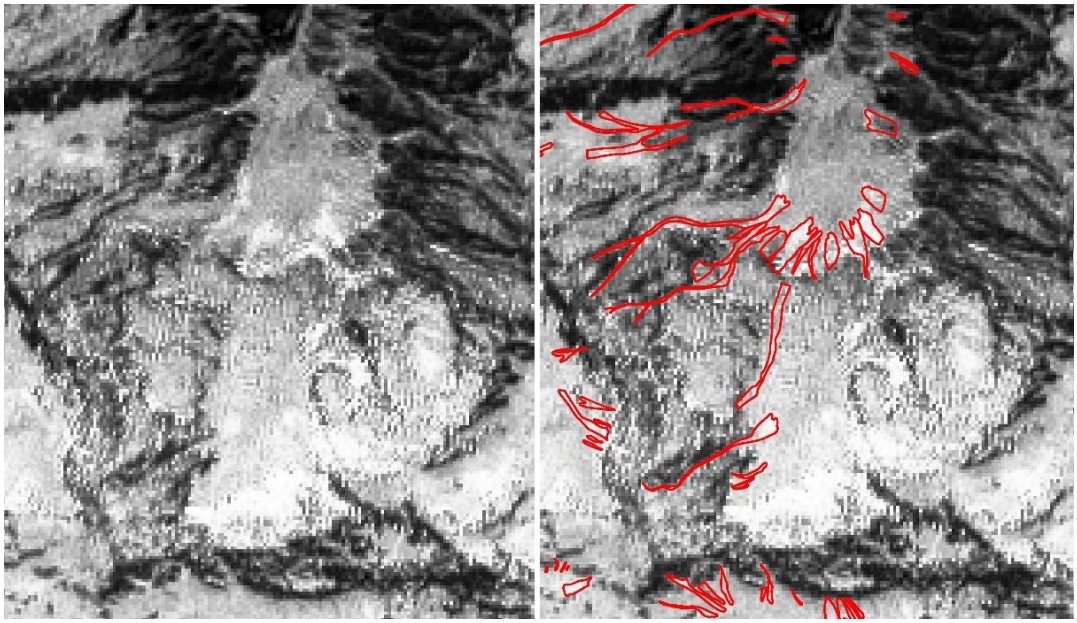

Figure 4.7.21: NDI (normalized difference index) derived from R and NIR bands of Sentinel-2 (4th of Aprilie 2016);
The white pixels suggest values indicating the potential presence of avalanches;
The avalanches mapped from the VHR image are outlined in red.

The use of Sentinel-2 images has proved to be inefficient for the detection of small and medium size avalanches, specific for Southern Carpathians. The 10 m resolution is too coarse for avalanches smaller than 1000m length and around 26 m width. Spectral limitation of NIR band, and the NDI that used that band are not suitable for avalanche detection in this type of images, although have been applied with good results in VHR images. Because of the high percentage of cloud cover during the winter season, only a small number of images were useful. In the same time , in December and January the Sun altitude is low, causing shadow effect, and no details can be observed in most areas of the image. All these factors suggest that for Southern Carpathians, the Sentinel-2 images cannot be used in avalanche detection or for monitoring the changes in snow cover during an entire season.

More details are presented in the deliverable D7.2: „Validated algorithms for detection of changes in land and snow cover caused by avalanches in HR SAR and optical satellite images".

*4.7.2. **Activity 7.3.** Avalanche simulation*

For snow avalanche hazard in the potential affected mountain areas, the existence of snow avalanche databases with historical records of past avalanche events related to the triggering factors, extent and volume, regular observations are very important. The approaches for identification of hazard prone areas can be divided into two types of models - topographic-statistical models and dynamic models. Simulation of avalanche trajectories is considered an important step in hazard analysis and has an important influence on the separation of hazard levels.
The simulations were tested with RAMMS (Christen et al., 2010) in the area surrounding the Transfăgărășan highway, this being the most affected by snow avalanche events, that caused damages, as are mentioned in the records. The friction parameters (Bartelt et al., 1999; Salm et al., 1990) as input variables were calculated using the automatic procedure implemented in this model. The procedure classifies terrain parameters, altitude, slope gradient, and plan curvature, in types like flat terrain / open slope, channelled / gully and forested or non-forested areas (Bartelt et al., 2013).
Potential release areas are the starting points that drive the simulation of the extent, height and snow pressure for several snow conditions. These areas can be delineated manually by experts (Figure 4.7.22) or in a more automated approach using morphometric parameters derived from a DEM. For this stage, in the identification of release areas, we used slope with values of 25-60 degrees, plan curvature (excluding the convex area such as peacks, ridges), terrain ruggedness (excluding area with high values that are not suitable to snow accumulation). Landcover data related to vegetation type were used to exclude classes that are not favorable for potential release areas.

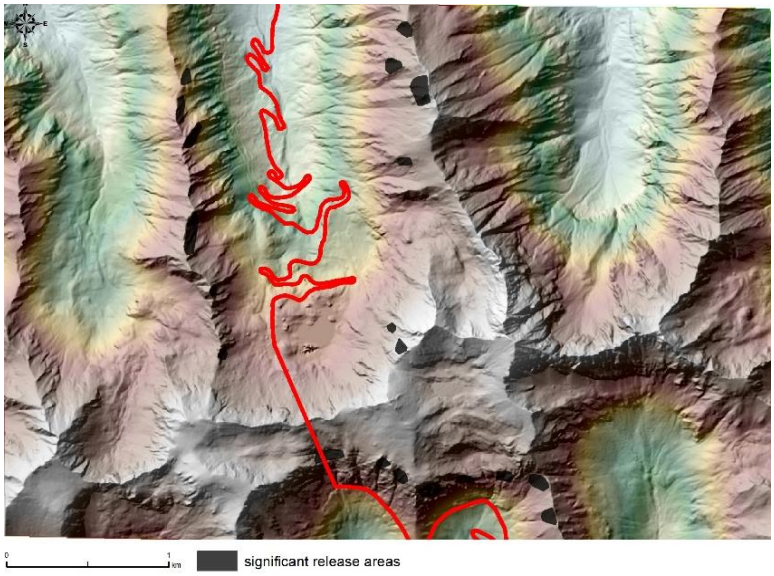

Figure 4.7.22: Example of potential release areas located in central part of Transfăgărășan area based on data extracted from past events.

Several release areas have been selected for further simulations in the central area of Făgăraș Mts., near Transfăgărășan highway. Calculation and classification of friction parameters was based on DEM

derived data (altitudine, slope, curvature), forest cover and global parameters (volume and return period).
For the estimation of the return period of avalanches in the areas, data from dendrochronologic reconstructions from other studies have been used (with values of 10 and 30 years).
For the size of the avalanches, small and medium size events were used as resulted from the database calculations. Trajectories simulation have been tested considering several high impact past avalanches identified in statistics. For the snow depth, values of 0.5 - 2 m have been tested in simulation. The avalanche trajectories, snow depth, velocity, pressure and spatial extent of the snow deposits have been simulated and exported as raster for further analysis.
The results of the simulation showed that in most of the cases, parts of the highway and forested areas will be affected, especially in the southern slope (Figure 4.7.23).

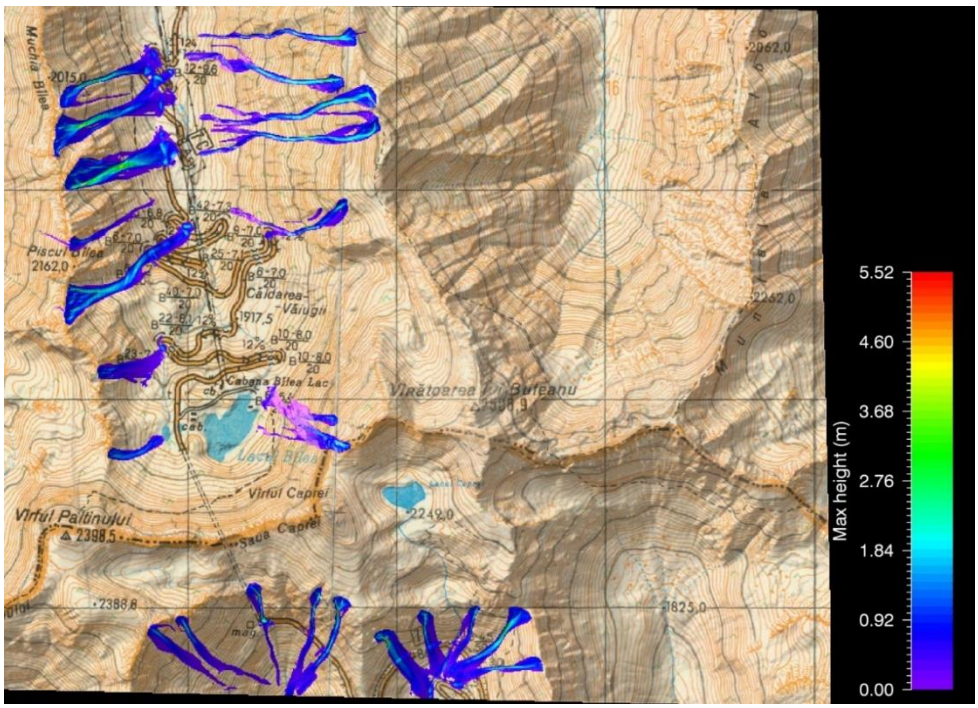

Figure 4.7.23: Example of a simulation - extent and snow height in Transfăgărășan area, based on return period of 30 years and medium size events; topographic map and hillshaded terrain in the background

4.8. *WP8* Promotion and Dissemintion

4.8.1. Activity 8.1. Project website

There was updated the project website (http://snowball.meteoromania.ro), being included information about the Snowball consortium activity for the current stage of the project: obtained results, meetongs, disseminations, etc (figure 4.8.1). Also, have been realised the Romanian version of the website.

Figure 4.8.1: The web page of the project SnowBall

4.8.2. Activity 8.3. Dissemination and training actions.

The dissemination and education actions have been conducted according to the project dissemination strategy included in the Publicity Plan: awareness of the user community about the opportunities offered by the Snowball project; communication of the results achieved in the project; preparation of the support materials for the products created within the project (eg. documentations, flyers, posters, etc.); ensuring project visibility at national and international level.
The communication channels that have been used in the Snowball project included oral ones (seminars, conferences, workshops, formal and informal meetings, etc.) and written communication channels (brochures, newsletters, articles in scientific journals, articles in generalist publications, postings on social networks, etc.
The following outlines are followed for each dissemination activity:

- Consistent visual identity;
- The project logo has to be visible;
- Mention of partners and financiers;
- All documents have to include a standard paragraph that mention the name and the indicative of the project, the financier.

Attending national and international conferences

One of the best appropriate ways to disseminate the scientific results of the project SnowBall is the scientific conferences message. Snowball consortium has participated with oral presentations and posters at relevant events for the topics addressed in the the project. There have also been submitted some articles for publication in relevant journals for the project objectives. At the end of the project will be organized a conference dedicated to the presentation of the results.
Representatives of the Snowball consortium has participated with oral presentations and posters at relevant events for the topics addressed in the project. There have also been submitted some articles for publication in relevant national and international journals for the project objectives. At the end of the project will be organized a final conference dedicated to the presentation of the results.

The project brochure

The brochure contains information about the the project objectives and results structured in an attractive manner and in non-technical language, understandable by the general public. A first bilingual version was performed. The final version will be distributed before the official end of the project.

Newsletter

The second e-newsletter (electronic format) was elaborated and downloaded on the project website and distributed to the end-users of the project SnowBall.

More details are presented in the deliverables D8.4: „Project brochure - Version 2", D8.6: „Visibility products (banners, posters etc.)", D8.7: „Conference project presentation package", D8.8: „Dissemination action report", D8.9: „Project newsletter (e-zine) - digital form".

5. ANNEXES

- **ANNEX 1: Agenda of the 2nd Workshop on Geoinformatics in the framework of SYNASC 2016. 18th International Symposium on Symbolic and Numeric Algorithms for Scientific Computing**
  Timisoara, Romania, September 27, 2016
- **ANNEX 2: Agenda of the 3rd Annual Progress Meeting (2016)**

ANNEX 1

2nd Workshop on Geoinformatics
in the framework of
SYNASC 2016
18th International Symposium on Symbolic and Numeric Algorithms for Scientific Computing
Timisoara, Romania
September 27, 2016

Workshop description

Geoinformatics is a relatively new field concerned with manipulation, modeling, and visualization of the geospatial data. The aim of this workshop is to facilitate discussion of the latest achievements in Geoinformatics as well as applications of geospatial technologies and methods in various fields, such as Geosciences, Environmental sciences, Archeology etc. The workshop particularly promotes collaboration between computer scientists and geoscientists to address scientific and practical challenges in this field. The workshop welcomes submissions of original, high-quality papers reporting on experiments, models or systems that have been or are being implemented. We encourage participation of the young scientists and PhD students.

Topics

Specific topics of this workshop include, but are not limited to, the following:

+ Acquisition of geospatial data
+ Spatial analysis
+ Simulation, prediction, forecasting
+ Location-based services
+ Satellite image analysis
+ Change detection and monitoring
+ High Performance Computing of geospatial data\

Session 1: Tuesday, September 27 (10:50-12:30) Chair: Gheorghe Stancalie

- Arnt B. Salberg, Jarle Bauck Hamar, Florina Ardelean, Thomas Johansen and Michael Kampffmeyer. *Automatic detection and segmentation of avalanches in remote sensing images using deep convolutional neural networks*
- Rune Solberg, Øystein Rudjord, Øivind Due Trier, Gheorghe Stancalie, Andrei Diamandi and Anisoara Irimescu. *Single and multi-sensor snow wetness mapping by Sentinel-1 and Sentinel-3 data*
- Ion Nedelcu, Anișoara Irimescu, Andrei Diamandi, Denis Mihăilescu, Vasile Crăciunescu, Gheorghe Stancalie and Radu Constantin Gogu. *Some Considerations on Using Copernicus Sentinel Satellite Data for Characterizing the Snow Cover in the Romanian Mountains*
- Marius Matreata and Simona Matreata. *Snow water equivalent estimation using a data fusion approach*
- Alexandru Dumitrescu, Roxana Bojariu, Sorin Ionut Dascalu, Madalina Gothard, Marius - Victor Birsan, Roxana Cica, Liliana Velea, Gheorghe Stancalie and Anisoara Irimescu. *High Resolution Temperature and Precipitation under Present and Future Climate Scenarios*

Session 2: Tuesday, September 27 (13:30-15:30) Chair: Marcel Torok-Oance

- Vasile Crăciunescu, Gheorghe Stancalie and Anisoara Irimescu. *MODIS-based, mapping and analysis platform for flood affected areas. Case study: 2006 Danube floods*
- Andrei Diamandi, Elena Mateescu, Gheorghe Stancalie,Oana Nicola, Anisoara Irimescu, Denis Mihailescu,Vasile Craciunescu, Luca Eduard, Ionut Sandric and Daniela Saizu. *Assessment of SMOS and SMAP soil moisture products over Romania with in-situ data*
- Marcel Török-Oance, Anişoara Irimescu, Narcisa Milian, Andrei Diamandi, Florina Ardelean and Mircea Voiculescu.*Snow avalanche hazard assessment in Făgăraș Mountains, Southern Carpathians*
- Florina Ardelean, Marcel Török-Oance, Arnt-Børre Salberg, Mircea Voiculescu, Narcisa Milian and Anișoara Irimescu.*Numerical simulation of documented snow avalanche events in Făgăraș Mountains*

- Andra Moldovan and Marcel Torok-Oance. *Using OBIA for delineating eligible grassland parcels for agricultural subsidies in L.P.I.S. (Land Parcel Identification System)*
- Tiberiu Banu and Marcel Torok-Oance. *Using OBIA for delineating management units in forest planning projects. Case study: National Park Cozia.*

Publication

Extended/revised versions of the best papers presented at the workshop will be included in the SYNASC post-proceedings published by the Conference Publishing Services. Other publishing opportunities in journals will be announced later.

Acknowledgments

This workshop is supported by the Project "Remote sensing, model and in-situ data fusion for snowpack parameters and related hazards in a climate change perspective (SnowBall-19SEE/2014)", financed from the Economic European Area Financial Mechanism 2009-2014.

Annex 2

SnowBall – Remote sensing, model and in-situ data fusion for snowpack parameters and related hazards in a climate change perspective

Annual Progress Meeting (2016) - AGENDA
Date: 7-10 of November 2016
Venue: Radisson Blu Mountain Resort, Beitostølen & NR, Oslo, Norway

7th of November 2016 (Beitostølen)

17:05 – 20:59	Bus transfer from Oslo Bus Terminal to Beitostølen

8th of November 2016 (Beitostølen)

9:00 – 9:10	Welcome NR Round Table - Introduction of Partners	All
	WPs Progress Reports	
9:10 – 9:55	**WP2 – In-situ snow parameters measurements** Activity 2.2. – Snowpack parameters observation and measurements. Activity 2.4. – Elaboration of spatial products using the spatial database.	NMA, NR, NIHWM, WUT
9:55 – 10:40	**WP3 – Satellite remote sensing, data fusion and modelling of snow parameters (snow wetness products)** Activity 3.2. – MWS algorithm and product. Activity 3.3. – New multilayer snow model module in NOAH.	NR, NMA, NIHWM
10:40 – 10:55	**Coffee break**	
10:55 – 11:40	**WP4 – Climate change impact on snow-related hazards** Activity 4.1. – Snow-related climate variability and change and associated impact. Activity 4.2. – Variability and change in flash floods with snow melt contribution. Activity 4.3. – Variability and change in avalanche statistics.	NMA, UTCB, NIHWM, WUT
11:40 – 12:25	**WP5 – Aquifer replenishment modelling from snow melt infiltration** Activity 5.2. – Aquifer modelling. Activity 5.3. – Pattern matching and climate scenarios.	UTCB, NIHWM
12:25 – 14:00	**Lunch break**	
14:00 – 14:45	**WP6 – Assimilation of snowpack parameters in the National Flood Forecasting and Warning System** Activity 6.3. – Implementation of the methodology for data assimilation of snowpack parameters in the main operational hydrological forecasting models.	NIHWM, NMA, NR

14:45 – 15:30	**WP7 – Avalanche inventory, release and hazard mapping** Activity 7.2. – Change-detection algorithm for Sentinel-1 and Sentinel-2. Activity 7.3. – Avalanche simulation.	WUT, NR, NMA
15:30 – 15:45	**Coffee Break**	
15:45 – 16:15	**WP8 – Promotion and Dissemination** Activity 8.1. – Project website. Activity 8.3 – Dissemination and training actions.	NMA / All
16:15 – 18:00	**Discussions**	All

9th of November 2016 (Beitostølen)

9:00 – 9:45	Project management Technical / Financial Reporting, Deliverables, Templates	NMA / All
9:45 – 10:45	Progress report 2016 and 2017 – 30 March 2017 Final project report - 30 April 2017 Field campaigns: winter 2016-2017	NMA / All
10:45 – 11:00	**Coffee break**	
11:00 – 12:00	Steering committee meeting	All
12:00 – 13:30	**Lunch break**	
13:30 – 16:00	Field trip to the Jotunheimen snow study area	All
18:00 – 21:58	Bus transfer from Beitostølen to Oslo Bus Terminal	

10th of November 2016 (Oslo)

9:00 – 11:30	Discussions for next SEE Program Call; Meeting with possible Norwegian end-users;	All
11:30 – 12:30	Final discussions / Conclusions	NMA

6. CONCLUSIONS

This report presents the results obtained during 2016 in implementing the objectives of the Snowball project, according to the work plan, broken down by work packages, activities and related deliverables.

WP1 Management

Activity 1.1. Project Management

The Project Steering Committee, made up of individuals responsible on behalf of partner institutions and led by the project manager contined to ensuring, during 2016 an efficient and concrete project management which comprised scientific, administrative, financial and communications matters with the contracting authority.

From 16 March 2016 to 6 May 2016 the operational audit mission for SnowBall project took place, performed by the Central Harmonisation Unit for Internal Public Audit within the Ministry of Public Finance. To elaborate a point of view regarding the findings and recommendations from the audit report, a series of meetings took place in the 6-27 May 2016 interval at the headquarters of MeteoRomania with individuals responsible on behalf of the Romanian partner institutions. The point of view resulted following the discussions contained explanations and justifications on the grounds of administrative and financial documents and was supported on the occasion of the reconciliation meeting on 27 May 2016.

The annual meeting of Project 19 SEE/ 30 June 2014 SnowBall took place in Beitostølen and Oslo in Norway on 8 – 10 November 2016. During the meeting, a session of the Project Steering Committee also took place, that analysed the project implementation stage, in accordance with the activity plan and issues were discussed that may affect fulfilment of the project's objectives. The Project Management Plan was also verified and updated and there was a discussion about the latest instructions received from the contracting authority regarding the verification of expenses borne at project level at the accomplishment of the indicators within the Annual 2016 Scientific and Technical Report.

WP2 In-situ snow parameters measurements

Activity 2.2. Snowpack parameters observation and measurements

The spectral data set obtained so far (more than 200 spectra) is covering a wide range of weather and snow conditions (sun angles, spectro-radiometer viewing angles, air temperature, illumination, etc). Close examination of the snow spectra shows all the known features associated with the snow spectral characteristics for different conditions and confirm therefore the quality of the acquired data.

The Decagon 5TM sensor has been selected for capacitive snow wetness mesurements in the SnowBall project. The 5TM probe is much less expensive than the Denoth or the Snow Fork instruments and can be easily interfaced with microcontroller based data loggers of the type used in the project. The probes will be deployed at the project cal/val sites an weather stations within the project test area.

Activity 2.4. Elaboration of spatial products using the spatial database

During this stage (achieving gridded climatology, 2nd version), the mean multiannual monthly data (1 October 2005 - 30 December 2016) for the parameters of interest were used for spatial interpolation. The gridded climatology – mean multiannual monthly maps – was realized at this stage for the parameters of interest. Auxiliary data derived from the DEM were also used for spatialization: altitude, mean altitude in a 20-km radius, latitude, distance to the Black Sea and distance to the Adriatic Sea.

An overview of the analysed variables is provided by the maps obtained in this stage. However, the accuracy is directly influenced by scale, by spatial estimation errors specific to the geostatistical

methods, and by the spatial density of ground data (weather stations operated by the National Meteorological Administration).

WP3 Satellite remote sensing, data fusion and modelling of snow parameters
Activity 3.2. MWS algorithm and product

The products have been demonstrated, studied and evaluated for the general quality over the whole product domains, Romania and southern Norway. The snow wetness maps seem in general quite consistent with the air temperatures. In most cases retrieval results of dry snow correspond with air temperatures below freezing point, and retrieval results of one of the wet-snow classes with air temperatures above freezing point. The highest temperatures usually gave the wettest snow classes. Furthermore, the MWS maps are usually internally consistent in the way that the content follows the topography and local climate well.
As an overall preliminary conclusion, the novel multi-sensor/multi-temporal wet snow maps have further confirmed the approach of fusing temporal optical and SAR observations to make an estimate of the daily snow surface wetness.

Activity 3.3. The new module of the multilayer model for snow in NOAH

Estimating the spatial distribution of snow water equivalent (SWE) in mountainous terrain, characterized by high elevation and spatially varying topography, is currently the most important unsolved problem in snow hydrology.
In order to reduce the errors associated with the estimation of the snow water equivalent, was designed and implemented within SNOWBALL Project a specific data fusion type approach.
The use of the new snow module in multilayer architecture, allowed the elaboration of a more complex procedure of data fusion, a better use of future available satellite products that relate to the characteristics from the snow layer surface.
Was finalized the deliverable D3.6. “Gridded SWE prototype products generated using data fusion methodology – Version 1”.

WP4 Climate change impact on snow-related hazards
Activity 4.1. Snow-related climate variability and change and associated impact

For the snow-related climate variability and change and associated impact, we have shown that the number of days with good ski conditions in a season is significantly decreasing in the Romanian Carpathians under climate change. Exceptions in this regard are the locations at altitudes higher than 2000 m. Also, we applied the hydrologic modelling to the sub-basins corresponding to the rivers Argeş (up to the hydrometric station Căteasca) and Dâmboviţa (left tributary of the Argeş River, up to the hydrometric station Lunguleţu), located mainly in mountain areas.

Activity 4.2. Variability and change in flash floods with snow melt contribution

The results of the hydrologic model (CONSUL) indicate that multiannual averages of maximum discharges during the interval from November to April show increases compared with present climate (1981-2010) under best (RCP 2.6) and worst (RCP 8.5) climate change scenarios. For sub-basins with larger areas, the increases are systematically larger under the worst scenario compared to those under the best one showing how the climate change signal overcome the noise (climate variability) beyond specific spatial scales of river basins.

Activity 4.3. Variability and change in avalanche statistics

In order to predict the avalanche conditions, we used a multifield analog approach and as a predictive metric we used the Euclidean distances between the past events and the actual conditions, in the hyperspace defined by the first 4 empirical orthogonal function (EOFs) modes. However, the states associated with avalanche events do not significantly cluster themselves, so the skill of the model is not high.

WP5 Aquifer replenishment modelling from snowmelt infiltration

Activity 5.1. Snowmelt infiltration assessment for the unsaturated zone

For the selection of the 3 sites, we considered the recharge process of 3 large hydro-structures, namely: the fissuered mountain aquifers - the Bucegi Mountain massif, the regional aquifers cantonated in alluvial areas - the Prahova-Teelejen alluvial cone and the last Small aquifer area located in the Romanian Plain, where the study area is the Colentina area (Colentina Laboratories Complex, Bucharest).

In Romania, areas with fissured aquifers, the hydrogeological parameters are highly complex and the lack of data makes it difficult to asses and model the behaviour of these aquifers. Bucegi area was chosen because it fulfills the main condition, namely that fissuered aquifers and a complex network of springs that can be monitored are found. From the lithological point of view and the fissured system, the selected area has observation points, and groundwater flows through fissure and voids in conglomerates and limestone.

For the area of the regional aquifers cantonated in the alluvial areas, it was chosen to evaluate the area of the alluvial cone Prahova-Teleajen, where under this deposists is the formation the Candesti strata. The two layers have a similar lithological composition (sand, gravel, interleaved clay), and the modeling of infiltration through the alluvial cone can be extrapolated to the Cândeşti aquifer.

In the last area of the small aquifers was chosen the reference area of Colentina - Bucharest, where the aquifer formation is the Colentina layer that meets the essential characteristics, namely: there is an alluvial aquifer in this area, the area is urban. In this area there is an experimental hydrogeological monitoring site composed of five hydrological wells and a geophysical drilling study.

In order to achieve the conceptual model for aquifer recharge from snow melting, a diagram of the processes and factors involved in soil infiltration was made.

The modeling and predicting of infiltration processes in frozen soils can be used to assess risks and damages related to climate change, especially for mountain regions and permafrost regions.

Activity 5.2. Aquifer modelling

As a result of the activities carried out in 2016, it was possible to identify the scheme of processes involved in determining soil infiltration, including the following:

- Weather conditions include weather data such as temperature, wind speed, relative humidity, atmospheric pressure, precipitation, cloud cover, and solar radiation. This data influences the melting process of snow.
- Garnier and Ohmura (1970) calculated the theoretical global radiation, including direct and diffuse solar radiation, the maximum number of sun-hours based on latitude and altitude, the slope of the soil and the azimuth, which provide radiation input data in the hours calculation module with sun, the snow melting module in the equilibrium energy equation, the net radiation wave pattern.
- Ellis et al. (2010) estimated the interception of forested areas with snow and fallen rain as well as losses from sublimation and evaporation at the interface with the forest.
- Pomeroy and Li (2000) simulated the redistribution of wind over snow and estimated snow accumulation and density changes throughout the winter.
- Atmospheric conditions influence the snow layer, causing different phenomena, such as depositing snow when rainfall falls in solid form, melting when rainfall falls in liquid form, and the rest of meteorological data, changing the water content in the snow layer.
- The snow state is influenced by the following parameters: temperature, thickness and density of the snow layer, Albedo factor, snow equivalent, as well as snow water content.
- The melting phenomenon is influenced by the weather conditions, but also by the heat of the soil, as well as the vapor-sublimation phenomenon.
- Essery and Etchevers (2004) have estimated Albedo snow factor throughout the winter and during the melting of snow.

- Marks et al (1998) developed a model (SNOBAL) for estimating snow melt by calculating the energy balance of radiation, latent heat, sensitive heat, soil layer, precipitation advection, and internal energy exchange of two layers of snow.
- Snow melting or excessive rainfall leads to surface runoff.
- Soil infiltration from snow melting is estimated in two ways, namely: Gray's parameter of snow melt infiltration (Zhao and Gray, 1999), which estimates the melting of snow infiltrated into frozen soils and is based on soil temperature, layer thickness, Porosity, soil moisture and soil saturation, and Ayers' infiltrations (Ayers, 1959) estimate infiltrations from snow melting and from rain in non-frozen soils based on soil texture, base rock exposure, root characteristics, degree Vegetation cover, soil moisture, porosity, air inlet pressure, hydraulic conductivity (KS and Kψ), saturated water content (θS) and residual water content (θr). Both infiltration algorithms are related to soil moisture.
- When the frozen soil has cracks, the amount of snow melting water infiltrates directly into the unsaturated zone, and when the ice lenses are present, the water flows to the surface water body.
- Evaporation of water is done by two methods: Granger and Gray (Granger and Gray, 1989; Granger and Pomeroy, 1997) estimate the actual evaporation (evaporation and perspiration) of unsaturated surfaces and the evaporation expression of Priestley and Taylor (Priestley and Taylor 1972) That estimates actual evaporation after saturated surfaces, such as wetlands or open water bodies (lakes, canals). Both evaporation calculation methods update the moisture content of the soil column.
- Leavesley et al (1983) developed the equilibrium equation of soil moisture. Dornes et al (2008) and Fang et al (2010) modified this equation to calculate the soil moisture balance. The first layer of soil is called recharge layer, which receives inputs through infiltrations from surface waters, snow melting or precipitation.
- Evaporation primarily uses intercepting and deposited surface water, and then it can withdraw moisture by sweating from the first layer of soil or from other layers depending on the vegetation characteristics Armstrong et al (2010).
- Underground water recharge takes place by percolation from soil strata or directly from depression deposits through macropores. Part of the water in the soil evaporates, part is consumed by the plants by evapotranspiration and part refills the aquifer.

Activity 5.3. Pattern matching and climate scenarios

The effect of climate change on seasonal snowfall can be estimated by adjusting time series, observed temperatures, and precipitation through adjustable parameters. This is technically facilitated by the implementation of climate change parameters for the assumed temperature and precipitation trends. It is possible to simulate the evolution of a seasonal snow layer under climate change conditions by flexibly adjusting the temperature and / or the modified rainfall.

WP6 Assimilation of snowpack parameters in the National Flood Forecasting and Warning System

Activity 6.3. Implementation of algorithms and methodology for snowpack parameter assimilation in the operational hydrological forecasting

One of the main application of the improved detailed estimations of the snow water equivalent, is to update this important state parameter in the operational hydrological forecasting models.

The Romanian National Hydrological Forecasting and Modelling System is composed by specialized hydrological modelling modules, adequate for the real-time simulation and forecasting of hydrological processes at different spatial and temporal scales.

Taking into account that the gridded SWE product generated using the data fusion approach could be considered as the best estimate of this parameter using the available information, the direct insertion method is used as data assimilation approach.

The adjusted gridded SWE product, output from the data fusion methodology, is used to compute the mean SWE for the sub-basins configured within the NWSRFS and respectively ROFFG operational models implementation.
Starting with the next winter season the data assimilation will be applied in operational mode, using the output from the data fusion methodology.
Was finalized the deliverable D6.3. "Implementation of the snowpack parameter assimilation into the hydrological forecasting modelling system: NOAH-R, NWSRFS (U.S. National Weather Service River Forecast System) and ROFFG".

WP7 Avalanche inventory, release and hazard mapping
Activity 7.2. Change-detection algorithm for Sentinel-1 and Sentinel-2

The analysis of the inventoried events showed that in the Carpathians avalanches are almost in totally small and middle size events with only a few cases that are considered extreme, most of the events causing damages to forest, road infrastructure and generating injuries and fatalities. In the frame of activity 7.2, the benefit of SAR based (i.e. Sentinel-1) detection process is that there are no cloud issues. When the avalanches look like bright "blobs", the algorithm detects them in most cases. In the layover and shadow areas avalanche detection is not feasible. Using the algorithm for detection of changes in avalanches during the same season, the avalanche age was also estimated from the image where a given avalanche was first observed. The results of the processing using optical images, Sentinel-2, has proved to be inefficient for the detection of small and medium size avalanches, specific for Southern Carpathians, a high percentage of cloud cover being specific in most of the images.

Activity 7.3. Avalanche simulation

In this stage of the project, avalanche trajectories simulation was tested for several magnitude scenarios in the central area of Făgăraș Mts. The potential release areas have been extracted base don morphometric parameters derived from DEM. The results of the simulation showed that in most of the cases, parts of the highway and forested areas will be affected, especially in the southern slope.

WP8 Promotion and Dissemination
Activity 8.1. Project website

The project web site (http://snowball.meteoromania.ro) has been updated. There were included information concerning the Snowball consortium activity in the current stage: results, meetings, dissemination, etc. The project website is bilingual (in Romanian and English).

Activity 8.3. Dissemination and training actions

Dissemination and training actions were carried out in accordance with the project dissemination strategy included in the Project's Publicity Plan.
Oral presentations of the results of the SnowBall project took place at various scientific events (seminars, conferences, workshops, formal and informal meetings, etc.) as well as written materials (brochures, newsletters, articles in scientific journals, articles in general publications, etc.).

7. REFERENCES

Ambach, W., Bitterlich, W., Howorka, F., 1965, Ein Gerat zur Bestimmung des freien Wassergehaltes in der Schneedecke durch dielektrische Messung, *Acta Physica Austriaca*, Band XX, Heft 1-4.

Anderson, E. A., 1968, Development and Testing of Snow Pack Energy Balance Equations, *Water Resources Research*, **4(1)**, pp 19-37.

Anderson, E. A., 1973, National Weather Service River Forecast System - Snow Accumulation and Ablation Model, NOAA Technical Memorandum NWS HYDRO-17, 217 pp.

Anderson, E. A., 1976, A Point Energy and Mass Balance Model of a Snow Cover, NOAA; Technical Report NWS 19, 150 pp.

Bartelt, P., Bühler, Y., Christen, M., Deubelbeiss, Y., Salz, M., Schneider, M., Schumacher, M., 2013, A numerical model for snow avalanches in research and practice, RAMMS User Manual.

Barnett, T.P. and Preisendorfer, R.W., 1978, Multifield analog prediction of short-term climate fluctuations using a climate state vector, *J. Atmos. Sci*., **35(10)**, 1771–1787.

Bartelt, P., Salm, B., Gruber, U., 1999, Calculating dense-snow avalanche runout using a Voellmy-fluid model with active/passive longitudinal straining, *Journal of Glaciology*, **45(150)**, 242-254.

Baum, L. E. and Petrie, T., 1966. Statistical Inference for Probabilistic Functions of Finite State Markov Chains, The Annals of Mathematical Statistics, 37 (6), 1554–1563.

Bălan, I., 2001, Patericul Românesc, Mânăstirea Sihastria.

Birsan, M-V, Dumitrescu, A., 2014, Snow variability in Romania in connection to large-scale atmospheric circulation, *Int. J. Climatol*., **34**, 134–144, DOI: 10.1002/joc.3671.

Busuioc, A. et al., 2012, Scenarii de schimbare a regimului climatic în România pe perioada 2001-2030, ANM.

Bühler, Y., Meier, L., Ginzler, C., 2015, Potential of Operational High Spatial Resolution Near-Infrared Remote Sensing Instruments for Snow Surface Type Mapping, IEEE Geoscience and Remote Sensing Letters, 12(4), 821-825.

Carneiro, T., Andrade, P. R., Câmara, G., Monteiro, A. M. V., Pereira, R., 2013, An extensible toolbox for modeling nature-society interactions, *Environmental Modelling & Software*, 2013 (in press). DOI:10.1016/j.envsoft.2013.03.002.

Carneiro, T., Câmara, G., Maretto, R., 2008, Irregular Cellular Spaces: Supporting Realistic Spatial Dynamic Modeling using Geographical Databases, Brazilian Symposium on Geoinformatics, GeoInfo'08, Rio de Janeiro.

Christen, M., Kowalski, J., Bartelt, P., 2010, RAMMS: Numerical simulation of dense snow avalanches in three-dimensional terrain, Cold Regions Science and Technology, 63(1–2), 1-14.

Denoth, A., 1994, An electronic device for long-term snow wetness recording, Annals of Glaciology, 19.

Dozier, J., 1989, Spectral signature of alpine snow cover from the Landsat Thematic Mapper, Remote Sensing of Environment, 28, 9-22.

Dumitrescu, A., Birsan, M.-V., Manea, A., 2015, Spatio-temporal interpolation of sub-daily (6 h) precipitation over Romania for the period 1975–2010, *J. Climatology*, **7**, DOI: 10.1002/joc.4427.

Fitzharris, B.B, 1987, A climatology of major avalanche winters in Western Canada, *Atmosphere-Ocean*, **25 (2)**, pp. 115-136.

Frauenfelder, R., Lato, M.J., Biskupič, M., 2015, Using eCognition to automatically detect and map avalanche deposits from the spring 2009 avalanche cycle in the Tatra mts., Slovakia. Int. Arch. Photogramm, Remote Sens. Spatial Inf. Sci., XL-7/W3, 791-795.

Gaspar, R., Munteanu, S.A., 1968, Studii privind avalanşele de zăpadă şi indicarea măsurilor de prevenire şi combatere, Analele I.C.A.S.

Hansen, C., Underwood, S.J, 2012, Synoptic Scale Weather Patterns and Size-5 Avalanches on Mt. Shasta, California, *Northwest Science*, **86**, pp. 329-341.

Hengl, T., Heuvelink, G.B.M., Rossiter, D.G., 2007, About Regression-Kriging: From Equations to Case Studies, *Computers & Geosciences*, **33 (10)**, 1301–1315.

Höller, P., 2009, Avalanche cycles in Austria: an analysis of the major events in the last 50 years, *Nat. Hazards*, **48 (3)**, pp. 399-424.

Isaaks, E.H., Srivastava, R.M., 1989, An Introduction to Applied Geostatistics, Oxford University Press.

Julien, P. Y., Saghafian B., Ogden F. L., 1995, Raster-based hydrological modeling of spatially-varied surface runoff. *Water Resour. Bull*., AWRA, **31(3)**, 523-536.

Malnes, E., Eckerstorfer, M., Larsen, Y., Fraunfelder, R., Jónsson, Á., Jaedicke, C., Solbø, S., 2013, Remote sensing of avalanches in northern Norway using Synthetic Aperture Radar ISSW International Snow Science Workshop, Chamonix Mont Blanc, October 07-11, 2013, pp. 955-959.

Mather, P.M., 2004, Computer processing of remotely-sensed images-An introduction, John Wiley & Sons, ISBN: 978-0-470-02101-9, 442 p.

Meinshausen, M. et al. 2011, The RCP greenhouse gas concentrations and their extensions from 1765 to 2300, *Climatic Change*, **109 (1-2)**, 213–241, doi:10.1007/s10584-011-0156-z.

Milian, N. et al., 2010, Avalanşele mortale din iarna 2009-2010, Sesiunea anuală de Comunicări Ştiinţifice a ANM.

Milian, N., Stăncescu M., 2012, Avalanches - Extreme Winter Events. Monitoring and Avalanche Risk - Conferinţa Aerul şi Apa Componente ale Mediului, pp. 220-226.

Mitchell, K., 2005, The community Noah land-surface model (LSM), user's guide, public release version 2.7.1. NCEP/EMC, USA.

Moţoiu, D. M., 2008, Avalanşele şi impactul lor asupra mediului. Studii de caz în Carpaţii Meridionali, *Edit. Proxima*, Bucureşti, 280 p.

Mualem, Y., 1976, A new model for predicting the hydraulic conductivity of unsaturated porous media, *Water Resour. Res*., **12(3)**, 513-522.

Niu, G. Y., et al., 2011, The community Noah land surface model with multiparameterization options (Noah-MP): 1. Model description and evaluation with local-scale measurements, *J. Geophys. Res*., **116**, D12109, doi: 10.1029/2010JD015139.

Paşol A.A. et al., 201), Winter extreme events - Romanian Carpathian Avalanches, in Air and Water Components of the Environment, Casa Cărţii de Stiinţă, Cluj-Napoca, pp. 101-107.

Rudjord, Ø., Salberg, A.-B., and Solberg R., 2015. Global Snow Cover Mapping Using a Multi-Temporal Multi-Sensor Approach. Proceedings of 8th International Workshop on the Analysis of Multitemporal Remote Sensing Images, July 22-24, 2015, Annecy, France.

Sihvola, A., Nyfors, E., Tiuri, M.,1985, Mixing formulae and experimental results for the dielectric constant of snow, *Journal of Glaciology*, **31(108)**.

Šimůnek, J., Šejna, M., Saito, H., Sakai, M., van Genuchten, M. Th., 2013, The HYDRUS-1D Software Package for Simulating the One-Dimensional Movement of Water, Heat, andMultiple Solutes in Variably-Saturated Media.

Solberg R, Huseby RB, Koren H, Malnes E. 2008. Time-series fusion of optical and SAR data for snow cover area mapping. Proceedings of EARSeL LIS-SIG Workshop, Berne, February 11-13 February, 2008.

Solberg R, Rudjord Ø, Salberg A-B, Killie MA. 2015. Advancements and validation of a global snow product fusing optical and passive microwave radiometer data. Proceedings for the 2015 EUMETSAT Meteorological Satellite Conference, 21-25 September 2015, Toulouse, France.

Stein, J., Laberge, G., and L´evesque, D., 1997, Measuring the dry density and the liquid water content of snow using time domain reflectometry, Cold Reg. Sci. Technol., 25, 123–136.

Stiles, W.H., Ulaby, F.T., 1981, Dielectric properties of snow, Interim Technical Report (Kansas Univ. Center for Research, Inc.) NASA-CR-166764.

Techel, F., C. Pielmeier, 2011, Point observations of liquid water content in wet snow – investigating methodical, spatial and temporal aspects, The Cryosphere, 5, 1–14.

Tiuri, M., Sihvola, A., 1986, Snow fork for field determination of the density and wetness profiles of a snow pack, Hydrology Applications of Space Technology (Proceedings of the Cocoa Beach Workshop, Florida, August 1985), IAHS Publ. no. 160.

Tiuri, M., Sihvola, A., Nyfors, E., Hallikainen, M., 1984, The complex dielectric constant of snow at microwave frequencies, IEEE Journal of Oceanic Engineering, OE-9 (5), 377-382.

Tiuri, M., Sihvola, A., Nyfors, E., 1982, Microwave sensor for snowpack wetness and density profile measurement, 12th European Microwave Conference, Helsinki, Microwave Exhibitions and Publishers Ltd, Kent, England.

USDA, 2004: Chapter 11: Snowmelt, National Engineering Handbook.

Viterbi, A. J., 1967, Error bounds for convolutional codes and an asymptotically optimum decoding algorithm, *IEEE Transactions on Information Theory*, **13**, pp: 260–269, doi:10.1109/TIT.1967.1054010

Voigt, S., Kleindienst, H., Baumgartner, M. F., 2003, Chapter 4.11: Snowmelt Forecasting as a Contribution to Operational Flood Warning: A System Integrating Remote Sensing Data and Meteorological Model Output, Early Warning Systems for Natural Disaster Reduction, Springer Berlin Heidelberg.

Wiesmann, A., Wegmüller, U., Honikel, M., Strozzi, T., Werner, C., 2001, Potential and methodology of satellite based SAR for hazard mapping, IGARSS International Geoscience and Remote Sensing Symposium, Sydney, Australia, 9 - 13 July 2001.

Wigmosta, M. S., Vail, L. W. and Lettenmaier, D. P., 1994, A distributed hydrology- vegetation model for complex terrain, *Water Resour. Res*., **30(6)**, 1665-1679.

Wigmosta, M. S., Lettenmaier D. P., 1999, A comparison of simplified methods for routing topographically driven subsurface flow, *Water Resour. Res*., **35(1)**, 255-264.

Zadeh, L. A., 1965, Fuzzy Sets, Information and Control, **8**, pp: 338-353.

5TM Water Content and Temperature Sensors, Decagon Devices, Inc., Version: March 11, 2016.

*** Bilanţul nivologic al sezonului de iarnă – publicaţie anuală, începând din 2004, Administraţia Naţională de Meteorologie, Bucureşti.

LIST of ACRONIMS

ANCSI	National Authority of Scietific and Inovation Research
ASAR	Advanced Synthetic Aperture Radar
CMIP5	Coupled Model Intercomparison Project Phase 5
DEM	Digital Elevation Model
EEA	European Economic Area
EO	Earth Observation
ESA	European Space Agency
FSC	Fractional Snow Cover
GIS	Geographic Information Systems
GPS	Global Positioning System
HR	High Resolution
HRLDAS	Data Assimilation System for High Resolution
IR	Infrared
LC/LU	Land Cover / Land Use
LSM	Land Surface Model
MODIS	Moderate Resolution Imaging Spectroradiometer
MWS	Multi-Sensor/Multi-Temporal Wet Snow
NASA	National Aeronautics and Space Administration
NIHWM	National Institute of Hydrology and Water Management
NIR	Near-infrared
NMA	National Meteorological Administration
NR	Norsk Regnesentral
NWSRFS	National Weather Service River Forecast System
OLCI	The Ocean Land Colour Instrument
OWS	Optical Wet Snow
PSC	Project Steering Committee
RCPs	Representative Concentration Pathways
ROFFG	Romanian Flash Flood Guidance System
RS	Remote Sensing
SAR	Synthetic-Aperture Radar
SCE	Snow Cover Extent Area
SGEM	International Multidisciplinary Scientific GeoConferences
SGS	Snow Grain Size
SLSTR	Sea Land Surface Temperature Radiometer
SPOT	Satellite for observation of Earth
SSW	Snow Surface Wetness
STG	Scientific and Technical Group
STS	Snow Surface Temperature
SW	Snow Wetness
SWCC	Soil Water Characteristic Curve
SWE	Snow Water Equivalent
SWS	SAR Wet Snow
TDR	Time-Domain Reflectometer
USGS	U.S. Geological Survey
UTCB	Technical University of Civil Engineering
UTM	Universal Transverse Mercator
VHR	Very-High Resolution
WUT	West University of Timisoara